POWER AMPLIFIER LINEARIZATION BY PREDISTORTION

A THESIS

SUBMITTED TO THE DEPARTMENT OF ELECTRICAL AND

ELECTRONICS ENGINEERING

AND THE INSTITUTE OF ENGINEERING AND SCIENCES

OF BILKENT UNIVERSITY

IN PARTIAL FULFILLMENT OF THE REQUIREMENTS

FOR THE DEGREE OF

MASTER OF SCIENCE

By

MUSTAFA DURUKAL

September 2006

I certify that I have read this thesis and that in my opinion it is fully adequate, in scope and in quality, as a thesis for the degree of Master of Science.

Prof. Dr. ABDULLAH ATALAR(Supervisor)

I certify that I have read this thesis and that in my opinion it is fully adequate, in scope and in quality, as a thesis for the degree of Master of Science.

Prof. Dr. ERDAL ARIKAN

I certify that I have read this thesis and that in my opinion it is fully adequate, in scope and in quality, as a thesis for the degree of Master of Science.

Prof. Dr. MURAT AŞKAR

Approved for the Institute of Engineering and Sciences:

Prof. Dr. Mehmet Baray
Director of Institute of Engineering and Sciences

ABSTRACT

POWER AMPLIFIER LINEARIZATION BY PREDISTORTION

MUSTAFA DURUKAL
M.S. in Electrical and Electronics Engineering
Supervisor: Prof. Dr. ABDULLAH ATALAR
September 2006

Power amplifiers are important elements in communication systems but they are inherently nonlinear. This nonlinearity shows itself in the form of amplitude and phase distortion. One way to get rid of this nonlinear behaviour is to apply backoff which means to operate the amplifier at an output power smaller than its saturated output power. As the backoff is increased, the amplifier will behave more linearly. But this will also reduce the efficiency of the amplifier, which is undesirable. This tradeoff between efficiency and linearity is solved by linearization techniques. By using linearization techniques, the amplifier can be operated near to saturation with good efficiency and linearity.

This thesis focuses on polar polynomial predistortion and polar look-up table predistortion, which are popular linearization techniques. A polar polynomial predistorter and a polar look-up table predistorter are implemented and tested with simulations in software. The implementation and testing is done by using IT++ which is a C++ library of mathematical, signal processing, speech processing, and communications classes and functions. The testing of the predistorters is done by using a baseband system model which consists of a 16-QAM modulator, an upsampler, a raised cosine filter, the predistorter and a baseband

behavioural amplifier model. The performance of the predistorters is evaluated in terms of adjacent channel power ratio, AM/AM & AM/PM responses and BER under AWGN. Simulation results show that the predistorters have good performance. In the simulations, the polar polynomial predistorter achieved 20 dB reduction and the polar look-up table predistorter achieved 25 dB reduction in adjacent channel power ratio. The effect of polynomial order and table size on the performance of the predistorters is investigated. Furthermore, the effect of lowpass filtering on the performance of the predistorters is also investigated by placing a lowpass filter after the predistorters in the system model. It is observed that as the ratio of the bandwidth of the lowpass filter to the bandwidth of the raised cosine filter decreases, the negative effect of the lowpass filter on the performance of the predistorters increases.

Keywords: **polar polynomial predistortion**, **polar look-up table predistortion**, **linearization**, **AM/AM distortion**, **AM/PM distortion**, **amplifier nonlinearity**.

ÖZET

ÖNBOZULUM YOLU İLE GÜÇ YÜKSELTECİ DOĞRUSALLAŞTIRMASI

MUSTAFA DURUKAL
Elektrik ve Elektronik Mühendisliği Bölümü Yüksek Lisans
Tez Yöneticisi: Prof. Dr. ABDULLAH ATALAR
Eylül 2006

Güç yükselteçleri haberleşme sistemlerinin önemli elemanlarıdır fakat yapıları gereği doğrusal değillerdir. Bu doğrusal olmama kendini genlik ve faz bozulumu şeklinde gösterir. Bu doğrusal olmayan davranıştan kurtulmanın bir yolu yükselteci doymuş çıkış gücünden daha az bir çıkış gücünde çalıştırmaktır. Çıkış gücü azaltıldıkça, yükselteç daha doğrusal davranacaktır. Fakat bu sırada yükseltecin verimi de düşecektir ve bu istenmeyen bir durumdur. Verimlilik ve doğrusallık arasındaki bu ikilem doğrusallaştırma teknikleri ile çözülebilir. Doğrusallaştırma teknikleri kullanılarak, yükselteç iyi bir verim ve doğrusallıkla doyuma yakın bir noktada çalıştırılabilir.

Bu tez popüler doğrusallaştırma teknikleri olan kutupsal polinomsal önbozulum ve kutupsal başvuru tablosu önbozulumu üzerine odaklanmaktadır. Yazılım kullanılarak bir kutupsal polinomsal önbozucu ve bir kutupsal başvuru tablosu önbozucusu yapıldı ve benzetimlerle denendi. Yapma ve deneme için matematiksel, sinyal işleme, ses işleme ve haberleşme sınıflarının ve işlevlerinin oluşturduğu bir C++ kütüphanesi olan IT++ kullanıldı. Önbozucuların denenmesi bir 16'lık dördün genlik kipleyici, bir yukarı örnekleyici, bir tabanlı cosinüs süzgeci, önbozucu ve bir taban bant davranışsal yükselteç modeli içeren bir taban

bant sistem modeli kullanılarak yapıldı. Önbozucuların performansları komşu kanal güç oranı, genlik kiplenimi/genlik kiplenimi & genlik kiplenimi/faz kiplenimi yanıtları ve toplanır beyaz Gauss gürültüsü altındaki bit hata oranı kıstasları kullanılarak değerlendirildi. Benzetim sonuçları önbozucuların iyi bir performansa sahip olduklarını gösteriyor. Benzetimlerde komşu kanal güç oranında kutupsal polinomsal önbozucu 20 dB, kutupsal başvuru tablosu önbozucusu ise 25 dB azalma sağladı. Polinom derecesi ve tablo boyutunun önbozucular üzerindeki etkisi araştırıldı. Aynı zamanda sistem modelinde önbozucuların arkasına bir alçak geçiren süzgeç yerleştirilerek alçak geçiren süzgeçlemenin önbozucular üzerindeki etkisi araştırıldı. Alçak geçiren süzgecin bant genişliğinin tabanlı cosinüs süzgecinin bant genişliğine oranı azaldıkça alçak geçiren süzgeçlemenin önbozucuların performansı üzerindeki olumsuz etkilerinin arttığı gözlemlendi.

Anahtar Kelimeler: **kutupsal polinomsal önbozulum**, **kutupsal başvuru tablosu önbozulumu**, **doğrusallaştırma**, **genlik kiplenimi/genlik kiplenimi bozulumu**, **genlik kiplenimi/faz kiplenimi bozulumu**, **yükselteç doğrusalsızlığı**.

ACKNOWLEDGMENTS

I would like to thank my supervisor Prof. Dr. Abdullah Atalar for his guidance, suggestions and encouragement throughout the development of this thesis.

I am deeply grateful to Dr.Tarık Reyhan for the guidance and help that he provided during my M.S. study.

I would like to express my special thanks to the members of the thesis committee for reviewing the thesis.

I would like to thank my parents, my sister and my brother for their love and support that they gave me all my life without asking for any return.

I would like to thank my friend Cihan Hakan Arslan for his friendship and the help that he provided during my M.S. study.

I would like to express my special thanks to my friend Rohat Melik. His friendship has always been very valuable for me. He was always near me when I needed him and when there was nobody else to support me.

Contents

1 INTRODUCTION **1**

2 POWER AMPLIFIER LINEARIZATION TECHNIQUES **4**

2.1 Feedback 4

2.1.1 RF Feedback 6

2.1.2 Envelope Feedback 7

2.1.3 Cartesian Loop Feedback 8

2.1.4 Polar Loop Feedback 10

2.1.5 Other Feedback Schemes 11

2.2 Feedforward 13

2.3 Envelope Elimination and Restoration 16

2.4 LINC(Linear Amplification using Nonlinear Components) 18

2.5 CALLUM(Combined Analogue Locked Loop Universal Modulator) 20

2.6 Predistortion 22

2.6.1 RF/IF Predistortion 23

2.6.2 Baseband Predistortion 26

2.6.2.1 LUT Predistorters that use direct predistorter adaptation 30

2.6.2.2 Memoryless Polynomial Predistorters that use direct predistorter adaptation 36

3 EFFECTS of POWER AMPLIFIER NONLINEARITY in COMMUNICATION SYSTEMS and MODELING of THIS NONLINEARITY 39

3.1 Common Measures of Power Amplifier Nonlinearity 40

3.1.1 1 dB compression point 40

3.1.2 Third order intercept point(IP3) 42

3.2 AM/AM and AM/PM characteristics 45

3.2.1 Saleh model 47

3.2.2 Rapp model 48

3.2.3 Arctan model 49

3.2.4 Third order polynomial model 50

3.3 Effects of Power Amplifier Nonlinearity 51

3.3.1 Harmonic Generation(Distortion) 52

3.3.2 Intermodulation Distortion 52

3.3.3 Spectral Regrowth 53

3.3.4 Cross Modulation 55

3.3.5 Desensitization 56

4 IMPLEMENTATION and TESTING of a LOOK-UP TABLE PREDISTORTER and a POLYNOMIAL PREDISTORTER in software 57

4.1 System Model 58

4.1.1 QAM modulator 58

4.1.2 Upsampling 60

4.1.3 Raised Cosine filter 60

4.1.4 Power Amplifier 64

4.1.5 Digital Baseband Predistorter 66

4.1.5.1 Polar Polynomial Predistorter 66

4.1.5.2 Polar Look-up Table Predistorter 69

4.2 Simulations, Results and Discussion 74

5 Summary, Conclusions and Future Work 110

APPENDIX 114

A 16-QAM-OFDM System Performance in the Presence of Adjacent Channel Interference Caused by Amplifier Nonlinearity 114

A.1 Introduction 114

A.2 Simulated System Model 117

A.2.1 OFDM modulator and demodulator 118

A.2.2 Nonlinear Power Amplifier 120

A.3 Simulations, Results and Discussion 121

A.4 Conclusion 130

List of Figures

2.1 Block diagram of feedback principle 5

2.2 Envelope Feedback Linearization 7

2.3 Cartesian Loop Feedback Transmitter 8

2.4 Polar Loop Feedback Transmitter 9

2.5 Second harmonic feedback with amplitude and phase adjustment . 11

2.6 Feedforward linearization 12

2.7 Multiple feedforward(2 loops) 15

2.8 Adaptive feedforward 15

2.9 Envelope Elimination and Restoration Technique 16

2.10 LINC technique 18

2.11 CALLUM block diagram 20

2.12 The basic idea of predistortion 21

2.13 RF predistortion(a), IF predistortion(b), Baseband predistortion(c) 21

2.14 (a)RF Cubic Predistorter, (b)IF Cubic Predistorter 23

2.15 Adaptive digital baseband predistortion 25

2.16 Direct Predistorter Adaptation 28

2.17 PA Modelling with Consecutive Inverse Estimation 28

2.18 Predistortion using Postdistorter Adaptation(Indirect learning) . . 29

2.19 Mapping predistorter block diagram 31

2.20 Mapping done by mapping predistorter 31

2.21 Complex Gain predistorter block diagram 33

2.22 Polar Predistorter block diagram 35

3.1 1 dB compression point 42

3.2 Third Order Intercept Point 43

3.3 An example AM/PM characteristics 46

3.4 Saleh model AM/AM and AM/PM responses 48

3.5 Rapp model AM/AM response 49

3.6 Arctan model AM/AM and AM/PM responses 50

3.7 Third order polynomial model AM/AM response 51

3.8 Spectral Regrowth 53

3.9 Adjacent Channel Interference 54

3.10 Upper and Lower Adjacent Channel Bands 55

4.1 Simulated System Model 57

4.2 16-QAM constellation 59

4.3 The impulse response and transfer function of a raised cosine filter for various roll-off factor(β) values 62

4.4 Impulse response of the FIR raised cosine filter 63

4.5 Transfer function of the FIR raised cosine filter 64

4.6 AM/AM response & AM/PM response & Gain of the amplifier model used in the simulations 65

4.7 Block diagram of the implemented polar look-up table predistorter 70

4.8 System model during training 75

4.9 System model during testing 75

4.10 Gain of polar polynomial predistorter of order 10, amplifier and polar polynomial predistorter & amplifier combination 76

4.11 AM/AM response of polar polynomial predistorter of order 10, amplifier and polar polynomial predistorter & amplifier combination 76

4.12 AM/PM response of polar polynomial predistorter of order 10, amplifier and polar polynomial predistorter & amplifier combination 77

4.13 Power Spectral Density of the input signal to the polar polynomial predistorter 78

4.14 Power Spectral Density of the output signal of the amplifier . . . 79

4.15 BER performance of the polar polynomial predistorter under additive white gaussian noise 79

4.16 Gain of the polar polynomial predistorter-amplifier combination for different polynomial orders 80

4.17 AM/PM response of the polar polynomial predistorter-amplifier combination for different polynomial orders 82

4.18 Gain of polar look-up table predistorter, amplifier and polar look-up table predistorter & amplifier combination 82

4.19 AM/AM response of polar look-up table predistorter, amplifier and polar look-up table predistorter & amplifier combination . . . 83

4.20 AM/PM response of polar look-up table predistorter, amplifier and polar look-up table predistorter & amplifier combination . . . 83

4.21 Power Spectral Density of the input signal to the polar look-up table predistorter 85

4.22 Power Spectral Density of the amplifier output signal 85

4.23 BER performance of the polar look-up table predistorter under additive white gaussian noise 86

4.24 Gain of the polar look-up table predistorter-amplifier combination for different table sizes 87

4.25 AM/PM response of the polar look-up table predistorter-amplifier combination for different table sizes 88

4.26 Simulated system model including lowpass filter 90

4.27 Transfer function of the lowpass filter for filter length = 1001, cutoff frequency = 0.2 91

4.28 Spectral performance of the polar polynomial predistorter which has AM/AM & AM/PM polynomials of order 10 for the case where ratio of filter bandwidths = 4.27 92

4.29 Spectral performance of the polar polynomial predistorter which has AM/AM & AM/PM polynomials of order 10 for the case where ratio of filter bandwidths = 3.2 93

4.30 Spectral performance of the polar polynomial predistorter which has AM/AM & AM/PM polynomials of order 10 for the case where ratio of filter bandwidths = 2.13 94

4.31 AM/AM performance of the polar polynomial predistorter which has AM/AM & AM/PM polynomials of order 10 for the case where ratio of filter bandwidths = 4.27 95

4.32 AM/PM performance of the polar polynomial predistorter which has AM/AM & AM/PM polynomials of order 10 for the case where ratio of filter bandwidths = 4.27 95

4.33 AM/AM performance of the polar polynomial predistorter which has AM/AM & AM/PM polynomials of order 10 for the case where ratio of filter bandwidths = 3.2 96

4.34 AM/PM performance of the polar polynomial predistorter which has AM/AM & AM/PM polynomials of order 10 for the case where ratio of filter bandwidths = 3.2 97

4.35 AM/AM performance of the polar polynomial predistorter which has AM/AM & AM/PM polynomials of order 10 for the case where ratio of filter bandwidths = 2.13 98

4.36 AM/PM performance of the polar polynomial predistorter which has AM/AM & AM/PM polynomials of order 10 for the case where ratio of filter bandwidths = 2.13 98

4.37 BER performance of the polar polynomial predistorter of order 10 under AWGN for different filter bandwidth ratio values 99

4.38 BER performance of the polar polynomial predistorter of order 10 as a function of ratio of filter bandwidths for $E_b/N_0 = 10\,dB$ . . . 100

4.39 Spectral performance of the polar look-up table predistorter which has a table size of 128 for the case where ratio of filter bandwidths = 4.27 100

4.40 Spectral performance of the polar look-up table predistorter which has a table size of 128 for the case where ratio of filter bandwidths = 3.2 102

4.41 Spectral performance of the polar look-up table predistorter which has a table size of 128 for the case where ratio of filter bandwidths = 2.13 102

4.42 AM/AM performance of the polar look-up table predistorter which has a table size of 128 for the case where ratio of filter bandwidths = 4.27 103

4.43 AM/PM performance of the polar look-up table predistorter which has a table size of 128 for the case where ratio of filter bandwidths = 4.27 104

4.44 AM/AM performance of the polar look-up table predistorter which has a table size of 128 for the case where ratio of filter bandwidths = 3.2 105

4.45 AM/PM performance of the polar look-up table predistorter which has a table size of 128 for the case where ratio of filter bandwidths = 3.2 105

4.46 AM/AM performance of the polar look-up table predistorter which has a table size of 128 for the case where ratio of filter bandwidths = 2.13 106

4.47 AM/PM performance of the polar look-up table predistorter which has a table size of 128 for the case where ratio of filter bandwidths = 2.13 106

4.48 BER performance of the polar look-up table predistorter of size 128 under AWGN for different filter bandwidth ratio values 107

4.49 BER performance of the polar look-up table predistorter of size 128 as a function of ratio of filter bandwidths for $E_b/N_0 = 10\,dB$. 108

A.1 Simulated baseband system model 116

A.2 Adjacent Channel Interference faced by the middle channel 117

A.3 OFDM modulator and demodulator block diagram 118

A.4 BER of the middle transmitter as a function of channel spacing for different average transmitted power ratio values where amplifier model = Rapp model, IBO = 0 dB 124

A.5 BER of the middle transmitter as a function of channel spacing for different average transmitted power ratio values where amplifier model = Rapp model, IBO = 2 dB 125

A.6 BER of the middle transmitter as a function of IBO for different average transmitted power ratio values where amplifier model = Rapp model, Channel Spacing = 2*Channel Bandwidth 126

A.7 BER of the middle transmitter as a function of IBO for different average transmitted power ratio values where amplifier model = Rapp model, Channel Spacing = 3.2*Channel Bandwidth 128

A.8 BER of the middle transmitter as a function of average transmitted power ratio for different channel spacing values where amplifier model = Rapp model, IBO = 0 dB 129

A.9 BER of the middle transmitter as a function of average transmitted power ratio for different channel spacing values where amplifier model = Rapp model, IBO = 3 dB 130

Dedicated to my father and my mother who brought me up

Chapter 1

INTRODUCTION

Power amplifiers have become a bottleneck for modern telecommunication systems. Their purpose is to amplify the signal before transmitting it, and since relatively high power levels are used, they are major power consumers while doing this. Since all other electronic and digital signal processing equipment in a handset or terminal usually operate at much lower power levels, the total efficiency of the system is significantly determined by the efficiency of the PA at the time of transmitting. This means that the operating time in a handset is greatly dependent on the efficiency of the PA, while high efficiency is also preferred in base stations in order to achieve low power consumption and avoid problems of overheating.

From a PA point of view, the difficulties in modern telecommunications systems arise from spectral efficiency. The number of users is increasing rapidly, and at the same time high data-rates have become a more and more important issue, as moving pictures and other data-expensive applications are gaining popularity. Since the available spectrum is limited and expensive, attempts are being made to transmit the maximum amount of data using the minimum amount of spectrum.

Large amounts of data can be transmitted using sophisticated modulation techniques. Such modulation techniques generally have highly varying envelopes and as a result, they require linear amplification to avoid distortion. Unfortunately, power amplifiers which will provide the necessary amplification are inherently nonlinear. They introduce amplitude(AM/AM distortion) and phase(AM/PM distortion) distortions to the input signal. These distortions cause spectral broadening of the input signal, which threatens spectral efficiency. It is possible to get linear behaviour from power amplifiers by operating them at a large backed-off output power but this will result in a low efficiency and high power dissipation. It seems that there is a tradeoff between linearity and efficiency. This problem is solved by linearization techniques. By applying linearization to the power amplifier, the linearity is improved, the required backoff is decreased and as a result, the efficiency is increased.

Power amplifier linearization techniques can be divided into 3 main groups:feedback, feedforward and predistortion. Nowadays, predistortion is the most commonly used linearization technique. Predistortion aims to introduce inverse nonlinearity that can compensate the AM/AM and AM/PM distortions generated by the nonlinear power amplifier. The most common form of predistortion is baseband predistortion in which the nonlinearity is applied at baseband. Baseband predistorters are generally implemented digitally by using digital signal processing. This type of baseband predistortion is called digital baseband predistortion. Two common types of digital baseband predistorters are polar look-up table predistorters and polar polynomial predistorters. In this thesis, a polar look-up table predistorter and a polar polynomial predistorter is implemented and tested in software by using a behavioural power amplifier model. The organization of the thesis is as follows: Chapter 2 describes the common linearization techniques found in the literature in detail. Chapter 3 describes the effects and modelling of power amplifier nonlinearity. It defines common measures of nonlinearity like 1 dB compression point and 3^{rd} order intercept point.

It describes AM/AM response & AM/PM response and the common AM/AM response & AM/PM response models found in the literature. It describes common effects of amplifier nonlinearity like harmonic distortion, intermodulation distortion, spectral regrowth, cross modulation and desensitization. Chapter 4 describes the implementation and testing of the polar polynomial predistorter and polar look-up table predistorter in software in detail. It describes the simulated system model. It describes the implementation and update mechanism of the predistorters. It also describes the simulations done with the predistorters and simulation results. Finally chapter 5 gives the conclusions and describes the future work that can be done.

Chapter 2

POWER AMPLIFIER LINEARIZATION TECHNIQUES

This chapter describes common power amplifier linearization techniques. There is a wide range of power amplifier linearization techniques. These techniques can be roughly classified into three groups:

- Feedback
- Feedforward
- Predistortion

Each of these 3 groups contain several techniques which will be described in the following sections.

2.1 Feedback

Feedback linearization is the first general category of linearization. Feedback is used extensively in automatic plant control and in audio amplifiers but it can

also be used to linearize power amplifiers [1]. Feedback achieves linearization by causing the amplifier output to follow the amplifier input. Figure 2.1 shows a general block diagram of feedback principle.

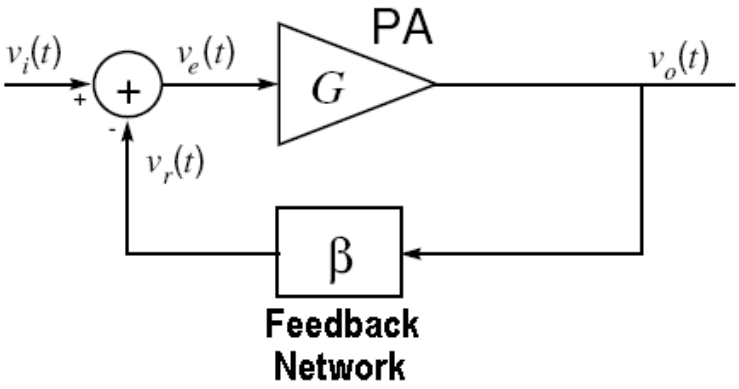


Figure 2.1: Block diagram of feedback principle [1]

The output $v_0(t)$ of the power amplifier is fed back through the voltage divider. The voltage divider has gain β. The input of the amplifier is driven by the error input

$$v_e(t) = v_i(t) - v_r(t) = v_i(t) - \beta v_0(t) = v_i(t) - \beta G v_e(t). \tag{2.1}$$

In equation 2.1 $v_i(t)$ is the original input signal, $v_r(t)$ is the signal fed back and G is the gain of the nonlinear power amplifier. G depends on the amplitude and frequency of the input signal to the power amplifier. The closed loop gain $G_c = \dfrac{v_0(t)}{v_i(t)}$ is given by:

$$G_c = \frac{G}{1 + \beta G} \tag{2.2}$$

The relative variation of G_c with respect to G_c is given by:

$$\frac{dG_c}{G_c} = \frac{1}{1 + \beta G} \frac{dG}{G} \tag{2.3}$$

Equation 2.3 shows us the main advantage of feedback linearization. The relative variations of the closed loop gain G_c is smaller than the relative variations of G by the factor $\dfrac{1}{1 + \beta G} \cdot$ As a result, if G shows great variation, the variation of G_c will be much smaller. But the disadvantage is that there is a reduction in overall gain. Another disadvantage is the delay introduced by the feedback. This delay

may cause stability problems. To ensure stable operation, the gain-bandwidth product must be limited. As a result, the input signals that can be used with feedback are limited by the choice of signal bandwidth.

The feedback can be directly applied to the RF signal(RF feedback) or indirectly to the modulation(modulation feedback), i.e. envelope, phase or I(in-phase) and Q(quadrature) components [2]. In RF feedback, the RF signal is fed back from the output to the input without any downconversion as seen in Figure 2.1. In modulation feedback, the output signal is first downconverted to baseband to get (envelope,phase) or (I,Q) components and then fed back to the input. In the following sections RF feedback and different forms of modulation feedback are described.

2.1.1 RF Feedback

The principle of RF feedback is illustrated in Figure 2.1. The output signal is fed back through a feedback network to the input without any downconversion and subtracted from the original input signal. The output of the subtractor drives the power amplifier. The feedback network used can be active or passive. An amplifier can be used as an active feedback network or resistors, transformers can be used as passive feedback networks [3]. Voltage-controlled current feedback and current-controlled voltage feedback are commonly used in the feedback network because they are simple and their distortion performance is predictable [2].

RF feedback reduces distortion at the output of the power amplifier with the help of the feedback network. This feedback network is simple and easy to implement and this is one of the advantages of RF feedback. However, the feedback reduces gain and introduces delay to the system. This delay can cause loop stability problems. To ensure stable operation the bandwidth of the input signal must be smaller than a certain value determined by the delay introduced.

As a result, RF feedback is limited to narrowband systems. The reduction in gain and narrowband operation are the main disadvantages of RF feedback.

2.1.2 Envelope Feedback

Envelope feedback is a form of modulation feedback. Figure 2.2 shows an envelope feedback scheme.

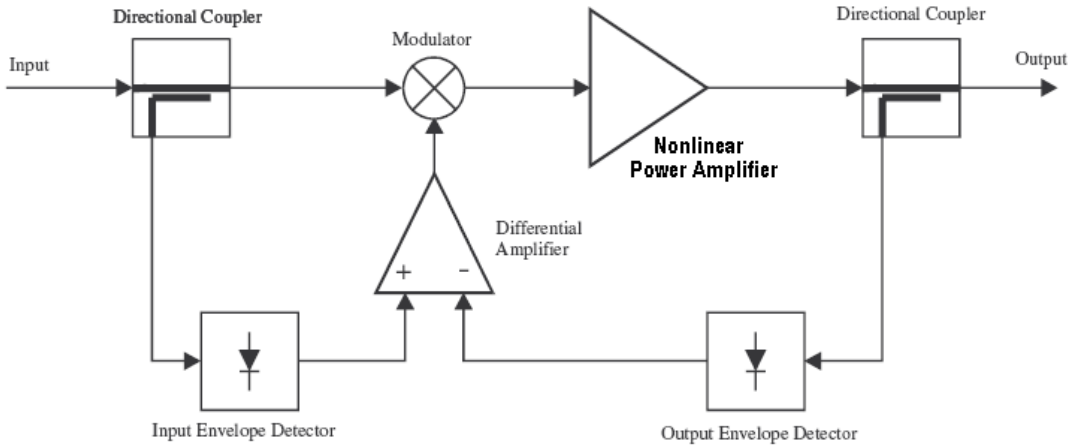


Figure 2.2: Envelope Feedback Linearization [3]

As seen in Figure 2.2, the input and output signals are sampled by couplers and then their envelopes are extracted by envelope detectors. The resulting input and output envelopes are subtracted by using a differential amplifier [3]. The resulting error signal controls a modulator, which modifies the envelope of the input signal [3]. The output of the modulator is amplified by the power amplifier.

In envelope feedback, there is no phase feedback. As a result, envelope feedback can only correct the distortion in the signal amplitude(AM-AM distortion). It can't correct the distortion in the signal phase(AM-PM distortion).

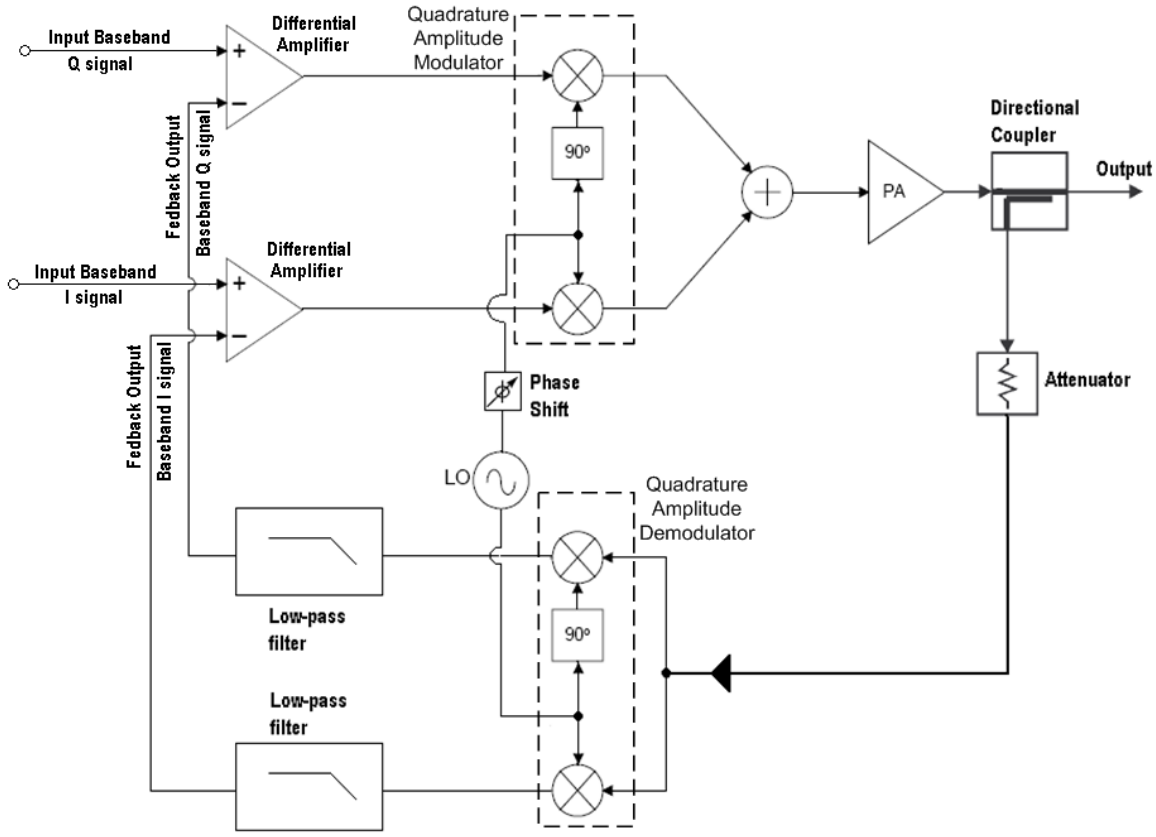


Figure 2.3: Cartesian Loop Feedback Transmitter [4]

2.1.3 Cartesian Loop Feedback

Cartesian Loop Feedback is depicted in Figure 2.3. In this technique the input and output baseband signals are processed in cartesian form. The input signal is available in baseband as quadrature(I and Q) components. These input I and Q components are fed to differential amplifiers and then upconverted to RF frequency by a quadrature amplitude modulator. The quadrature amplitude modulator consists of two mixers and a 90 degree phase shift network to create in-phase and quadrature components. After upconversion, these two signals are summed to form the modulated RF signal and the resulting RF signal drives the power amplifier. The output of the power amplifier is sampled, attenuated and downconverted to get the baseband output I and Q signals. These output I and Q signals are fed back to the input where they are compared with the input I

and Q signals with the help of differential amplifiers. In this way, the distortion in both I and Q signals is corrected. There is a delay between upconversion and downconversion processes in the cartesian loop system. To prevent the asynchronisation of upconversion/downconversion caused by this delay and to make them synchronised, there is a phase shift ϕ in the upconverter [1].

Cartesian Loop Feedback actually forms a complete transmitter [3] and it actually linearizes the complete transmitter [4]. As a result, nonlinearities of all blocks in the transmitter including quadrature amplitude modulator/demodulator are compensated. Since this is a closed loop feedback system, there is a delay around the loop and this delay affects the linearization performance. For high frequency signals this delay can cause stability problems. To prevent any unstable behaviour, this feedback system is limited in bandwidth and the linearization performance of this system depends on its bandwidth [3].

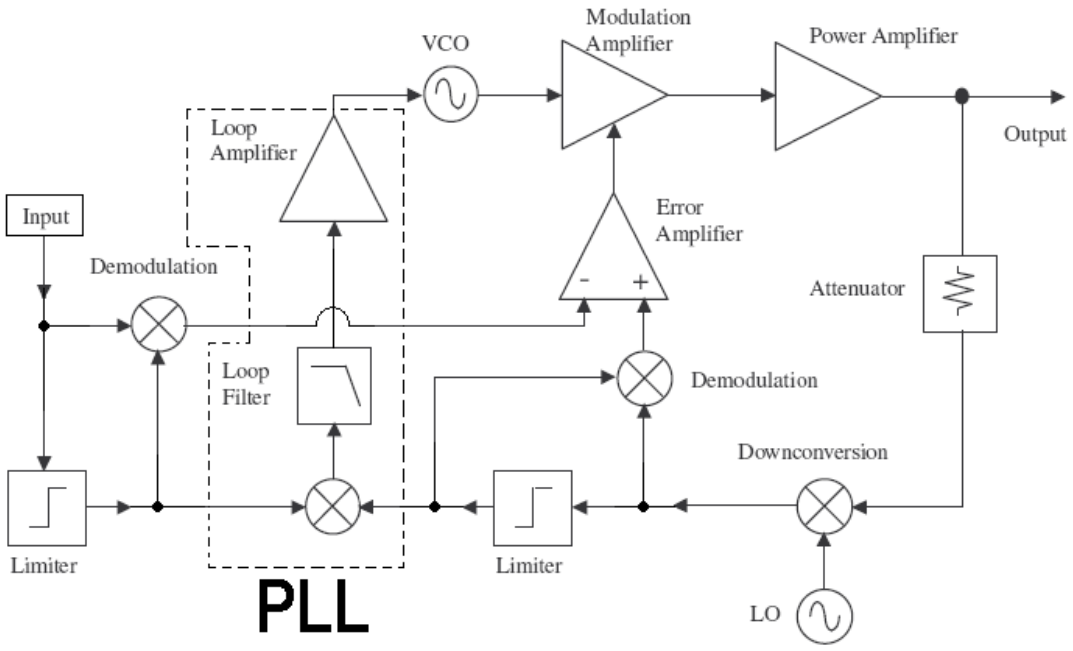


Figure 2.4: Polar Loop Feedback Transmitter [3]

2.1.4 Polar Loop Feedback

Polar Loop Feedback is an improved version of envelope feedback [3]. Envelope feedback can only compensate amplitude distortion but polar loop feedback can compensate both amplitude distortion and phase distortion. Polar loop feedback is also similar to cartesian loop feedback except that the envelope and phase are fed back rather than I and Q components. In polar loop feedback, envelope and phase comparison generally take place at an intermediate(IF) frequency [3]. Polar loop feedback typically linearizes a complete transmitter rather than a single power amplifier [3].

Polar loop feedback is depicted in Figure 2.4. As seen in the figure, the output signal is sampled and then downconverted to a convenient intermediate frequency(IF) by the local oscillator(LO). The resulting IF signal is resolved into its amplitude and phase(polar form) by the demodulator and limiter, respectively. (The limiter sets the amplitude of the signal to a constant value so that it removes the amplitude modulation and amplitude information of the signal.) At the input side the input signal is also resolved into its amplitude and phase by the demodulator and limiter, respectively. An error amplifier compares the input and output signal amplitudes and as a result of this comparison, an amplitude error signal is obtained. This error signal controls a modulation amplifier. What the error signal does is to modulate the collector/drain voltage of the modulation amplifier. The phase signals of input and output are multiplied by a mixer. The resulting signal passes through a loop filter and then it is amplified by a loop amplifier. As a result of these operations, the phase error signal is obtained and this error signal controls a voltage controlled oscillator(VCO). Actually the mixer(acts as the phase detector), loop filter, loop amplifier and VCO form a phase locked loop(PLL) which tries to lock the phases of input and output signals. VCO gives the phase signal(constant amplitude, phase modulated signal) as the output. The amplitude modulation is obtained by modulating the collector/drain

voltage of the modulation amplifier by the amplitude error signal. The phase and amplitude signals are combined by the modulation amplifier. The resulting signal is amplified by the nonlinear power amplifier.

The polar loop feedback has some disadvantages. It contains a PLL in the phase feedback path. This PLL can have locking problems at low amplitude values and when abrupt changes occur in the phase [4]. Another problem with this method is that the required feedback bandwidths for the amplitude and phase components are different from each other for most modulation formats [4]. This limits the available loop gain to either the amplitude or phase path since one path will require a feedback bandwidth that reduces the available loop gain, while the other path may need a larger loop gain [4]. This effectively limits the overall linearity improvement [4].

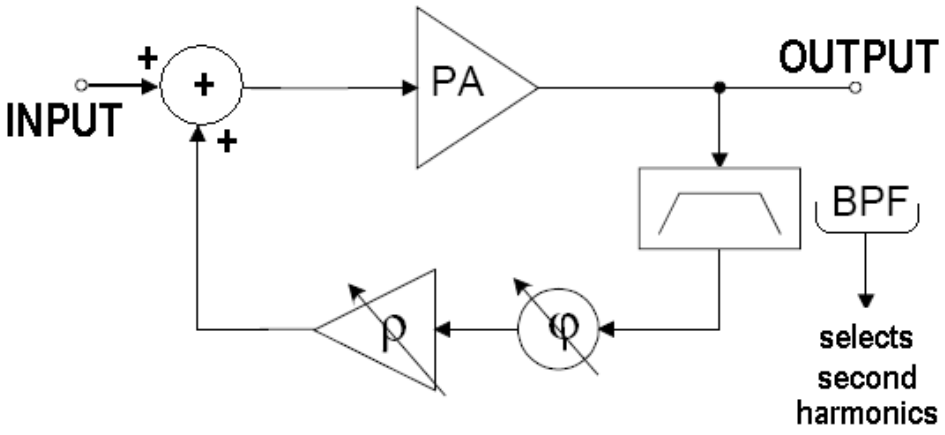


Figure 2.5: Second harmonic feedback with amplitude and phase adjustment [4]

2.1.5 Other Feedback Schemes

There is another form of feedback that can be called *distortion feedback*. In this technique, the distortion components at the output of the amplifier are fed

back to the input to achieve linearization. One example of distortion feedback is second harmonic feedback. In second harmonic feedback, the second harmonic signal produced at the PA output is fed back to the PA input to reduce third order intermodulation distortion. As the amplifier is nonlinear, an interaction occurs between the source signals and their fed-back second harmonics. If the amplitude and phase of the fed-back second harmonics are adjusted appropriately, the third order intermodulation distortion produced by the second harmonics and the original third order intermodulation distortion can be out of phase and equal in amplitude. As a result, ideally, the third order intermodulation distortion can be totally eliminated. However, this technique has some limitations. In order to get ideal elimination of the third order intermodulation, the phase and amplitude of the fed-back second harmonics must be accurately selected and very precisely adjusted. Even small mismatches in phase or amplitude will affect the elimination/reduction performance badly.

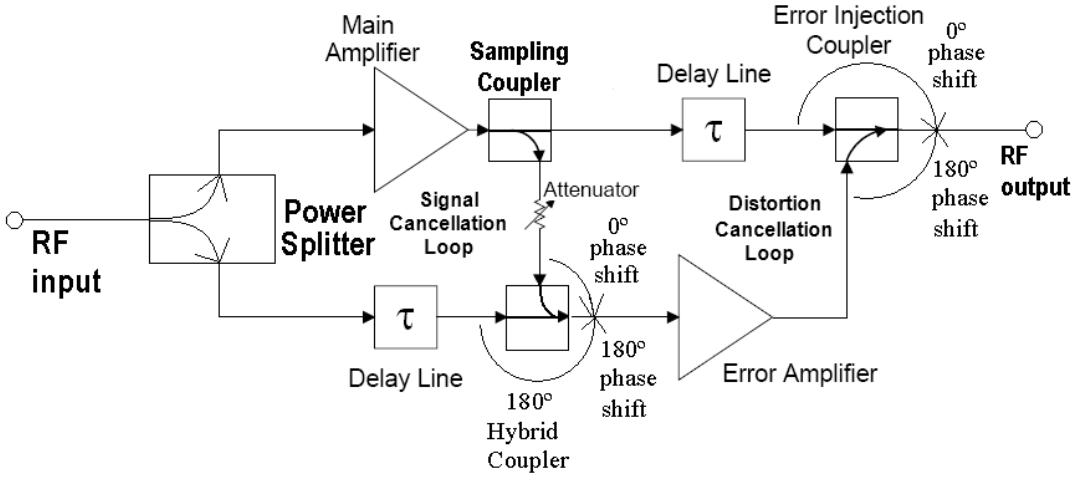


Figure 2.6: Feedforward linearization [4]

2.2 Feedforward

Feedforward is another linearization technique. It was invented by H. S. Black in 1928. In contrast to feedback it doesn't suffer from stability problems. It is unconditionally stable. As a result it can be used to linearize wideband signals. The theory behind this technique is simple but it can be rather costly to implement it in hardware [4].

Feedforward linearization technique is depicted in Figure 2.6. As seen in the figure the input signal is split into two paths by a power splitter(divider). The signal in the upper path goes to the nonlinear power amplifier to be linearized, which is denoted as main amplifier in Figure 2.6. The output of the amplifier contains the amplified input signal plus the distortion generated by the amplifier. This signal is sampled by a coupler and then goes to the 180° hybrid coupler passing through an attenuator. The signal in the lower path also goes to the same coupler after being delayed by a delay element. This delay is necessary to compensate for the delay introduced by the amplifier. These two signals are subtracted from each other by the 180° hybrid coupler and ideally the signal at the output of the coupler only contains the distortion generated by the amplifier. The main signal is cancelled. This signal at the output of the 180° hybrid coupler is generally called the error signal. This error signal is amplified by an amplifier which is denoted as error amplifier in Figure 2.6. The output of the error amplifier, which contains the amplified distortion components of the main amplifier, goes to the error injection coupler. A delayed version of the main amplifier output also goes to the error injection coupler. This second delay compensates for the delay introduced by the error amplifier. These two signals are subtracted from each other by the error injection coupler. Ideally this subtraction cancels the distortion introduced to the input signal by the main amplifier. So to sum

up it can be said that the first loop cancels the main signal and isolates the distortion of the main amplifier. In the second loop the isolated distortion is used to cancel the distortion of the main amplifier.

There are some issues that must be mentioned about feedforward linearization technique. Feedforward ideally cancels the distortion of the main amplifier completely but for this to occur, perfect gain matching is required in the signal and distortion cancellation loops. For gain matching in the signal cancellation loop, the total loss due to the sampling coupler and the attenuator must match the gain of the main amplifier. Also the delay of the delay line must match the group delay of the main amplifier to time align the main amplifier output and the signal in the lower path before subtracting them from each other. For gain matching in the distortion cancellation loop, the gain of the error amplifier must match the total loss due to sampling coupler, attenuator, hybrid coupler and error injection coupler to increase the error signal to the same level as the distortion component of the main amplifier output signal. Also the delay of the delay line must match the group delay of the error amplifier to time align the main amplifier output and error amplifier output before subtracting them from each other. When these conditions are not satisfied so that there is gain or delay mismatch in the system, complete cancellation of the main amplifier distortion will not occur. The system will have a finite distortion cancellation and the level of cancellation will depend on the level of gain/delay mismatch. The error amplifier in the system is a critical component for distortion cancellation. It must be highly linear so that it doesn't create additional distortion. It must provide sufficient gain. It must have a small group delay so that the required delay line length in the upper path is not large.

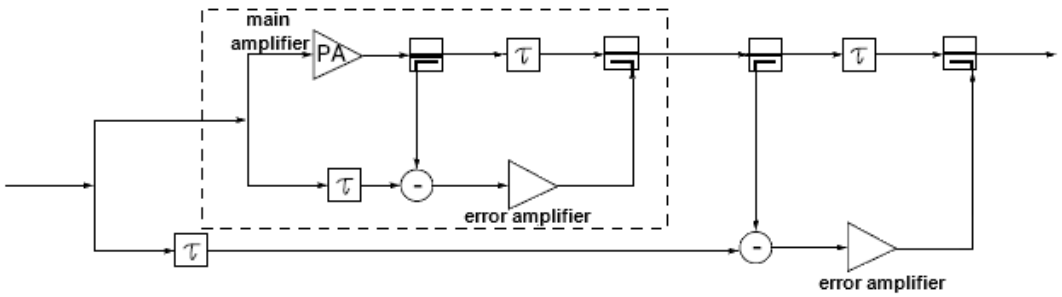


Figure 2.7: Multiple feedforward(2 loops) [1]

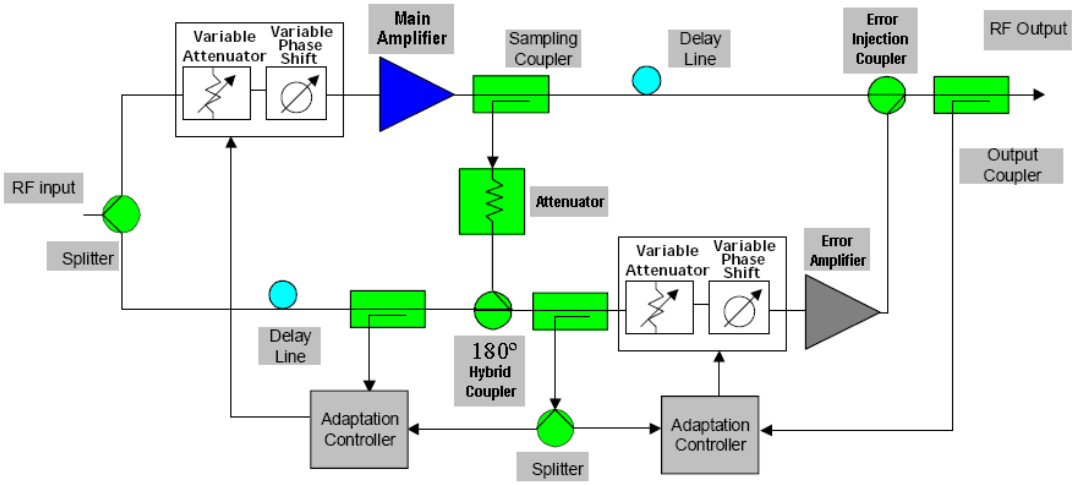


Figure 2.8: Adaptive feedforward [5]

The basic feedforward system shown in Figure 2.6 does not take the alterations that can occur in the element responses with aging and temperature changes into account. But such changes occur and this degrades the linearization performance. One way to reduce such effects is to use multiple feedforward loops as seen in Figure 2.7 [2]. In this configuration a feedforward loop acts as main amplifier and is placed within another feedforward loop. This process can be continued and 3, 4, etc. feedforward loops can be used. But this also increases the complexity of the system fast, which is a disadvantage. Another way is to make the system adaptive(Figure 2.8). With adaptation the linearization performance is under control and any change in the element responses can easily be accounted for. But adaptation has also a disadvantage. It introduces feedback to the system and this can result in stability and bandwidth problems.

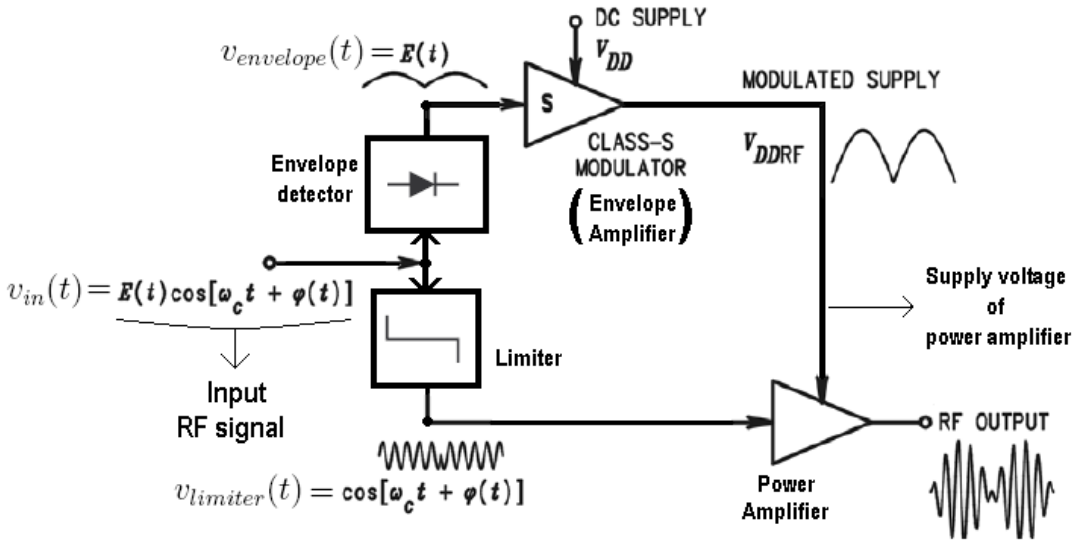


Figure 2.9: Envelope Elimination and Restoration Technique [6]

2.3 Envelope Elimination and Restoration

Envelope elimination and restoration is a technique which increases linearity and power efficiency simultaneously [3]. It depends on the principle that any narrow-band signal can be produced by simultaneous amplitude(envelope) and phase modulations [3]. Using this principle, the input RF signal is resolved into amplitude modulation and phase modulation components and they are combined back after amplification [3]. The block diagram of envelope elimination and restoration can be seen in Figure 2.9. The limiter in the figure extracts the phase information from the input signal and the envelope detector extracts the amplitude information. If the input RF signal is represented by $v_{in}(t) = E(t)\cos(w_c t + \varphi(t))$, the signal at the output of the limiter will be a constant amplitude phase modulated RF signal $v_{limiter}(t) = \cos(w_c t + \varphi(t))$ and the signal at the output of the envelope detector will be $v_{envelope}(t) = E(t)$, which is relatively low frequency with respect to w_c. The constant amplitude phase modulated RF signal is amplified by a highly nonlinear but efficient power amplifier. The nonlinearity of the power amplifier is no problem because the input signal is constant amplitude.

This power amplifier is chosen to have switched-mode operation so it is chosen to be of type class C, class D, class E or class F. The signal at the output of the envelope detector, the envelope signal, is amplified by the envelope amplifier. The output of the envelope amplifier, the amplified envelope signal, modulates the supply voltage of the switched-mode power amplifier. The envelope of the RF output of a switched-mode PA is directly proportional to its supply voltage [7]. So when the signal containing the phase information is given as input to the switched-mode power amplifier and the envelope signal modulates the DC supply of the power amplifier, they will be combined by the power amplifier and the output signal of the power amplifier will be an amplified replica of the amplitude and phase modulated input signal.

The envelope elimination and restoration can be employed to a complete transmitter or a single PA [3]. If it is used to design a transmitter, a DSP is typically utilized to generate the envelope and phase information [3]. Envelope elimination and restoration provides high efficiency and good linearity. The level of linearity does not depend on the power amplifier much because it is driven by a constant amplitude signal. A factor which affects the level of linearity is time alignment of the envelope and phase modulation signals. If they are misaligned in time, this will degrade the linearization performance. Another problem that can occur is that large envelope variations may drive the PA transistor bias into cutoff and this results in significant distortion [4].

It is possible to introduce feedback to envelope elimination and restoration technique. Examples of this are seen in the literature in [7] and [8]. In the proposed feedback procedure, envelopes of input and output signals are detected and compared with a differential amplifier and then the output of the differential amplifier modulates the final stage amplifier [3]. However the resulting feedback causes stability problems and poses a bandwidth limitation [3]. It also increases the complexity of the system [3].

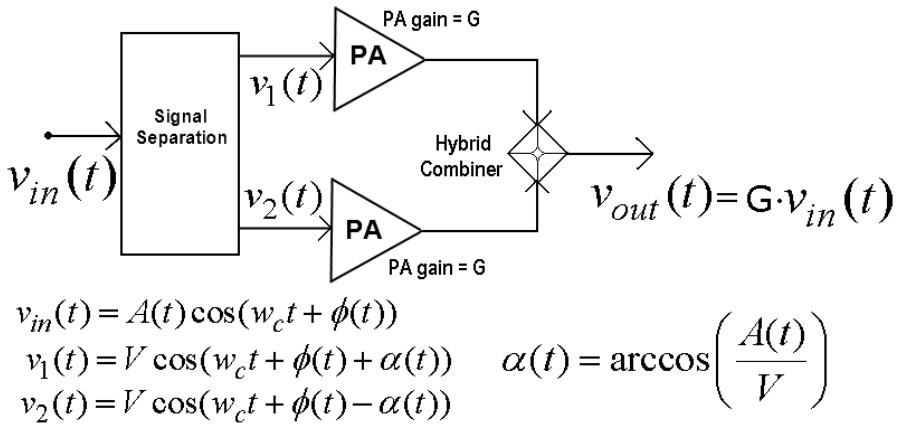


Figure 2.10: LINC technique [2]

2.4 LINC(Linear Amplification using Nonlinear Components)

LINC is another linearization technique. It stands for linear amplification using nonlinear components. Like the envelope elimination and restoration technique described previously, the LINC scheme avoids the nonlinear characteristic of the power amplifier by feeding it with a constant envelope signal. Also like envelope elimination and restoration, LINC can linearize a complete transmitter. A block diagram of LINC scheme is given in Figure 2.10. As seen in the figure, the amplitude and phase modulated input RF signal is split into two constant amplitude phase modulated signals [2]. These two signals are fed to identical power amplifiers. Power amplifiers amplify them by the same amount. The resulting amplifier outputs are combined and ideally an amplified replica of the input signal with no added distortion is obtained.

The separation of the input signal into two constant envelope signals needs explanation. Let the input RF signal be given by

$$v_{in}(t) = A(t)\cos(w_c t + \phi(t)) \tag{2.4}$$

where w_c is the carrier frequency, $A(t)$ is the amplitude modulation(envelope) and $\phi(t)$ is the phase modulation. As mentioned before, this input signal is split into two constant amplitude phase modulated signals $v_1(t)$ and $v_2(t)$, which are given by

$$v_1(t) = V\cos(w_c t + \phi(t) + \alpha(t)) \quad (2.5)$$

$$v_2(t) = V\cos(w_c t + \phi(t) - \alpha(t)) \quad (2.6)$$

where V is a constant which satisfies $V \geq \max(|A(t)|)$ and $\alpha(t)$ is given by $\alpha(t) = \arccos\left(\frac{A(t)}{V}\right)$. $v_1(t)$ and $v_2(t)$ satisfy the condition $v_1(t)+v_2(t) = 2v_{in}(t)$. As a result if $v_1(t)$ and $v_2(t)$ are amplified by identical power amplifiers and then combined, an amplified replica of the input signal is obtained. Also since $v_1(t)$ and $v_2(t)$ are constant envelope signals, the effects of the nonlinearity of the power amplifiers are avoided to a great extent.

The LINC scheme requires the implementation of the arccos function. The analog implementation of this function is difficult. But it can be more easily implemented in baseband by DSP techniques. As a result, the signal separation operation of LINC is generally implemented in baseband by DSP and then the resulting signals are upconverted to the necessary carrier frequency before amplification.

The LINC architecture has some disadvantages. It is quite sensitive to mismatches between the two signal paths in terms of I-Q imbalance in upconversion and power amplifier characteristics [1]. Especially power amplifier characteristics are important. The characteristics of the two power amplifiers used should be as identical as possible. Another problem with LINC is the bandwidth occupied by the separated signal components $v_1(t)$ and $v_2(t)$ [1]. According to [1], the bandwidth they occupy can be 10 or more times larger than the original bandwidth.

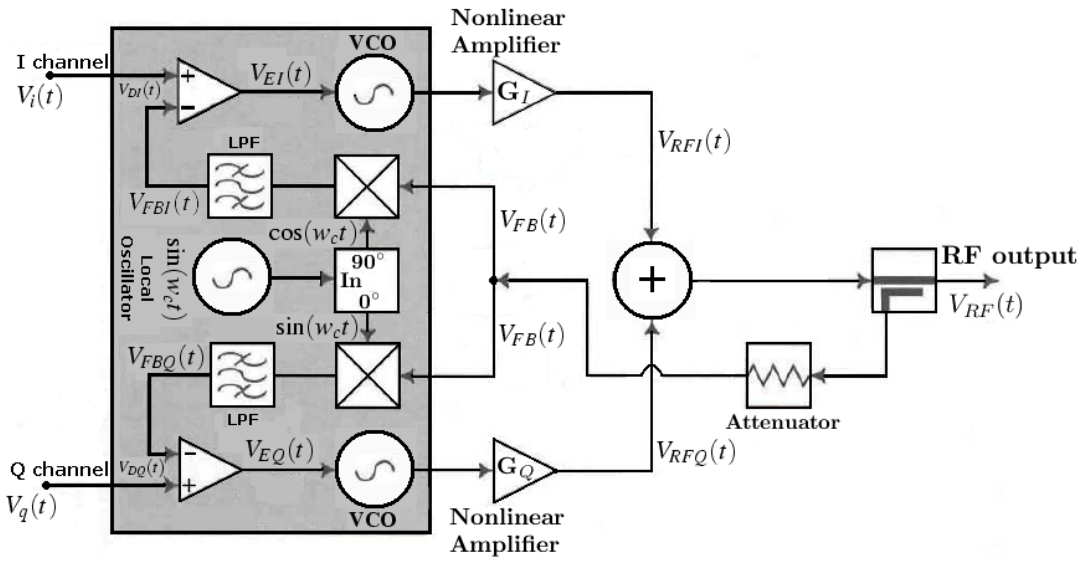


Figure 2.11: CALLUM block diagram [2]

2.5 CALLUM(Combined Analogue Locked Loop Universal Modulator)

CALLUM stands for combined analogue locked loop universal modulator. It is an improved version of LINC described in the previous section. It depends on the same basic principle of combining two amplified constant envelope components to form the output signal [9]. The way CALLUM generates the constant envelope components differs from LINC. It generates them by means of two feedback loops. Since there is feedback in CALLUM, it can compensate mismatches between the two nonlinear amplifiers and other imperfections in the transmitter. The block diagram of CALLUM is shown in Figure 2.11. As seen in the figure, CALLUM takes the input signal in Cartesian form and the feedback present in CALLUM is Cartesian feedback. The output signal is downconverted to baseband and demodulated to I and Q components. The resulting I and Q components of the output signal are fed back to input and compared with the I and Q components of the input signal. As a result of this comparison, two error signals are obtained,

one for I component and one for Q component. These error signals control two voltage controlled oscillators. The outputs of the voltage controlled oscillators are amplified by nonlinear power amplifiers and then the outputs of the two amplifiers are combined to form the RF output signal.

CALLUM contains feedback and as a result it suffers from the limitations of feedback. It suffers from stability problems. To ensure stability, it is limited to narrowband applications.

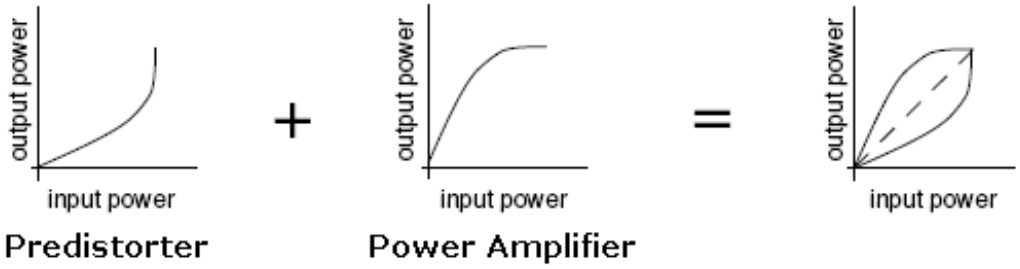


Figure 2.12: The basic idea of predistortion [1]

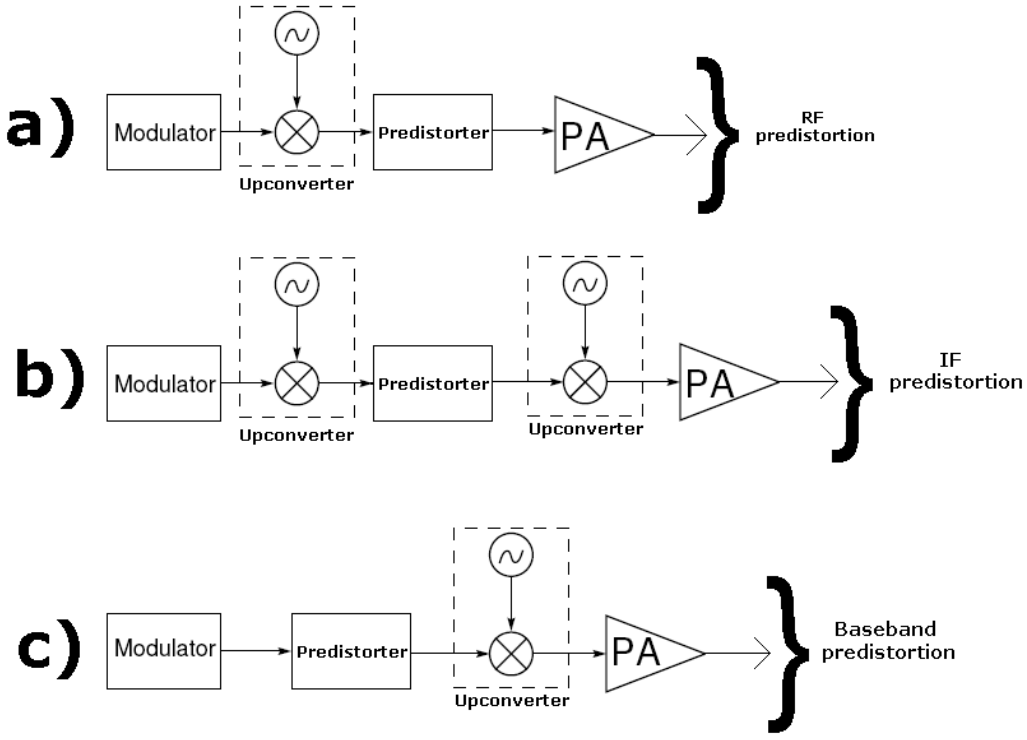


Figure 2.13: RF predistortion(a), IF predistortion(b), Baseband predistortion(c) [1]

2.6 Predistortion

Predistortion is one of the major linearization techniques. The basic idea of predistortion is to insert a nonlinear element which approximates the inverse of the characteristics of the power amplifier prior to the power amplifier so that the combined transfer characteristics of the two devices is linear. Figure 2.12 illustrates the underlying principle of predistortion. As observed in the figure, the transfer characteristics of the predistorter is the inverse of the transfer characteristics of the power amplifier. This results in a linear input-output relationship for the predistorter-amplifier combination. Predistortion can be divided into three main categories according to the position of the predistorter in the transmitter [1]:

- RF Predistortion
- IF Predistortion
- Baseband Predistortion

The position of the predistorter in the transmitter is shown in Figure 2.13 for these 3 cases. In RF predistortion, the nonlinear predistorting element/network operates at the final carrier frequency [2]. In IF predistortion, the predistorting element/network operates at a convenient intermediate frequency [2]. This allows the same design to be used for different carrier frequencies [2]. After predistortion, the signal is upconverted to the final carrier frequency. In baseband predistortion, predistortion is applied to the baseband signal to be transmitted. After predistortion, the baseband signal is upconverted to the final carrier frequency.

The characteristics of the power amplifier to be linearized by predistortion can be affected and changed by temperature changes, aging or output load changes. In such a case, to preserve linearity the characteristics of the predistorter should also change. This is achieved by making the predistortion system adaptive. By

using this criteria, predistortion can be further classified as *adaptive predistortion* and *non-adaptive predistortion* [1]. In adaptive predistortion, the information about the power amplifier output is used together with the input signal to adjust the predistortive characteristic [1]. Adaptation can be applied to RF predistortion, IF predistortion and baseband predistortion but it is more commonly applied to baseband predistortion. Baseband predistortion with adaptation is called adaptive baseband predistortion and it is a very popular linearization technique nowadays.

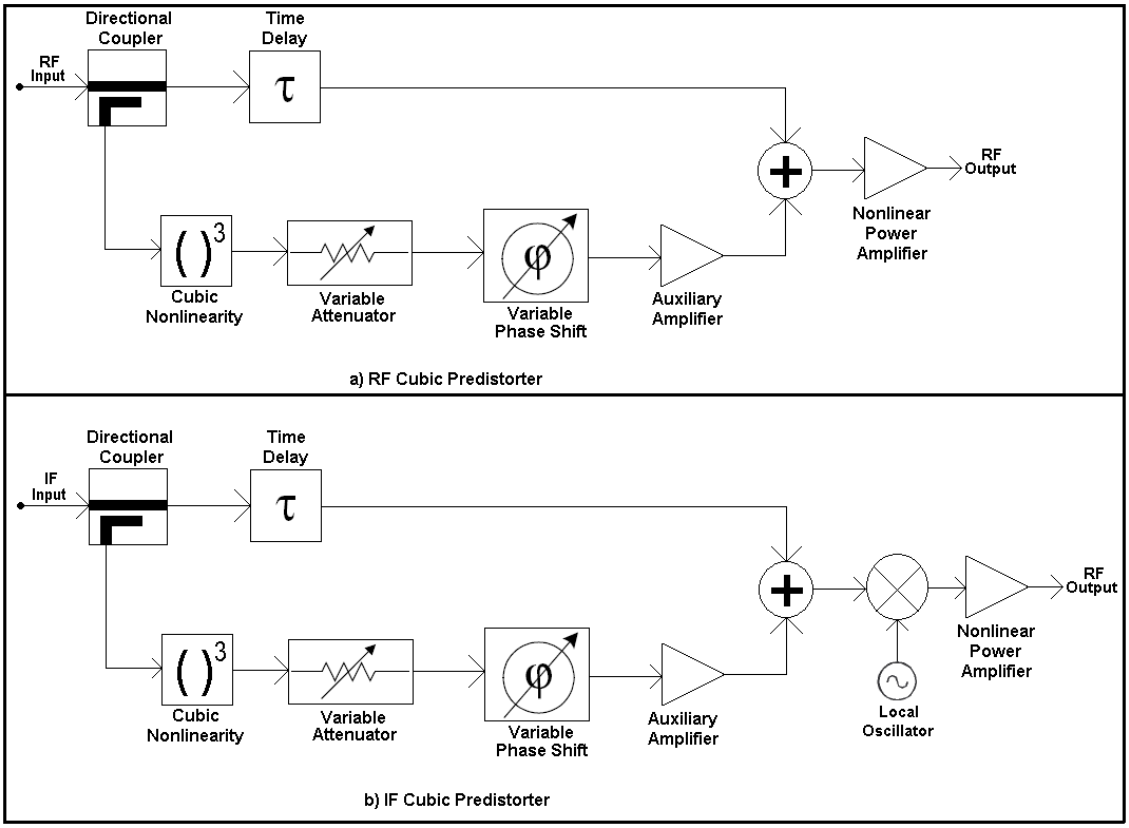


Figure 2.14: (a)RF Cubic Predistorter, (b)IF Cubic Predistorter [1]

2.6.1 RF/IF Predistortion

RF and IF predistortion are similar in operation. In RF predistortion, the predistorter operates at the final carrier frequency and works directly on the power amplifier input signal. Due to its high frequency of operation, it is difficult to

make it adaptive [1]. So RF predistorters are generally not adaptive. Because of this, the nonlinearity to be cancelled must be known in advance [3]. One of the main advantages of RF predistortion is its simple implementation.

IF predistortion operates at an intermediate frequency. This allows the use of the same predistorter for different RF carrier frequencies. Moreover, lowering the predistorter's frequency of operation allows to use some elements which cannot work with RF signals [1].

The fundamental advantage of RF/IF predistortion is their ability to linearize the entire bandwidth of an amplifier [2]. Because of this, they are ideal to use in wideband multicarrier systems such as satellite amplifiers or base-station applications [2].

The degree of linearity improvement provided by RF/IF predistortion mainly depends on the transfer characteristic of the power amplifier [2]. The better behaved the transfer characteristic is, the greater the degree of improvement which can be achieved and maintained over a variety of input conditions [2].

The main aim in RF/IF predistortion is to implement a circuit with a transfer function which approximates the inverse of the transfer characteristic of the power amplifier so that the combination of the two will produce a linear input-output relationship. This is not a trivial task and a large number of different networks have been utilized over the years for this purpose [2]. One famous and widely used configuration is the RF/IF cubic predistorter shown in Figure 2.14. It is based on 3^{rd} order intermodulation product cancellation [1]. As seen in the figure, the input signal is split into two paths. The first path only delays the input signal. This delay accounts for the delays in the second path and achieves synchronization between the two paths. In the lower path, there exist a cubic(3^{rd} order) nonlinearity, variable phase shifter and attenuator and an auxiliary amplifier. The cubic nonlinearity provides a compressive

input-output characteristic. The phase shifter and attenuator adjust the phase and amplitude to achieve cancellation of the distortion. The auxiliary amplifier compensates for the significant attenuation introduced by the cubic element [1]. The input power level to this amplifier is low and as a result it doesn't create additional distortion. By proper adjustment of the phase, the compressive characteristic provided by the cubic nonlinearity is subtracted from the input signal to obtain an expansive characteristic. This expansive characteristic will compensate for the compressive characteristic of the power amplifier. It is better to explain this mathematically. The upper path will provide(assuming it is synchronized with the lower path) $v_{upper} = a_1 v_{in}$. The lower path will provide $v_{lower} = a_2 v_{in} - b v_{in}^3$(Compressive Characteristic). When the signal of the lower path is subtracted from the signal of the upper path, the output signal of the predistorter is obtained, which is given by $v_{pd} = (a_1 - a_2) v_{in} + b v_{in}^3$. This is an expansive characteristic with a linear gain of $a_1 - a_2$ and it can be used to predistort any compressive amplifier characteristic by appropriate choice of a_1, a_2 and b [2].

There are various ways to implement the cubic nonlinearity in the cubic predistorter. It is generally implemented by using a single diode or a pair of anti-parallel diodes or by using FET transistors. Several examples using diodes and FET's can be found in [2].

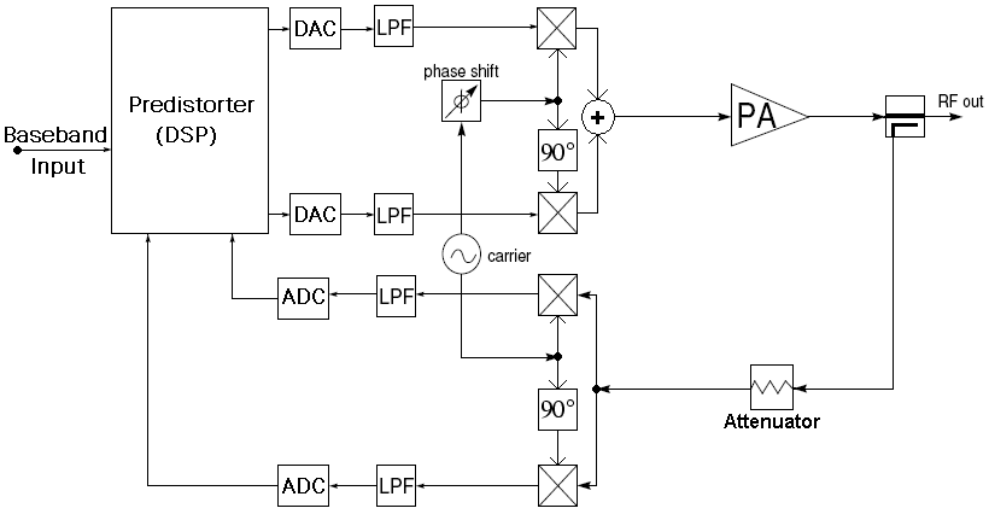


Figure 2.15: Adaptive digital baseband predistortion [1]

2.6.2 Baseband Predistortion

In baseband predistortion, the predistorter operates at baseband frequencies. This is an advantage because it is much simpler to implement the nonlinear inverse characteristic at baseband. The implementation of baseband predistorters is generally done in digital manner using digital signal processing technology. Digital Signal Processors(DSP), FPGA's(Field Programmable Gate Arrays) or ASIC's(Application Specific Integrated Circuits) serve as the main part of the baseband predistortion system [1]. As a result baseband predistortion generally takes the form of digital baseband predistortion and when the word ***baseband predistortion*** is used, it is generally meant ***digital baseband predistortion***. One advantage of digital baseband predistortion is the fact that it is simple to make it adaptive. The adaptive version of digital baseband predistortion is called adaptive digital baseband predistortion. It is depicted in Figure 2.15. As seen in the figure, the predistorter distorts the modulated signal. The output of the predistorter is converted to analog form by using D/A converters. The resulting signal is modulated onto the RF carrier and then amplified by the power amplifier. The power amplifier output is sampled, demodulated back into baseband, converted to digital form by using A/D converters and used to adapt the predistorter characteristic [1]. As both predistorter and amplifier introduce spectral regrowth, fast large-band data converters are needed [1].

Digital baseband predistorters can be classified by using different criteria. According to the position of the predistorter in the transmitter, digital baseband predistorters can be divided into two groups [1]:

- **Data Predistorters:** They try to compensate the deformation of the constellation diagram. They are simpler but they can't eliminate adjacent channel emissions. They are modulation-dependent.

- **Signal Predistorters:** They generally operate on the signal after modulation and baseband pulse shaping. Their adaptation is slower than data predistorters due to the wide range of signal amplitudes.

According to the form of predistortion characteristic, digital baseband predistorters have the following variants:

- **LUT(Look-up table) Predistortion:** The predistorter characteristic is stored in a look-up table. There are different approaches for the implementation of the look-up table. These will be explained later in this section. The addressing of the look-up table can be based on the amplitude or the power of the input signal.
- **Parametric Predistortion:** The predistorter is implemented as a nonlinear function. This function can be a polynomial, spline, Volterra serie etc. The most common form of parametric predistorters is polynomial predistorters.

In terms of adaptivity, the number of parameters to adapt in the case of parametric predistortion is generally significantly reduced with respect to LUT predistortion [1]. Because in parametric predistortion only the parameters of the nonlinear function has to be updated but in LUT predistortion every entry in the look-up table has to be updated.

According to their capability to work in the presence of power amplifier memory effects, the predistorters can be divided into two categories [1]:

- **Memoryless Predistorters:** They can't compensate for power amplifier memory effects. The predistortion characteristic has no memory. It depends only on the current value of the input.

- **Predistorters with memory:** They can compensate for power amplifier memory effects. The predistortion characteristic has memory. It not only depends on current value of the input but also depends on past values of the input.

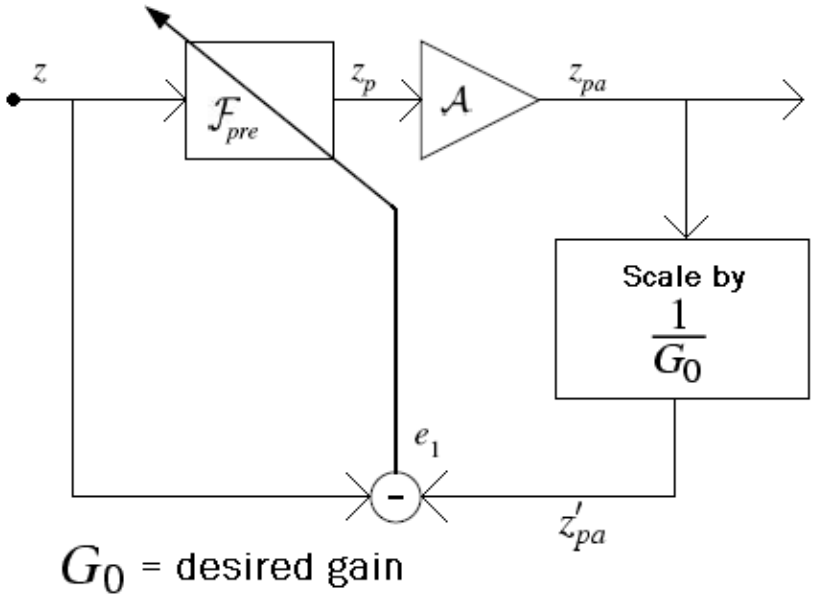


Figure 2.16: Direct Predistorter Adaptation [1]

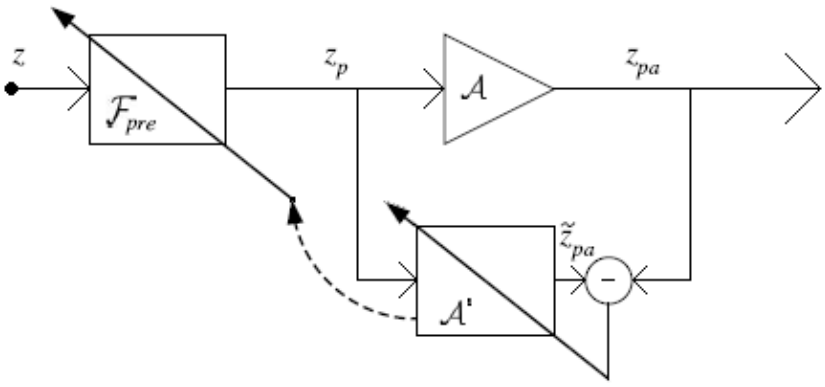


Figure 2.17: PA Modelling with Consecutive Inverse Estimation [1]

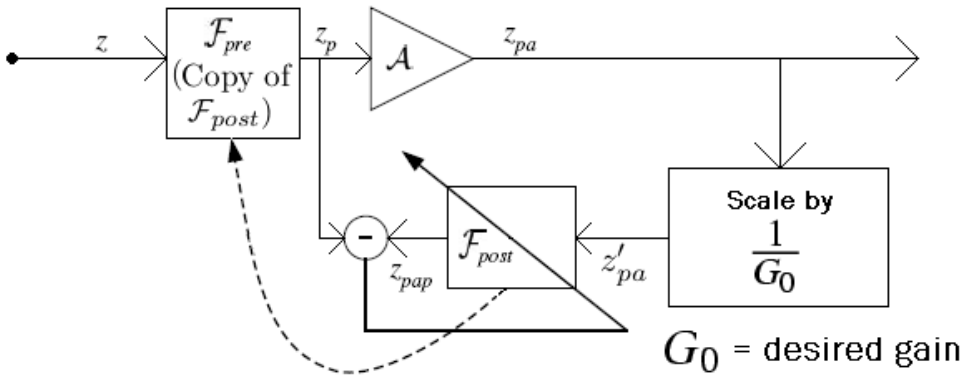


Figure 2.18: Predistortion using Postdistorter Adaptation(Indirect learning) [1]

The methods for digital baseband predistorter adaptation can be classified into 3 main groups [1]:

- **Direct predistorter adaptation(Figure 2.16)**
- **PA modelling with consecutive inverse estimation(Figure 2.17)**
- **Predistortion using postdistorter adaptation(Figure 2.18)**

In the direct predistorter adaptation architecture, the predistorter is adjusted in order to minimize the error between the attenuated output of the amplifier z'_{pa} and the original input signal z [1]. The observations that are used to obtain the predistorter function are z and $\mathcal{A}(\mathcal{F}_{pre}(z))$ [1]. As $\mathcal{A}$ is a nonlinear function, $\mathcal{F}_{pre}$, which should be the inverse of $\mathcal{A}$, can't be written explicitly from these observations and it has to be derived by classical iterative optimization techniques [1].

The second predistorter adaptation architecture, shown schematically in Figure 2.17, basically consists of 2 steps [1]. First, the power amplifier input z_p and output z_{pa} are used to calculate the power amplifier characteristic estimate $\mathcal{A}'$ and then this forward power amplifier model is used to calculate the power amplifier inverse $\mathcal{F}_{pre}$ [1].

The third possible way to adapt the predistorter, shown schematically in Figure 2.18, is based on the direct identification of the power amplifier inverse using the input and attenuated output of the power amplifier [1]. It can be viewed as searching for the equivalent post-distortion system $\mathcal{F}_{post}$ with the optimal solution $\mathcal{F}_{post}\left(\frac{\mathcal{A}(z_p)}{G_0}\right) = z_p$ or equivalently $\mathcal{F}_{post}(z) = A^{-1}(G_0 z)$ [9]. The predistorter characteristic $\mathcal{F}_{pre}$ is an exact copy of $\mathcal{F}_{post}$. $\mathcal{F}_{post}$ is obtained by iterative error minimization techniques and when $\mathcal{F}_{post}$ is obtained, this means that $\mathcal{F}_{pre}$ has also been obtained.

All of the adaptation methods described above can be applied to both LUT predistorters and parametric predistorters but in this thesis the discussion will only concentrate on predistorters using direct predistorter adaptation. The following sections describe different direct predistorter adaptation algorithms published in the literature for LUT and memoryless polynomial predistorters.

2.6.2.1 LUT Predistorters that use direct predistorter adaptation

Direct predistorter adaptation is the most commonly used adaptation method for LUT predistorters. The LUT-based predistorters can be classified as mapping predistorters and gain-based predistorters. Gain-based predistorters can be further classified as polar predistorters and complex gain predistorters.

Mapping Predistorter : Figure 2.19 shows the block diagram of a mapping predistorter. The mapping predistorter was first reported by Nagata in [10]. In this method, a two-dimensional look-up table is used to map any complex input signal represented by its cartesian components to a new complex signal in cartesian form. The mapping is done by summation. The sum of the input signal and the look-up table output approximates the inverse characteristics of the power amplifier, thereby canceling the distortion at the power amplifier output [11]. Adaptation, delay estimation and adjustment is also present in the system. For

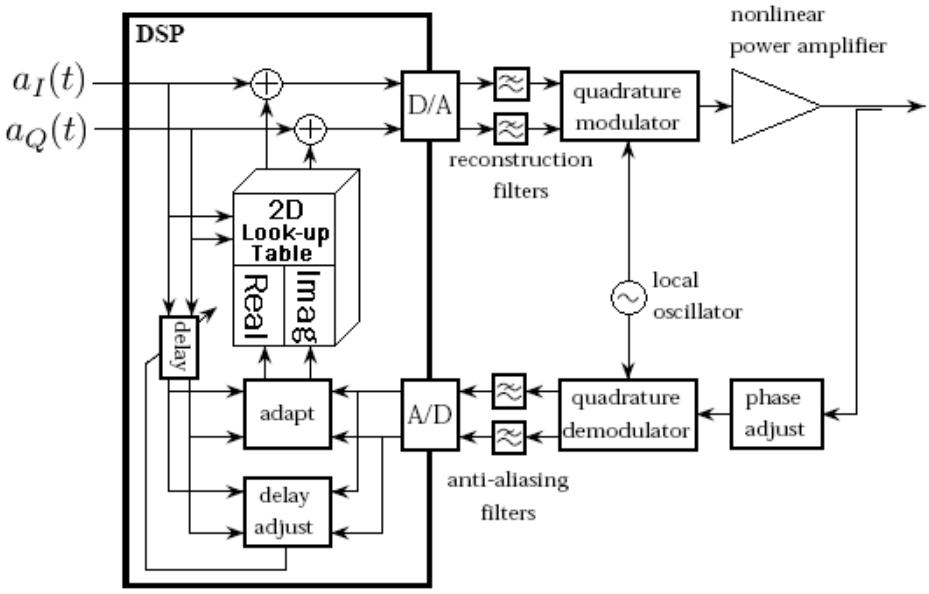


Figure 2.19: Mapping predistorter block diagram [9]

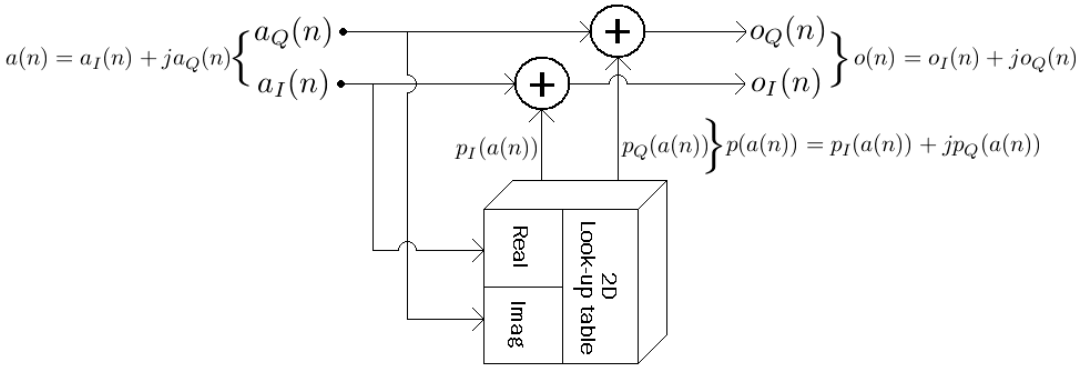


Figure 2.20: Mapping done by mapping predistorter

the purpose of adaptation, the amplifier output signal is synchronously demodulated and compared with the input signal [9]. The table entries are updated according to the results of this comparison. The details of the update algorithm will be described later in this section. Nagata also provided an algorithm for delay estimation and adjustment. The details of the algorithm can be found in [10]. The delay element in the DSP part of the system is necessary to correctly align the input signal and the fed-back demodulated amplifier output signal.

Figure 2.20 shows a closer look at the mapping operation of the predistorter. In the figure, $a(n)$ is the predistorter input, $p(a(n))$ is the correction generated

by the predistorter and $o(n)$ is the output signal. As seen in the figure, the predistortion is done in cartesian form. The following relations hold between $a(n), p(a(n))$ and $o(n)$:

$$\begin{aligned} a(n) &= a_I(n) + ja_Q(n) \\ p(a(n)) &= p_I(a(n)) + jp_Q(a(n)) = p_I(a_I(n), a_Q(n)) + jp_Q(a_I(n), a_Q(n)) \\ o(n) &= o_I(n) + jo_Q(n) \\ o(n) &= a(n) + p(a(n)) = a(n) + p(a_I(n), a_Q(n)) \quad (2.7) \\ o_I(n) &= a_I(n) + p_I(a(n)) = a_I(n) + p_I(a_I(n), a_Q(n)) \quad (2.8) \\ o_Q(n) &= a_Q(n) + p_Q(a(n)) = a_Q(n) + p_Q(a_I(n), a_Q(n)) \quad (2.9) \end{aligned}$$

As mentioned in equations (2.7), (2.8) and (2.9), the I component and Q component correction values, p_I and p_Q, generated by the predistorter are functions of both the I and Q components of the input signal,a_I and a_Q. These correction values reside in the 2D look-up table and they are indexed by using both the I and Q components of the input signal. In this way, the input complex plane is mapped to a predistorted complex plane by the 2D look-up table [1]. To achieve this, a large size LUT is necessary and this is one of the disadvantages of mapping predistorter. As a result of the large size LUT, the adaptation speed is slow and this is another disadvantage. The adaptation is achieved by using the simple algorithm given below [1]:

$$p_{ij}(m+1) = p_{ij}(m) + \mu \left(a(n) - \frac{a_{pa}(n)}{G} \right) \quad (2.10)$$

where m is the iteration number of the LUT cell which has index (i, j), $\mu \leq 1$ is the convergence constant, G is the desired amplifier gain, $a(n)$ is the predistorter input signal and $a_{pa}(n)$ is the corresponding fed-back demodulated amplifier output signal.

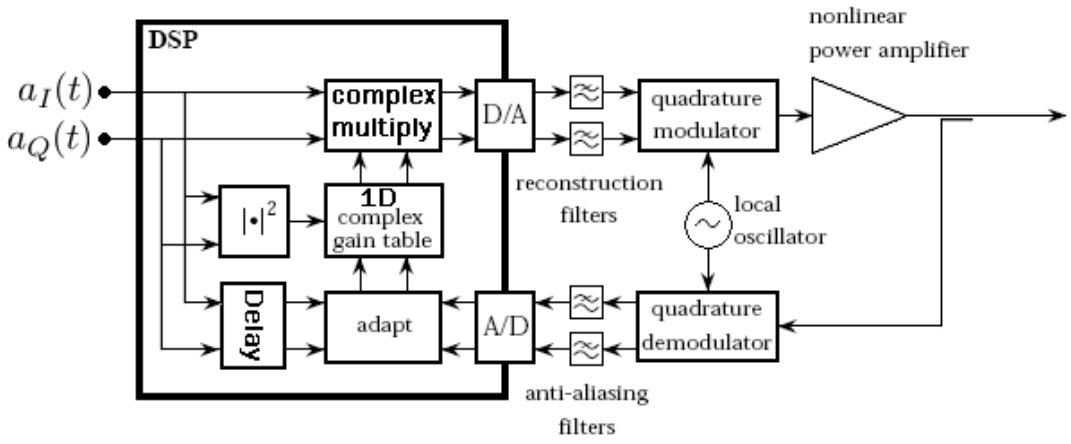


Figure 2.21: Complex Gain predistorter block diagram [9]

Complex Gain Predistorter : Figure 2.21 shows the block diagram of a complex gain predistorter. Complex gain predistorter was proposed by Cavers in [12]. In this approach, the LUT is one dimensional and it contains complex-valued gain values of the predistorter in cartesian(I,Q) format. The gain values of the predistorter have to be complex because the PA characteristic contains both amplitude and phase effects [1]. The predistortion is achieved by complex multiplication of the input signal and the corresponding predistorter gain in cartesian format. Since the LUT is one dimensional, its size is reduced compared to the mapping predistorter case. The LUT is addressed by the squared magnitude(power) of the input signal which gives a uniform distribution in power of the table entries [9]. The gain of the complex gain predistorter depends on the squared input magnitude(input power). If $z(n)$ denotes the input signal to the predistorter and $F_{pre}(|z(n)|^2)$ denotes the corresponding predistorter gain, the output of the predistorter will be $z(n)F_{pre}(|z(n)|^2)$ [1]. If the complex gain(complex envelope response) of the amplifier, which is a function of input power to the amplifier, is denoted by G and the desired linear gain is denoted by G_0, the following condition must be satisfied to achieve ideal linearization [1]:

$$z(n)F_{pre}\Big(|z(n)|^2\Big)G\left(|z(n)|^2\Big|F_{pre}\Big(|z(n)|^2\Big)\Big|^2\right) = G_0 z(n) \tag{2.11}$$

To satisfy the condition given in equation (2.11), the complex gains in the predistorter LUT must be adjusted adaptively. For this purpose, Cavers used two

different adaptation algorithms. They are secant adaptation algorithm and successive substitutions adaptation algorithm [1]. In the secant adaptation algorithm, the update rule is as follows [13]:

$$F_{pre,i}(k+1) = F_{pre,i}(k) + \alpha \frac{e(k)\Big(F_{pre,i}(k-1) - F_{pre,i}(k)\Big)}{e(k) - e(k-1)} \tag{2.12}$$

where α is a small iteration constant and k is the iteration index of the i^{th} LUT cell. In equation (2.12), $e(k)$ is the error signal for k^{th} iteration of i^{th} LUT cell and is given by $e(k) = z_{pa}(k) - G_0 z(k)$ where z_{pa} is the fed-back demodulated amplifier output, z is the predistorter input and G_0 is the desired linear gain [13]. To have this update, $|z(k)|^2$ must certainly fall in the range of predistorter entry $F_{pre,i}$.

In the successive substitutions adaptation algorithm, the update rule is as given below [1]:

$$F_{pre,i}(k+1) = F_{pre,i}(k)\left[1 - \mu\left(\frac{z_{pa}(k) - G_0 z(k)}{z_{pa}(k)}\right)\right] \tag{2.13}$$

where μ is a convergence constant smaller than 1.

Polar Predistorter : Figure 2.22 shows the block diagram of a polar predistorter. In polar predistortion, there are two one dimensional LUTs. One of these LUTs contains the magnitude gain values and the other LUT contains the phase rotation values. So in polar predistortion the complex gain of the predistorter is stored in polar form and in this way it differs from the complex gain predistorter which stores the complex gain values in cartesian form. Like the complex gain predistorter, predistortion is achieved by complex multiplication but before the multiplication, the magnitude gain and phase rotation output by the LUTs must be converted from polar to rectangular form. Also for the adaptation updates, the input signal and the fed-back demodulated amplifier output signal must be converted from rectangular to polar form. So rectangular to polar and polar to rectangular transformations are necessary and this increases the computational load. This is a disadvantage of the polar predistorter. The indexing of the LUTs

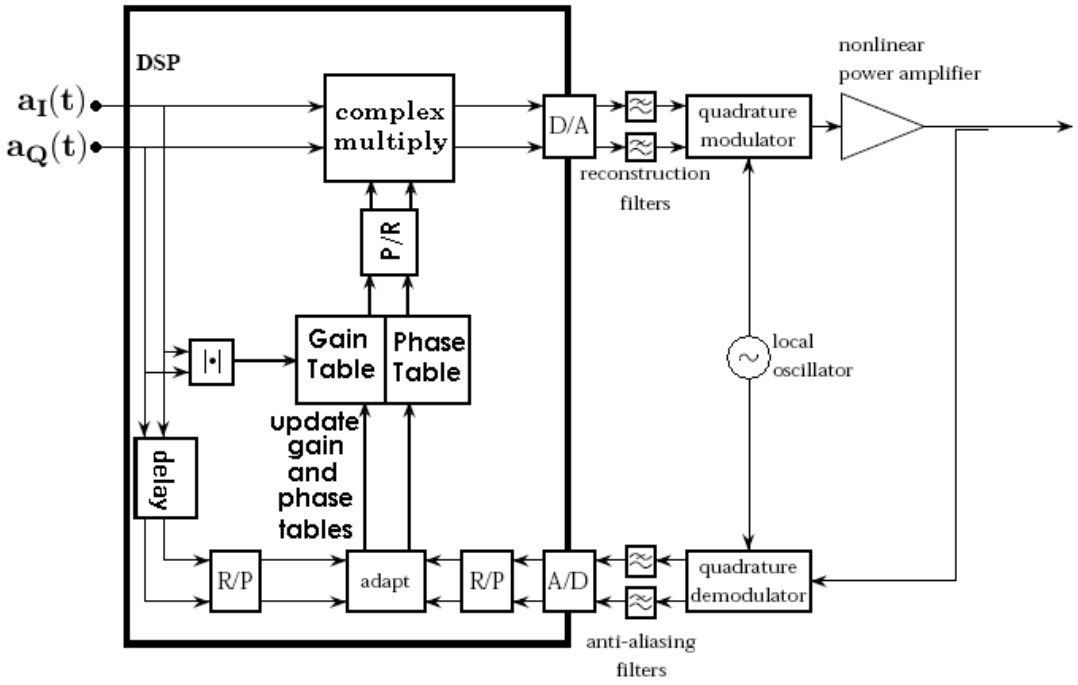


Figure 2.22: Polar Predistorter block diagram

is done by using the magnitude of the input signal. Different algorithms can be used for the adaptation of polar predistorters. A very simple algorithm is suggested in [14] and it is explained below:

The magnitude gain table characteristic is denoted by g_{pre}.

The phase table characteristic is denoted by θ_{pre}.

$$g_{pre,i}(m+1) = g_{pre,i}(m) + \mu_g\Big(G_0|z(n)| - |z_{pa}(n)|\Big) \tag{2.14}$$

$$\theta_{pre,i}(m+1) = \theta_{pre,i}(m) + \mu_\theta\Big(\arg(z(n)) - \arg(z_{pa}(n))\Big) \tag{2.15}$$

where G_0 is the desired linear gain, $z(n)$ is the input signal to the predistorter, $z_{pa}(n)$ is the fed-back demodulated amplifier output signal, μ_g is the positive convergence constant for amplitude correction, μ_θ is the positive convergence constant for phase correction and m is the iteration index of the i^{th} LUT cell.

g_{pre} and θ_{pre} depend on the magnitude of the input signal to the predistorter. So

if the input signal to the predistorter is $z(n)$, the output signal will be:

$$g_{pre}\Big(|z(n)|\Big)|z(n)|\exp\left(j\left(\angle z(n)+\theta_{pre}(|z(n)|)\right)\right)$$

2.6.2.2 Memoryless Polynomial Predistorters that use direct predistorter adaptation

Like LUT predistorters, direct predistorter adaptation is generally used for adaptation of memoryless polynomial predistorters. Memoryless polynomial predistorters can be classified as complex polynomial predistorters and polar polynomial predistorters.

Complex Polynomial Predistorter : In complex polynomial predistorters, the complex gain of the predistorter is implemented by a polynomial with complex coefficients. The complex gain provided by the polynomial is a function of the magnitude of the input signal. If the complex gain provided by this kind of a predistorter is denoted by F_{pre}, it is given by [1]:

$$F_{pre}\Big(|z|\Big)=\sum_{k=0}^{N}a_k\big|z\big|^k \tag{2.16}$$

where N is the order of the polynomial predistorter, $|z|$ is the magnitude of the input signal to the predistorter and $a_k(k=0,1,2,\ldots,N)$ are the complex coefficients of the polynomial predistorter. As noted in the equation, order is another important parameter of the complex polynomial predistorter and as it gets larger, the predistorter will be more successful in combating the nonlinear distortion introduced by the power amplifier. If the input signal to the complex polynomial predistorter is denoted by $z(n)$, the corresponding output signal will be $z(n)F_{pre}\Big(|z(n)|\Big)=z(n)\sum_{k=0}^{N}a_k\Big|z(n)\Big|^k$.

Polar Polynomial Predistorter : In polar polynomial predistorters, both the amplitude and phase corrections are implemented by using polynomials [1]. In this approach, there are two polynomials with real coefficients. One of the

polynomials gives the magnitude gain of the predistorter. The other polynomial gives the phase shift introduced by the predistorter. In this way, the complex gain of the predistorter is implemented in polar form. Both polynomials are function of the magnitude of the input signal to the predistorter. If the input signal to the polar polynomial predistorter is denoted by z, magnitude gain of the polar polynomial predistorter is denoted by g_{pre} and phase shift of the polar polynomial predistorter is denoted by θ_{pre}, g_{pre} and θ_{pre} are given by [1]:

$$g_{pre}(r) = \sum_{k=0}^{N} a_k r^k = (\overline{A})^T \overline{R}_a \tag{2.17}$$

$$\theta_{pre}(r) = \sum_{k=0}^{M} p_k r^k = (\overline{P})^T \overline{R}_p \tag{2.18}$$

where $r = |z|$, $\overline{A} = [a_0\ a_1\ a_2\ a_3 \dots a_N]^T$, $\overline{R}_a = [1\ r\ r^2\ r^3 \dots r^N]^T$, $\overline{P} = [p_0\ p_1\ p_2\ p_3 \dots p_M]^T$, $\overline{R}_p = [1\ r\ r^2\ r^3 \dots r^M]^T$ and N and M are the orders of the magnitude and phase polynomials. N and M don't have to be the same. They can take different values. If the input signal to the polar polynomial predistorter is $z(n)$, the output signal will be $z(n) g_{pre}\Big(|z(n)|\Big) \exp\left(j\theta_{pre}\Big(|z(n)|\Big)\right)$.

In the literature there are different adaptation algoritms applied to complex and polar polynomial predistorters. The most common ones are LMS(least mean squares) and RLS(recursive least squares) algorithms. An example of a LMS algorithm applied to a polar polynomial predistorter can be found in [15]. In that paper, the LMS algorithm was applied to adaptation to minimize the mean square error between the desired amplifier output and the observed amplifier output in the presence of a polar polynomial predistorter before the amplifier. This resulted in the following update rule for magnitude gain and phase polynomials [15]:

$$\overline{A}(n+1) = \overline{A}(n) + \mu_a \overline{R}_a(n) \left[G_0 r(n) - \left| G\Big(r(n)(\overline{A}(n))^T \overline{R}_a(n)\Big) \right| r(n) \right]$$

$$\overline{P}(n+1) = \overline{P}(n) + \mu_p \overline{R}_p(n) \left[-\arg\left(G\Big(r(n)(\overline{A}(n))^T \overline{R}_a(n)\Big) \right) - (\overline{P}(n))^T \overline{R}_p(n) \right]$$

where n is the iteration index, $r(n)$ is the magnitude of the input signal to the predistorter at the n^{th} iteration, μ_a and μ_p are small positive convergence constants, G_0 is the desired linear gain, G is the complex gain of the amplifier which is a function of input magnitude, $\overline{R}_a(n) = [1 \;\; r(n) \;\; r(n)^2 \;\; r(n)^3 \ldots r(n)^N]^T$, $\overline{R}_p(n) = [1 \;\; r(n) \;\; r(n)^2 \;\; r(n)^3 \ldots r(n)^M]^T$ and $\overline{A}(n)$ and $\overline{P}(n)$ are the vectors defined in equations (2.17) and (2.18) which contain the coefficients of the magnitude gain and phase polynomials at the n^{th} iteration.

Chapter 3

EFFECTS of POWER AMPLIFIER NONLINEARITY in COMMUNICATION SYSTEMS and MODELING of THIS NONLINEARITY

This chapter describes effects and modeling of power amplifier nonlinearity. In the first section, common measures of power amplifier nonlinearity(1 dB compression point and third order intercept point) are described. The second section describes AM/AM and AM/PM responses which characterize the distortion of power amplifiers. Finally the third section describes common effects of power amplifier nonlinearity like harmonic distortion, intermodulation distortion, spectral regrowth, cross modulation and desensitization.

If a power amplifier is weakly nonlinear and has no memory(means that the output at time instant t depends only on the input at time instant t), its input-output relationship can be described by a polynomial with real coefficients:

$$y(t) = \sum_{n=1}^{\infty} c_n \left(x(t)\right)^n = c_1 x(t) + c_2 \left(x(t)\right)^2 + c_3 \left(x(t)\right)^3 + \cdots\cdots\cdots \qquad (3.1)$$

where c_1 is the linear small-signal gain of the amplifier, $x(t)$ is the input signal and $y(t)$ is the output signal. This polynomial model will be used in the following subsections to find formulas for 1 dB compression point and 3^{rd} order intercept point, which are common measures of amplifier nonlinearity. In those analyses, the polynomial will be truncated to order 3.

3.1 Common Measures of Power Amplifier Nonlinearity

In order to get a better understanding of the level of nonlinear distortion of a power amplifier, measures which characterize the nonlinear behaviour of the amplifier are defined [3]. Two commonly used measures to describe nonlinearities of a power amplifier are 1 dB compression point and third order intercept point [3]. In the following subsections, these two are described.

3.1.1 1 dB compression point($P_{1\,dB}$)

The 1 dB compression point is a measure for gain compression of the amplifier which occurs as the input power to the amplifier increases. It is defined as the power level where the gain of the amplifier deviates from the linear small signal gain by 1 dB. As the input power to an amplifier is increased, the amplifier enters its nonlinear region and the gain of the amplifier starts to decrease from its small signal value. When the compression in the gain reaches 1 dB, the 1 dB

compression point is reached. The 1 dB compression point($P_{1\,dB}$) can be input power($IP_{1\,dB}$) or output power($OP_{1\,dB}$) referred and is usually given in units of dBm [3]. Generally the output power at the 1 dB compression point($OP_{1\,dB}$) is used to represent the 1 dB compression point. To measure the 1 dB compression point, a single tone signal $x(t) = A\cos(w_0 t)$ is applied to the power amplifier and the amplitude A is increased from zero to higher values. If the nonlinear characteristic of the amplifier is given by (3.1) up to third order $\Big($ $y(t) = c_1 x(t) + c_2\left(x(t)\right)^2 + c_3\left(x(t)\right)^3$ where c_1 is the linear gain and c_2&c_3 represent the second and third order nonlinearities of the amplifier$\Big)$, the corresponding output signal will be :

$$y(t) = \frac{1}{2}c_2A^2 + (c_1A + \frac{3}{4}c_3A^3)\cos(w_0t) + \frac{1}{2}c_2A^2\cos(2w_0t) + \frac{1}{4}c_3A^3\cos(3w_0t) \quad (3.2)$$

The gain at the fundamental frequency is given by $c_1 + \frac{3}{4}c_3A^2$. c_3 is negative and as a result, when the input amplitude A increases, the gain decreases. For small values of A, $c_1 \gg \frac{3}{4}c_3A^2$ and as a result, a linear gain of c_1 is obtained. As A increases, the gain compresses and when it compresses by 1 dB, the 1 dB compression point is reached. At the 1 dB compression point,

$$20\log\left(\frac{c_1}{c_1 + \frac{3}{4}c_3A^2}\right) = 1 \quad (3.3)$$

From (3.3), the input and output signal amplitudes at the 1 dB compression point are :

$$A_{in\,1\,dB} = \sqrt{\frac{4}{3}\frac{|c_1|}{|c_3|}(1 - 10^{-\frac{1}{20}})} \quad (3.4)$$

$$A_{out\,1\,dB} = 10^{-\frac{1}{20}}c_1\sqrt{\frac{4}{3}\frac{|c_1|}{|c_3|}(1 - 10^{-\frac{1}{20}})} \quad (3.5)$$

By using (3.4), another useful equation is obtained :

$$|c_3| = \frac{4}{3}|c_1|\frac{1 - 10^{-\frac{1}{20}}}{A^2_{in\,1\,dB}} \quad (3.6)$$

If the 1 dB compression point and small signal gain c_1 are known, c_3 can be found by using (3.6).

Figure 3.1 illustrates the 1 dB compression point graphically.

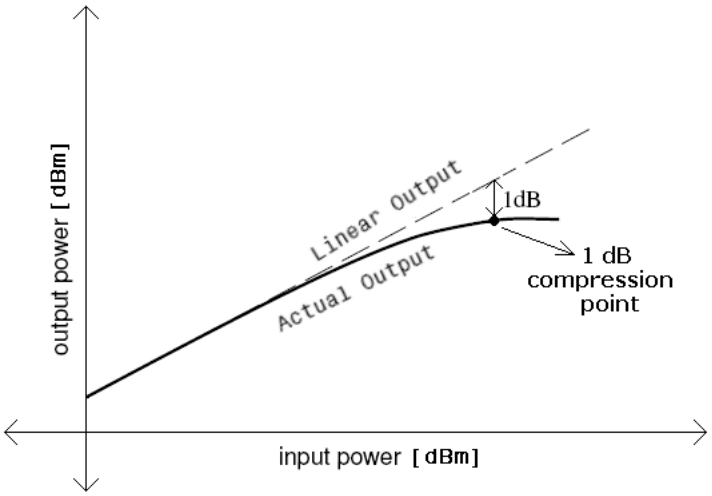


Figure 3.1: 1 dB compression point [1]

3.1.2 Third order intercept point(IP3)

When a two-tone signal $x(t) = A\cos(w_1 t) + A\cos(w_2 t)$ $(w_2 > w_1)$ is given as input to a nonlinear power amplifier, two main groups of distortion can be distinguished at the amplifier output - *intermodulation products* and *harmonics* [1]. The harmonics are produced at frequencies nw_1 and mw_2 (n, m are integers) which are multiples of the fundamental frequencies w_1 and w_2. The harmonic products are typically out-of-band and they can be eliminated by filtering. The intermodulation products are produced at frequencies $\pm nw_1 \pm mw_2$. Some of these intermodulation products cause problems because they are in-band meaning that they are close to the fundamental frequencies w_1 and w_2. Even-order intermodulation products $\Big(|n| + |m| \text{ even}\Big)$ are not so harmful because they are out-of-band and they can be eliminated by filtering. The odd-order intermodulation products $\Big(|n| + |m| \text{ odd}\Big)$ are more harmful because many of them are in-band. Among the odd-order intermodulation products, the third order intermodulation products at frequencies $2w_1 - w_2$ and $2w_2 - w_1$ have the most important influence because they are the intermodulation products which are closest to the fundamental frequencies w_1 and w_2. Since they are so close to fundamental frequencies, they can't be eliminated by filtering.

After defining third order intermodulation products, the third order intercept point can now be defined. It is the point where third order intermodulation products($2w_1 - w_2$ and $2w_2 - w_1$) at the amplifier output are equal in power to the fundamental components(w_1 and w_2) when the amplifier input is a two-tone signal$\Big(A\cos(w_1 t) + A\cos(w_2 t)\Big)$. Since both fundamental components and third order intermodulation products show compressive behaviour, this imaginary point is found by extrapolation from a plot of power of third order intermodulation products and power of the fundamental tones at the amplifier output versus input power per fundamental tone. This is illustrated in Figure 3.2. Figure 3.2 is a logarithmic plot. Both input and output powers are in dBm. As seen in the figure, before compression both the power of fundamental tones and third order intermodulation products increase linearly with increasing power. For high input powers compression occurs. If the linear portions of both curves are extrapolated and intersected as seen in the figure, the third order intercept point is obtained. In the linear portion of the power curves, the slope of the curve belonging to the third order intermodulation products is three times the slope of the curve belonging to the fundamental tones. This behaviour can be explained by using

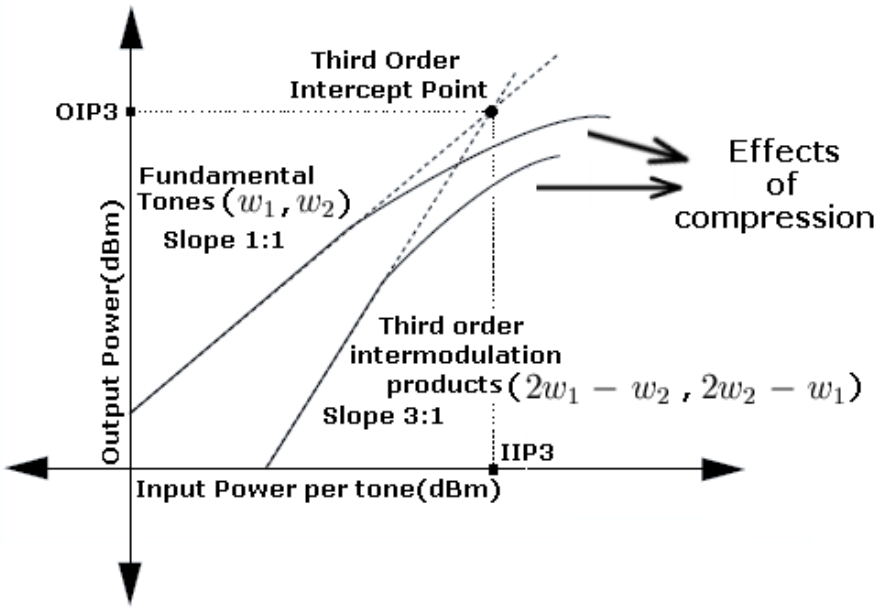


Figure 3.2: Third Order Intercept Point

the third order polynomial model which was used in the explaination of 1 dB compression point. In this case, the input $x(t)$ is $x(t) = A\cos(w_1 t) + A\cos(w_2 t)$ and the corresponding output $y(t) = c_1 x(t) + c_2 \left(x(t)\right)^2 + c_3 \left(x(t)\right)^3$ contains a lot of frequency components. The important ones are the frequency components at $w_1, w_2, 2w_1 - w_2$ and $2w_2 - w_1$. The amplitude of the frequency components at w_1, w_2 is $c_1 A + \frac{9}{4} c_3 A^3$. Since c_3 is negative, the term $\frac{9}{4} c_3 A^3$ causes compression and it is ignored in the calculations. The amplitude of the frequency components at $2w_1 - w_2, 2w_2 - w_1$ is $\frac{3}{4}|c_3|A^3$. At the third order intercept point, $c_1 A$ and $\frac{3}{4}|c_3|A^3$ should be equal to each other. By using this, the input amplitude at the third order intercept point is found as

$$A_{in\,IP3} = \sqrt{\frac{4}{3}\left|\frac{c_1}{c_3}\right|} \tag{3.7}$$

Since the amplitude of fundamental tones ($c_1 A$) is proportional to A and the amplitude of third order intermodulation products $\left(\frac{3}{4}|c_3|A^3\right)$ is proportional to A^3, in the logarithmic plot(Figure 3.2) the ratio of slopes becomes 3.

The third order intercept point can be input power or output power referred. If input power is used, it is called input third order intercept point and denoted by **IIP3**. If output power is used, it is called output third order intercept point and denoted by **OIP3**.

The 1 dB compression point and the third order intercept point are important parameters to characterize the nonlinearities of power amplifiers [1]. They are generally provided by the amplifier manufacturers and they can be obtained by relatively simple measurements$\Big($1-tone test[input : $A\cos(w_0 t)$] and 2-tone test[input : $A(\cos(w_1 t) + \cos(w_2 t))$]$\Big)$ [1]. Although these parameters give an idea about amplifier behaviour in single-tone or two-tone systems, they are not sufficient for modeling the effects of nonlinearity on modulated signals [1]. To model the effects of nonlinearity on modulated signals, the complex envelope

response of the amplifier given by *AM/AM* and *AM/PM* responses is used. In the following section, these two are described.

3.2 AM/AM and AM/PM characteristics

An ideal linear amplifier shows a linear input amplitude(power)-output amplitude(power) relationship and hence a constant gain. This is not the case in reality. As the input amplitude increases, the linear behaviour of the amplifier is disturbed, its gain compresses and starts to decrease. Figure 3.1 illustrates this behaviour. As seen in that figure, as the input amplitude(power) increases, the output amplitude(power) takes values smaller than the ideal linear value. This behaviour of the amplifier is called AM/AM distortion and it is described by AM/AM characteristics of the amplifier. Another important property of an ideal linear amplifier is that it applies a zero phase shift or a constant phase shift to the input signal as the input amplitude(power) changes. Again this is not the case in reality. As the input amplitude(power) increases, the phase shift applied to the input signal by the amplifier changes. This behaviour of the amplifier is called AM/PM distortion and it is described by AM/PM characteristics of the amplifier. Figure 3.3 shows an example AM/PM characteristics. By combining the AM/AM and AM/PM characteristics of the amplifier, the complex envelope response of the amplifier is obtained. The complex envelope response can be explained in mathematical terms as follows:

If the input signal to a power amplifier is

$$x(t) = A(t)\cos\Big(w_0 t + \phi(t)\Big) = \mathrm{Re}\Bigg(\underbrace{A(t)\exp\Big(j\phi(t)\Big)}_{\text{Input Complex Envelope}}\exp(jw_0 t)\Bigg) \tag{3.8}$$

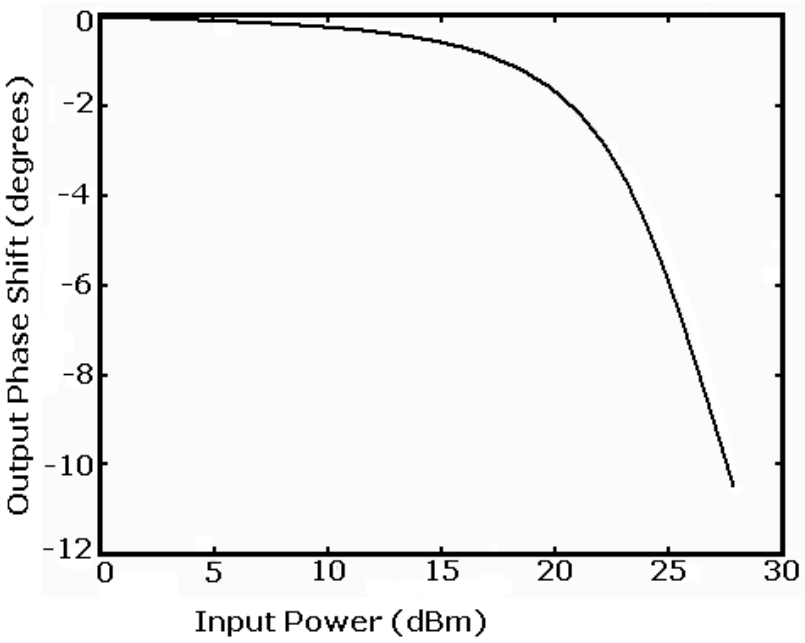


Figure 3.3: An example AM/PM characteristics

then the output signal is given by

$$y(t) = G(|A(t)|)\cos\Big(w_0 t + \phi(t) + \theta(|A(t)|)\Big) \tag{3.9}$$

$$= \mathrm{Re}\Bigg(\underbrace{\underbrace{G(|A(t)|)\exp\Big(j\theta(|A(t)|)\Big)}_{\text{Complex Envelope Response}}\exp\Big(j\phi(t)\Big)}_{\text{Output Complex Envelope}}\exp(jw_0 t)\Bigg) \tag{3.10}$$

In (3.10), $A(t)$ is the amplitude modulation of the input signal, $\phi(t)$ is the phase modulation of the input signal, $G\Big(|A(t)|\Big)$ is the AM/AM response of the amplifier, $\theta\Big(|A(t)|\Big)$ is the AM/PM response of the amplifier and the combination of AM/AM and AM/PM responses $G\Big(|A(t)|\Big)\exp\Bigg(j\theta\Big(|A(t)|\Big)\Bigg)$ is the complex envelope response of the amplifier. As observed in (3.10), the AM/AM and AM/PM responses depend only on the amplitude of the input signal. Both of them are only functions of amplitude of the input signal. Another observation in (3.10) is that the amplifier is assumed to be memoryless. Both AM/AM and AM/PM responses at time instant t depend only on the amplitude of the input signal at time instant t. For this assumption to be valid, the input signal $x(t)$ must be a narrowband signal. Otherwise if $x(t)$ is wideband, the AM/AM and

AM/PM responses will have memory and they will be affected by the past values of the input.

The AM/AM and AM/PM responses of a power amplifier can be measured by applying a single tone input signal to the amplifier and sweeping the power of this input signal. A model can then be fitted to the measured data [1]. There are some famous models in the literature used for modeling power amplifier AM/AM and AM/PM responses. These are Saleh model, Rapp model, third order polynomial model and arctan model.

3.2.1 Saleh model

Saleh model uses the following 2 functions to model AM/AM and AM/PM responses of a power amplifier [16]:

$$\underbrace{G(|x|)}_{\text{AM/AM response}} = \left\{ \begin{array}{ll} \dfrac{\alpha_a|x|}{1+\beta_a|x|^2} & \text{if } |x| \leq \dfrac{1}{\sqrt{\beta_a}} \\ \dfrac{\alpha_a}{2}\dfrac{1}{\sqrt{\beta_a}} & \text{if } |x| > \dfrac{1}{\sqrt{\beta_a}} \end{array} \right\} \quad \underbrace{\theta(|x|)}_{\text{AM/PM response}} = \frac{\alpha_p|x|^2}{1+\beta_p|x|^2} \tag{3.11}$$

where x is the complex envelope of the input signal(so $|x|$ corresponds to the amplitude of the sinusoidal input signal). As seen in (3.11), the Saleh model has four parameters $\alpha_a, \beta_a, \alpha_p$ and β_p. The parameter α_a is the linear small-signal gain. The parameter β_a controls how fast the gain of the amplifier compresses as the input amplitude increases. The AM/AM response saturates when the input amplitude reaches the value $1/\sqrt{\beta_a}$. At that point, the output amplitude takes the value $\dfrac{\alpha_a}{2}\dfrac{1}{\sqrt{\beta_a}}$ and stays constant at that value even if the input amplitude increases further. So the maximum value that the output amplitude can take in Saleh model is $\dfrac{\alpha_a}{2}\dfrac{1}{\sqrt{\beta_a}}$. The parameters α_p and β_p control how the phase shift of the amplifier changes as the input amplitude changes. From (3.11), as the input amplitude $|x| \to \infty$, the phase shift $\to \dfrac{\alpha_p}{\beta_p}$. So the maximum value that the phase shift can take in Saleh model is $\dfrac{\alpha_p}{\beta_p}$. Figure 3.4 shows an example

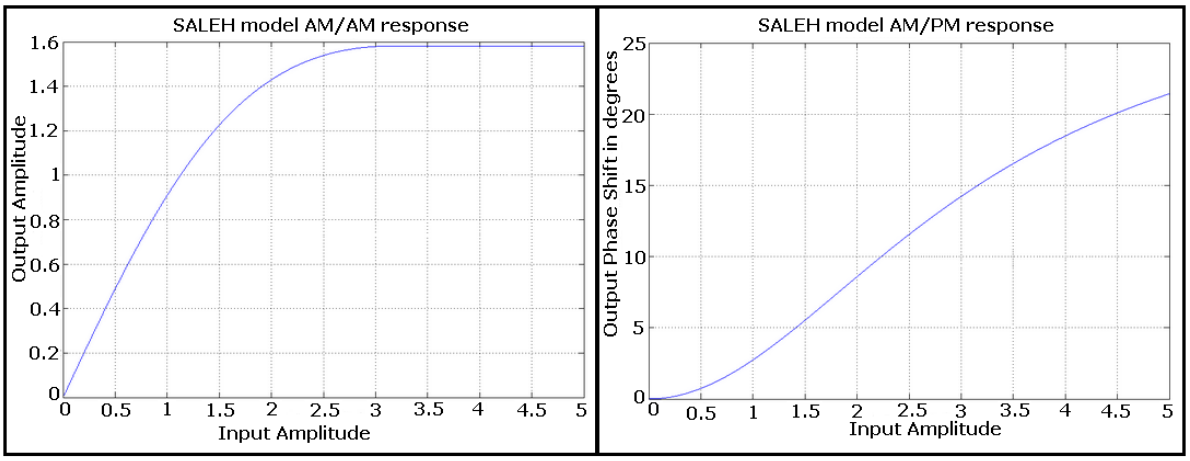


Figure 3.4: Saleh model AM/AM and AM/PM responses
($\alpha_a = 1, \beta_a = 0.1, \alpha_p = \frac{\pi}{60}, \beta_p = 0.1$)

of AM/AM and AM/PM responses of Saleh model for the following parameter values: $\alpha_a = 1,\ \beta_a = 0.1,\ \alpha_p = \frac{\pi}{60},\ \beta_p = 0.1$.

3.2.2 Rapp model

The Rapp model only models the AM/AM response of the amplifier. It assumes that the amplifier does not apply any phase shift to the input signal. The Rapp model AM/AM response is given by the following function [17]:

$$\underbrace{G(|x|)}_{\text{AM/AM response}} = \frac{v|x|}{\left(1 + \left(\frac{v|x|}{A_0}\right)^{2p}\right)^{\frac{1}{2p}}} \quad \text{where } x \text{ is the complex envelope of the input} \tag{3.12}$$

signal. As noted in (3.12), the Rapp model has three parameters $v,\ A_0$ and p . The parameter v is the linear small-signal gain [17]. The parameter p is the smoothness factor [17]. It controls the smoothness of the transition of the AM/AM response from the linear region to the limiting region [17]. As it increases, the smoothness of the transition decreases and the transition becomes more abrupt. The parameter A_0 is the limiting output amplitude [17]. From (3.12), as the input amplitude $|x| \to \infty$, the AM/AM response(output amplitude) $\to A_0$. So

A_0 is the maximum value that the AM/AM response of the Rapp model can take. Figure 3.5 shows an example of AM/AM response of Rapp model for the

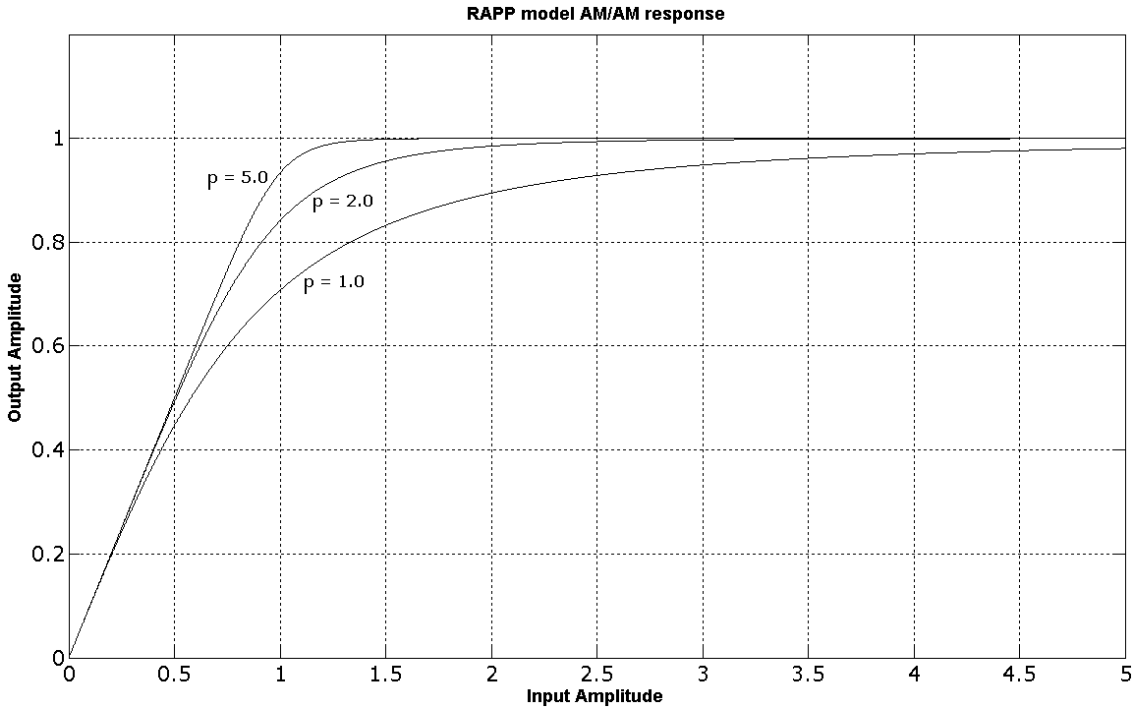


Figure 3.5: Rapp model AM/AM response
$\Big(p = (1.0, 2.0, 5.0),\ v = 1.0,\ A_0 = 1.0\Big)$

following parameter values: $p = (1.0, 2.0, 5.0)$, $v = 1.0$, $A_0 = 1.0$. As observed in the figure and as mentioned before, the smoothness of the response decreases as the parameter p increases.

3.2.3 Arctan model

The AM/AM and AM/PM responses of the Arctan model are given by the following functions [18]:

$$\underbrace{G(|x|)}_{\text{AM/AM response}} = \left|\gamma_1 \arctan\Big(\zeta_1|x|\Big) + \gamma_2 \arctan\Big(\zeta_2|x|\Big)\right| \tag{3.13}$$

$$\underbrace{\theta(|x|)}_{\text{AM/PM response}} = \angle\left(\gamma_1 \arctan\Big(\zeta_1|x|\Big) + \gamma_2 \arctan\Big(\zeta_2|x|\Big)\right) \tag{3.14}$$

As observed in the equations, Arctan model has 4 parameters γ_1, γ_2, ζ_1 and ζ_2. γ_1&γ_2 are complex numbers and ζ_1&ζ_2 are real numbers. These four parameters are found by curve fitting to the measured amplifier characteristics. Figure 3.6 shows an example of AM/AM and AM/PM responses of Arctan model for the following parameter values:

$\gamma_1 = 8.00335 - 4.61157i$, $\zeta_1 = 2.26895$, $\gamma_2 = -3.77167 + 12.03758i$, $\zeta_2 = 0.8234$.

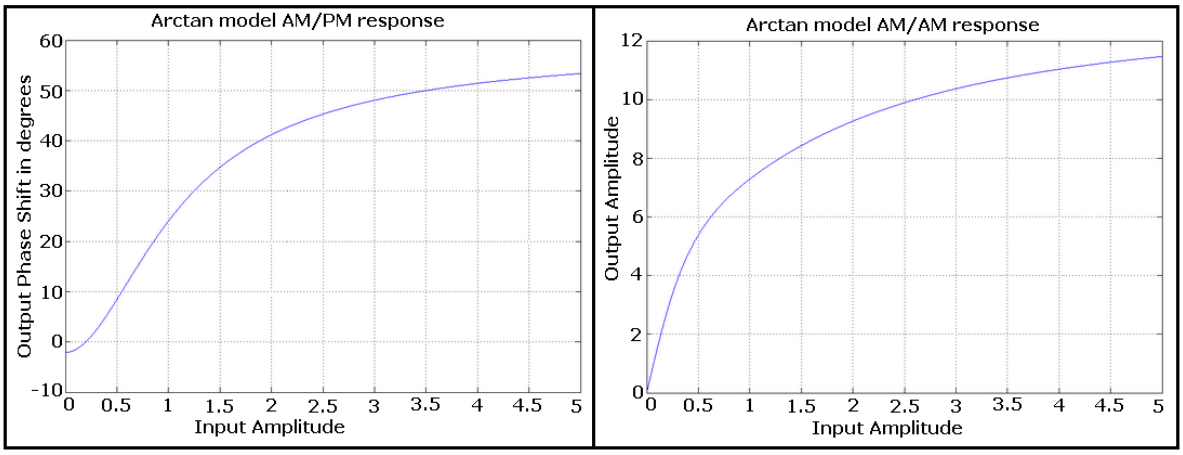


Figure 3.6: Arctan model AM/AM and AM/PM responses
$\left(\gamma_1 = 8.00335 - 4.61157i,\ \zeta_1 = 2.26895,\ \gamma_2 = -3.77167 + 12.03758i,\ \zeta_2 = 0.8234\right)$

3.2.4 Third order polynomial model

Like the Rapp model, the third order polynomial model only models the AM/AM response of the amplifier. It assumes that the amplifier does not apply any phase shift to the input signal. Its AM/AM response is given by the following function:

$$\underbrace{G(|x|)}_{\text{AM/AM response}} = \begin{cases} c_1\left(1 - \dfrac{4}{3A_{inIP3}^2}|x|^2\right)|x| & ;\ \text{if } |x| \le \dfrac{A_{inIP3}}{2} \\ \dfrac{c_1}{3}A_{inIP3} & ;\ \text{if } |x| > \dfrac{A_{inIP3}}{2} \end{cases} \tag{3.15}$$

As noted in (3.15), the third order polynomial model has 2 parameters A_{inIP3} and c_1. $c_1(>0)$ is the linear small-signal gain. A_{inIP3} is the input amplitude at the third order intercept point of the amplifier. It is a measure of the linearity of the third order polynomial model. As it gets larger, the gain

compression of the model decreases and the model behaves more linearly. Figure

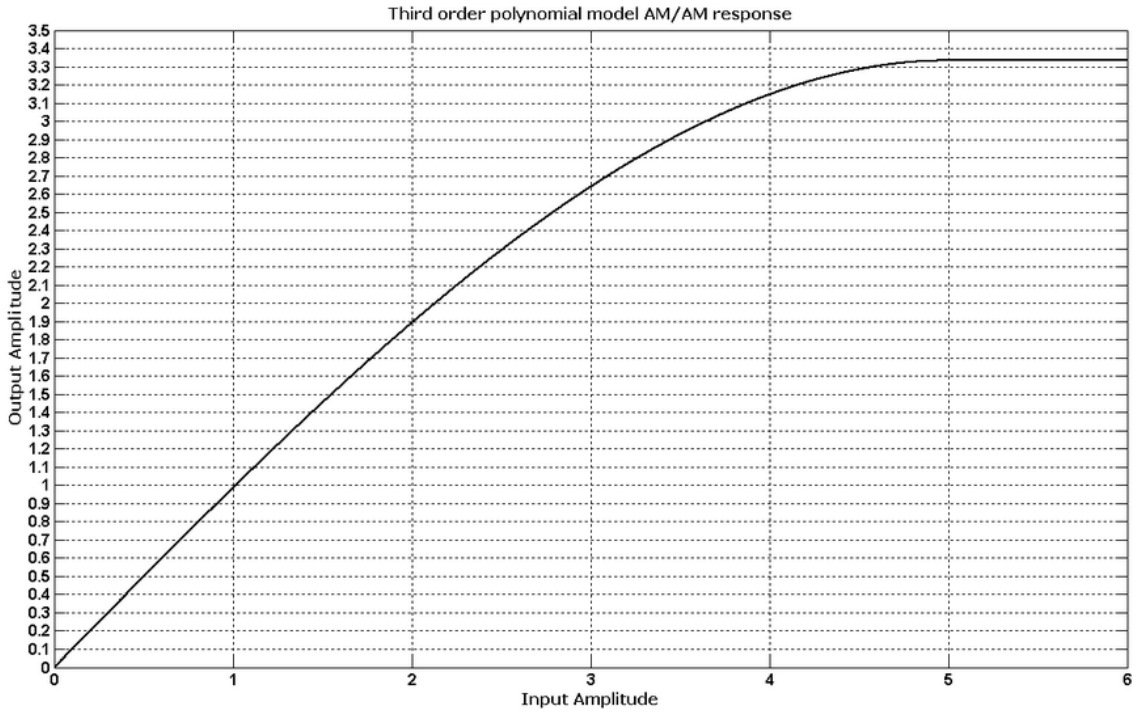


Figure 3.7: Third order polynomial model AM/AM response
($c_1 = 1.0$, $A_{inIP3} = 10.0$)

3.7 shows an example of AM/AM response of third order polynomial model for the following parameter values: $c_1 = 1.0$, $A_{inIP3} = 10.0$.

3.3 Effects of Power Amplifier Nonlinearity

In this section, the effects of power amplifier nonlinearity in communication systems are described. Some of these effects(AM/AM distortion, AM/PM distortion) were described before so they won't be repeated here. In the following subsections, the nonlinear effects harmonic generation(distortion), intermodulation distortion, spectral regrowth, cross modulation and desensitization are described.

3.3.1 Harmonic Generation(Distortion)

When a single-tone signal at frequency w_0 is given as input to a nonlinear power amplifier, at the output of the amplifier we won't only observe the excitation frequency w_0. Its harmonics at $nw_0(n$ integer) will also be present at the output due to the nonlinearity of the power amplifier. This generation of harmonics of the excitation frequency by the nonlinear power amplifier is called harmonic distortion and the harmonic at frequency nw_0 is called n^{th} harmonic. An important measure of harmonic distortion is THD(Total Harmonic Distortion). This figure of non-ideality is defined as the ratio between the square roots of total harmonic output power and output power at the fundamental signal [19].

3.3.2 Intermodulation Distortion

When a multi-tone signal(containing more than one fundamental frequency) is given as input to a nonlinear power amplifier, at the output of the amplifier we won't only observe the excitation frequencies and their harmonics. The linear combinations of the excitation frequencies will also be present at the output. For example if the input is a two-tone signal(w_1; w_2), at the output we will observe the harmonics nw_1 and mw_2 but we will also observe the frequencies $\pm mw_2 \pm nw_1$. These linear combinations of the excitation frequencies are called intermodulation products and this type of distortion is called intermodulation distortion. $k = |m| + |n|$ is the order of the intermodulation distortion and the corresponding intermodulation products at frequencies $\pm mw_2 \pm nw_1$ are called k^{th} order intermodulation products. An important measure of intermodulation distortion is IMR(intermodulation ratio). This figure of merit is defined as the ratio between the fundamental output power and intermodulation distortion output power.

3.3.3 Spectral Regrowth

The spectrum of the input signal to a power amplifier need not necessarily contain only discrete frequencies. If this input signal is a modulated signal commonly found in telecommunication systems, its spectrum will probably contain a continuous band of frequencies instead of discrete frequencies. When such a signal containing a continuous band of frequencies passes through a nonlinear power amplifier, this continuous band widens. This widening is called spectral regrowth. Figure 3.8 illustrates spectral regrowth of an OFDM signal caused by a

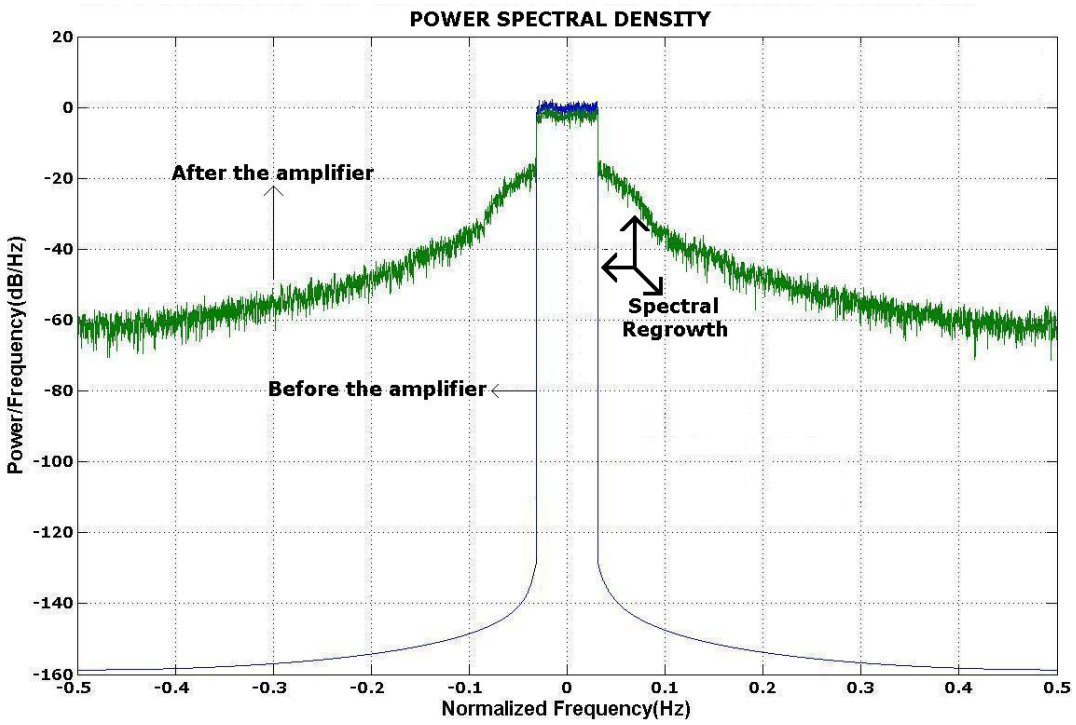


Figure 3.8: Spectral Regrowth

nonlinear amplifier. The widening of the bandwidth due to amplifier nonlinearity can be clearly observed in the figure. Due to spectral regrowth, leakage into adjacent bands(channels) occurs. This leakage causes interference for the adjacent channel and is called adjacent channel interference. Figure 3.9 illustrates adjacent channel interference. An important measure of adjacent channel interference is ACPR(Adjacent Channel Power Ratio). There are alternative definitions for ACPR. It may be defined as total adjacent channel power ratio($ACPR_T$)

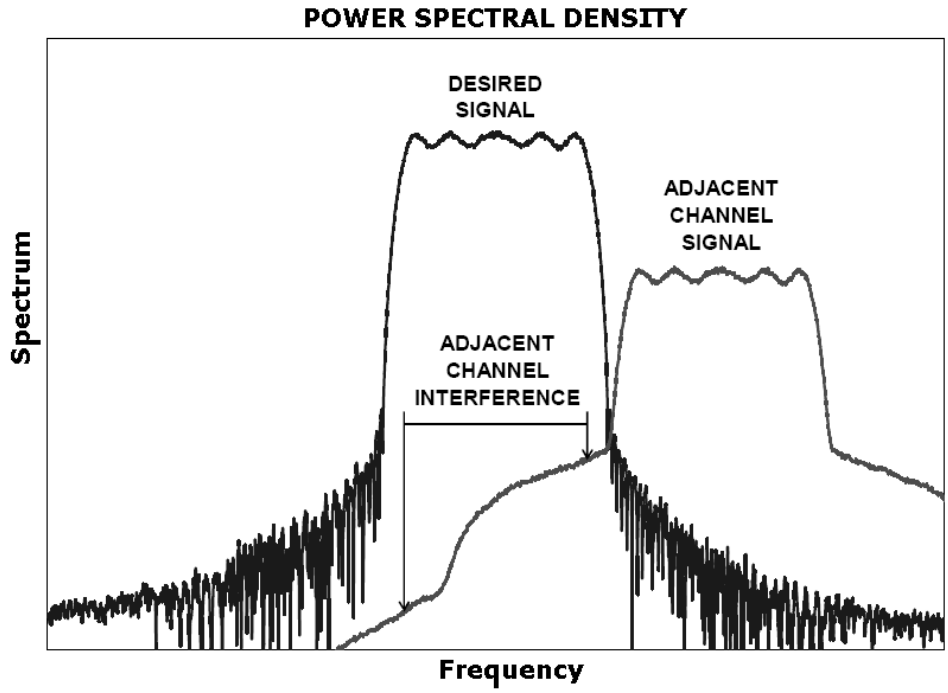


Figure 3.9: Adjacent Channel Interference [20]

which is the ratio of total output power measured in the main channel to the total power integrated in the lower and upper adjacent channel bands, shown in Figure 3.10 [19]. $ACPR_T$ is given by [19]:

$$\begin{aligned} ACPR_T &= \frac{P_{main\ channel}}{P_{upper\ adjacent\ channel} + P_{lower\ adjacent\ channel}} \\ &= \frac{\int_{f_1}^{f_2} S(f)df}{\int_{f_3}^{f_4} S(f)df + \int_{f_5}^{f_6} S(f)df} \end{aligned} \tag{3.16}$$

where $S(f)$ is power spectral density of the signal. ACPR can also be defined by taking the adjacent channel power only in the upper adjacent channel or lower adjacent channel. In that case, it is the ratio of total output power measured in the main channel to the total power measured in the lower adjacent channel or upper adjacent channel and is denoted by $ACPR_{lower}/ACPR_{upper}$ [19]. $ACPR_{lower/upper}$ are given by [19]:

$$ACPR_{lower} = \frac{P_{main\ channel}}{P_{lower\ adjacent\ channel}} = \frac{\int_{f_1}^{f_2} S(f)df}{\int_{f_5}^{f_6} S(f)df} \tag{3.17}$$

$$ACPR_{upper} = \frac{P_{main\ channel}}{P_{upper\ adjacent\ channel}} = \frac{\int_{f_1}^{f_2} S(f)df}{\int_{f_3}^{f_4} S(f)df} \tag{3.18}$$

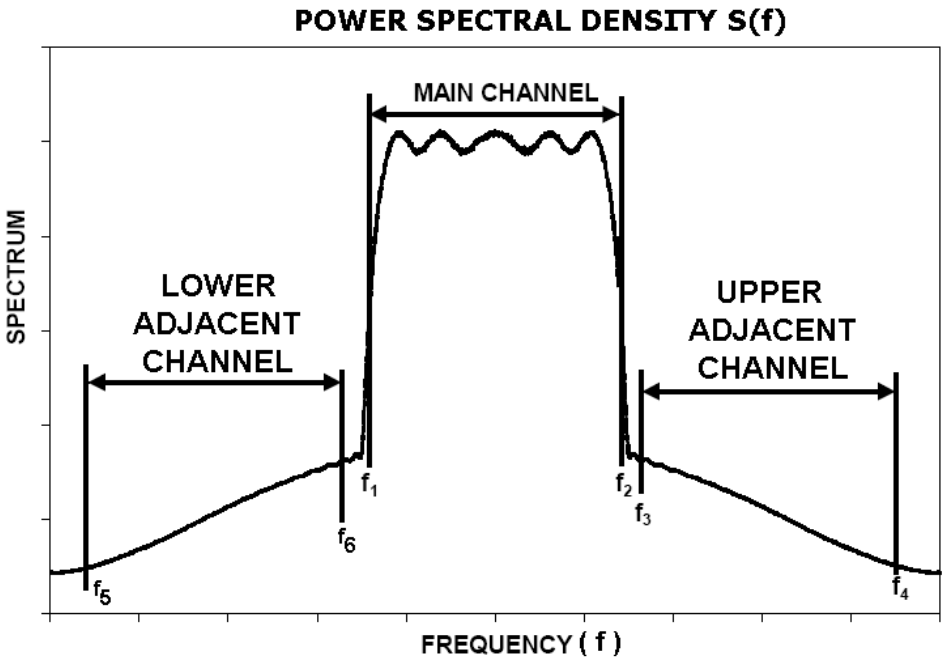


Figure 3.10: Upper and Lower Adjacent Channel Bands [20]

3.3.4 Cross Modulation

Cross modulation is a detrimental effect of amplifier nonlinearity in communication systems. It is the nonlinear effect where modulation from one carrier is transferred to another carrier [3]. To understand cross modulation, let us assume that the input signal to a nonlinear power amplifier is :

$$V_{in}(t) = V_1 \cos(w_1 t) + (1 + m(t)) \cos(w_2 t) \tag{3.19}$$

where $m(t)\Big(|m(t)| < 1\Big)$ is a modulating waveform. This input signal consists of an unmodulated carrier and an amplitude modulated signal. Let us use the polynomial model $y(t) = c_1 x(t) + c_2 x(t)^2 + c_3 x(t)^3$ for the amplifier. At the output of the amplifier, the signal at frequency w_1 will be :

$$\left(c_1 V_1 + \frac{3}{4} c_3 V_1^3 + \frac{3}{2} c_3 V_1 \Big(1 + m(t)\Big)^2 \right) \cos(w_1 t) \tag{3.20}$$

As observed in (3.20), the modulation of w_2 is transferred to the unmodulated carrier w_1 due to nonlinearity and this is an example of cross modulation. Cross modulation is especially critical in multi-carrier systems [3].

3.3.5 Desensitization

The nonlinearity of the amplifier can cause the blocking of weak signals by strong signals at different frequencies. This effect is called desensitization. It generally occurs when a receiver has to process a weak desired signal radiated from a remote transmitter in the presence of a strong signal emitted from a close transmitter. To understand this phenomenon, let us assume that the input signal to a nonlinear amplifier is :

$$V_{in}(t) = V_1 \cos(w_1 t) + V_2 \cos(w_2 t) \tag{3.21}$$

where the first term denotes the desired signal and the second term denotes the strong interferer signal. Since interference is strong, $V_2 \gg V_1$. If the polynomial model $y(t) = c_1 x(t) + c_2 x(t)^2 + c_3 x(t)^3$ is used for the amplifier, at the output the desired signal will be :

$$\left(c_1 V_1 + \frac{3}{4} c_3 V_1^3 + \frac{3}{2} c_3 V_1 V_2^2 \right) \cos(w_1 t) \tag{3.22}$$

As noted in (3.22), if c_1 and c_3 have opposite signs, the desired signal is effectively being weakened by the strong interferer signal due to the third term. This is an example of desensitization.

Chapter 4

IMPLEMENTATION and TESTING of a LOOK-UP TABLE PREDISTORTER and a POLYNOMIAL PREDISTORTER in software

This chapter describes the implementation and testing with simulations of a digital baseband look-up table predistorter and a digital baseband polynomial predistorter in software. The implementation and simulations were done by using IT++, which is a C++ library of mathematical, signal processing, speech processing and communications classes and functions. Figure 4.1 shows the system

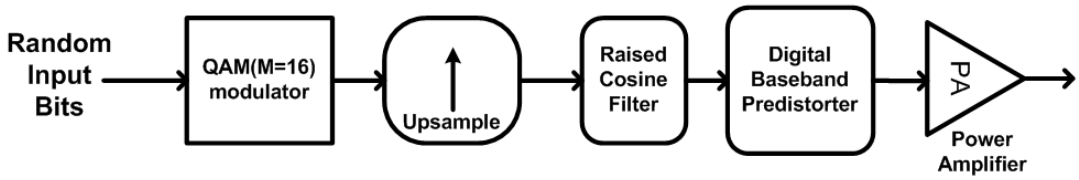


Figure 4.1: Simulated System Model

model used in the simulations. This is a baseband system model. Every element in the model is represented by their baseband equivalents. As mentioned before, two types of predistorters are implemented and used as the predistorter element in the simulations: **1)** a look-up table predistorter **2)** a polynomial predistorter. In the following sections, first the elements of the system model are described. In this description, the predistorter element is especially described in detail. After the description of the system model, the simulations done with the system model are described and their results and the analysis of the results are presented.

4.1 System Model

The system model shown in Figure 4.1 is actually the baseband model of a simple communication transmitter. As mentioned before, this is a totally baseband model and every element is represented by their baseband equivalents. This system model is used to test the performance of the implemented predistorters. The performance is evaluated in terms of BER(bit-error-rate) and adjacent channel power.

4.1.1 QAM modulator

QAM stands for quadrature amplitude modulation. It is a modulation technique which combines amplitude modulation and phase modulation. In this modulation technique, the amplitudes of two quadrature carriers(carriers at the same frequency but 90° out of phase) are changed(modulated) to represent the information bits. These two carriers are called I and Q channels. The carrier of I(in phase) channel is a cosine wave while the carrier of Q(quadrature) channel is a sine wave. So by amplitude modulating I and Q channels, QAM

modulation is obtained. There are different types of QAM modulation which differ in the number of points in their constellation. If the constellation contains M points, it is called M-QAM modulation. M(the number of points in the constellation of QAM) must be a power of two. It will also be better if M is a square of some integer in order to obtain a perfect rectangular constellation with no empty(unused) points. The constellation points of M-QAM modulation are complex numbers. Their real parts represent the I channel modulation and their imaginary parts represent the Q channel modulation. Every complex element in the constellation of M-QAM modulation corresponds to a sequence of information bits which has length $k = \log_2(M)$. This is because by using M different symbols, $k = \log_2(M)$ different bits can be represented. If the complex constellation points of M-QAM modulation are denoted by $c_n = a_n + jb_n$ where a_n is the I component and b_n is the Q component, c_n takes values from the alphabet $c_n \epsilon \left\{ \left[2k - 1 - \sqrt{M}\right] + j\left[2l - 1 - \sqrt{M}\right]; k, l = 1, 2, 3, \ldots, \sqrt{M} \right\}$. The QAM modulator used in the system model is a 16-QAM

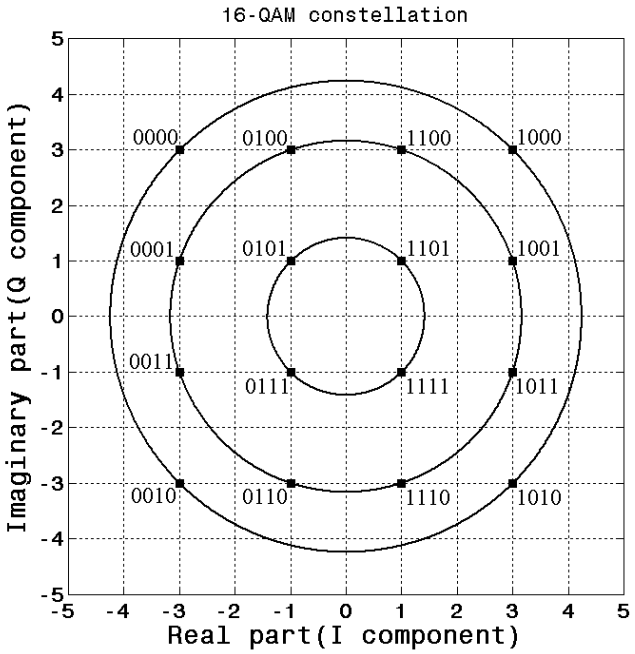


Figure 4.2: 16-QAM constellation

modulator. The constellation corresponding to 16-QAM modulation is shown in

Figure 4.2. In the constellation, gray coding is applied so that adjacent elements of the constellation differ only by one bit. As seen in Figure 4.2, the 16 different constellation elements have only 3 different amplitude levels. The maximum amplitude level is $\sqrt{2}\left(\sqrt{M}-1\right)\Big|_{M=16} = 3\sqrt{2}$. The 16-QAM modulator in the system model takes the input bits, groups them into sequences of length $\log_2 M\Big|_{M=16} = 4$ and maps each sequence to corresponding complex information symbols following the mapping in Figure 4.2. After this mapping, the complex information symbols are scaled by $\sqrt{\frac{2(M-1)}{3}}\Bigg|_{M=16} = \sqrt{10}$ to make the average energy of the constellation equal to $1\left(\text{the average energy of M-QAM constellation is } \frac{2(M-1)}{3}\right)$. So at the output of the 16-QAM modulator, we have complex information symbols which take values from the set $\frac{1}{\sqrt{10}}\Big\{\pm 1 \pm j, \pm 3 \pm 3j, \pm 1 \pm 3j, \pm 3 \pm j\Big\}$.

4.1.2 Upsampling

Upsampling in the system model is performed by inserting $\alpha - 1$ zeros between consecutive complex information symbols coming from the 16-QAM modulator where α is the upsampling factor. Upsampling increases the sampling frequency and the observable spectral range. This is necessary because since the simulations are done in discrete time, the observable spectral range is limited by the sampling frequency. Both the predistorter and the amplifier produce out-of-band spectral components. To be able to observe these components, the observable spectral range must be increased and this is achieved by upsampling. The upsampling factor α is one of the parameters of the simulations performed.

4.1.3 Raised Cosine filter

Raised cosine filters are widely used in telecommunications systems. They are used as pulse-shaping filters to limit the bandwidth of the transmitted signal. The

reason why they are chosen is that they eliminate ISI(intersymbol interference). The impulse response $h(t)$ and the transfer function $|H(f)|$ of a raised cosine filter are as follows:

$$h(t) = \text{sinc}\left(\frac{t}{T}\right)\frac{\cos\left(\pi\beta\frac{t}{T}\right)}{1-\left(2\beta\frac{t}{T}\right)^2} \tag{4.1}$$

$$|H(f)| = \begin{cases} 1 & ; |f| \leq \frac{1-\beta}{2T} \\ \frac{1}{2}\left[1+\cos\left(\frac{\pi T}{\beta}\left[|f|-\frac{1-\beta}{2T}\right]\right)\right] & ; \frac{1-\beta}{2T} < |f| \leq \frac{1+\beta}{2T} \\ 0 & ; |f| > \frac{1+\beta}{2T} \end{cases} \tag{4.2}$$

where the parameter β is called the roll-off factor of the raised cosine filter and T is symbol duration. β can take values in the range $[0, 1]$. It controls the bandwidth and the shape of the transfer function of the raised cosine filter. Figure 4.3 shows the impulse response and the transfer function of the raised cosine filter for various roll-off factor(β) values. As seen in the figure, the transfer function approaches a rectangular window and the impulse response approaches a sinc function as β decreases. Also the decay of the tails of the impulse response gets slower as β decreases. Another effect of the decrease of β is the decrease of the bandwidth of the filter which is equal to $\frac{1+\beta}{2T}$. In the simulations that take place in discrete time, the raised cosine filter is implemented as a discrete-time *FIR* filter which has a finite-length impulse response. The impulse response of this FIR filter is obtained by sampling the continuous-time raised cosine filter impulse response given in (4.1). The finite interval over which (4.1) is sampled to obtain the impulse response of the FIR filter is determined by the parameter *delay*(which is a positive integer) in the simulations. The *delay* parameter also determines the length of the impulse response and group delay of the FIR filter. The continuous-time raised cosine filter impulse response given in (4.1) is sampled over the interval $[-delay * T, delay * T](T =$ symbol duration) with sampling period $\frac{T}{\alpha}(\alpha =$ upsampling factor used in the upsampling block) to obtain the impulse response of the FIR filter. As a result, the length of the impulse response

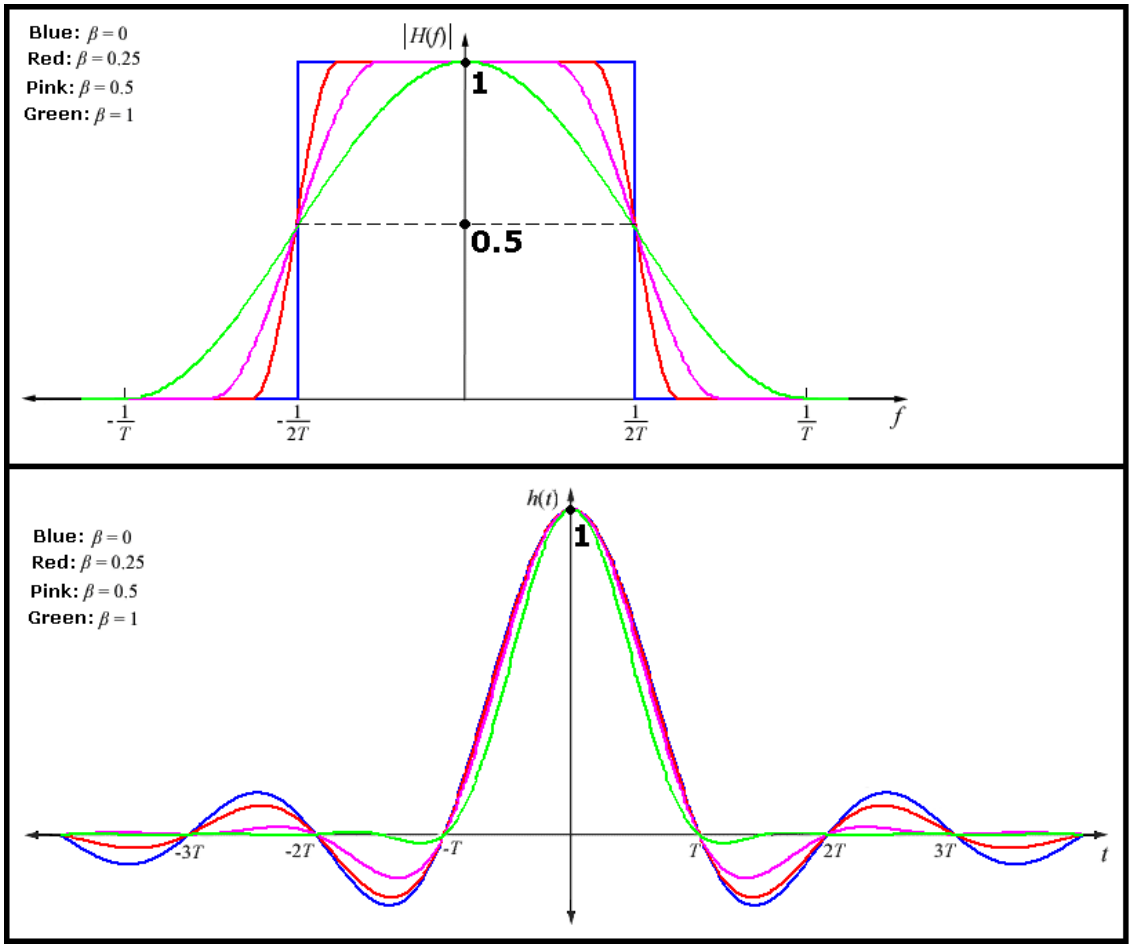


Figure 4.3: The impulse response and transfer function of a raised cosine filter for various roll-off factor(β) values

of the FIR filter is (2∗delay∗upsampling factor+1). The FIR filter has a constant group delay given by (delay $*$ upsampling factor) samples. The impulse response of the FIR filter is as follows:

$$h[n] = \text{sinc}\left(\frac{t}{T}\right)\frac{\cos\left(\pi\beta\frac{t}{T}\right)}{1-\left(2\beta\frac{t}{T}\right)^2}\Bigg|_{t=\left(-delay+\frac{n}{\alpha}\right)*T} \tag{4.3}$$

$$= \text{sinc}\left(-delay+\frac{n}{\alpha}\right)\frac{\cos\left(\pi\beta\left(-delay+\frac{n}{\alpha}\right)\right)}{1-\left(2\beta\left(-delay+\frac{n}{\alpha}\right)\right)^2} \tag{4.4}$$

where $n = (0, 1, 2, 3, \ldots\ldots, 2 * \text{delay} * \alpha)$, T is the symbol period, α is the upsampling factor used in the upsampling block and β is the roll-off factor.

Figure 4.4 shows the impulse response of the FIR raised cosine filter for the

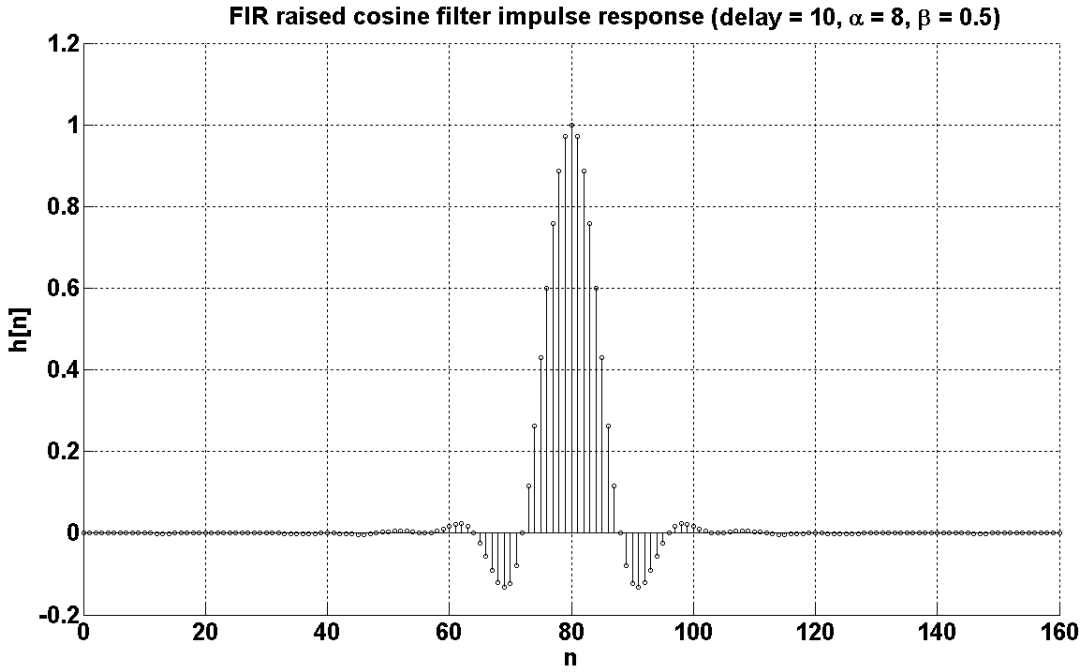


Figure 4.4: Impulse response of the FIR raised cosine filter
$(delay = 10, \alpha = 8, \beta = 0.5)$

following parameter values: $delay = 10$, $\alpha = 8$, $\beta = 0.5$. As seen in the figure, the impulse response of the FIR filter is a delayed raised cosine response. The delay in the response is necessary. It is set so that the impulse response before time zero is negligible and can safely be ignored by the function. In this way, the filter becomes causal. At the same time, this delay is the group delay of the filter and is given by (delay $*$ upsampling factor) samples as mentioned before. Figure 4.5 shows the transfer function of the FIR raised cosine filter for the same parameter values on a normalized frequency axis. How the axis should be interpreted is also shown on the figure. As the figure shows, the raised cosine response is approximated very well.

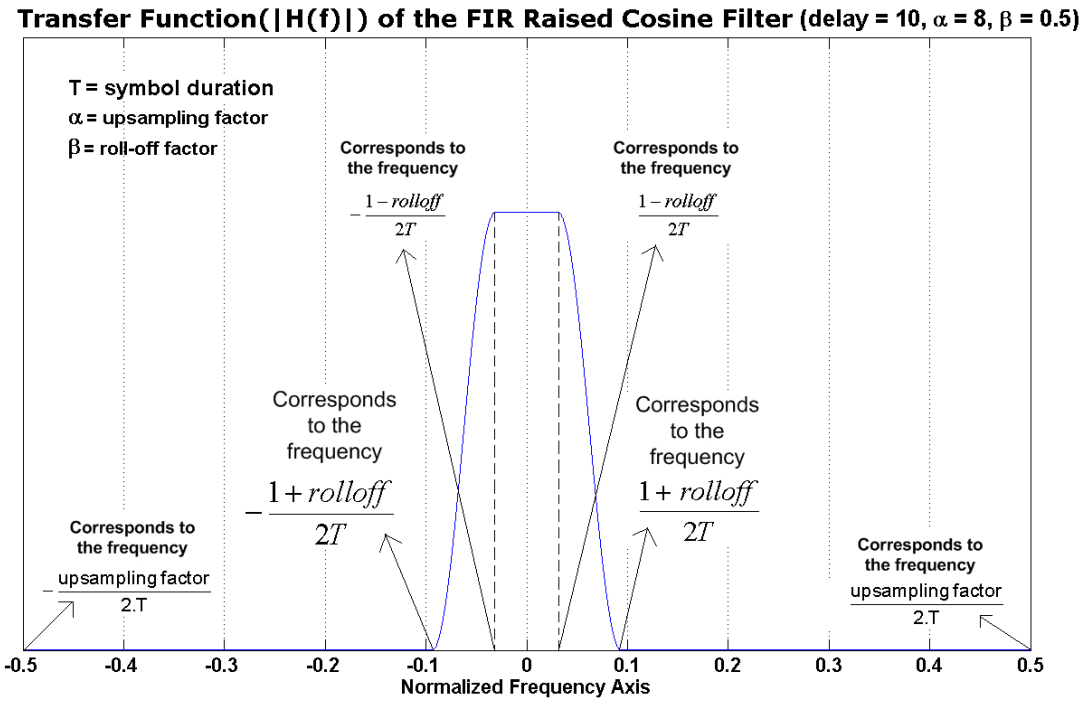


Figure 4.5: Transfer function of the FIR raised cosine filter
$(delay = 10, \alpha = 8, \beta = 0.5)$

4.1.4 Power Amplifier

The modelling of nonlinear behaviour of power amplifiers was discussed in detail in chapter 3. Since the simulated system model is a baseband model, a baseband model is needed for the power amplifier in the simulations. For this purpose, the complex envelope response(AM/AM response and AM/PM response) which is a baseband behavioural model is used in the simulations to model the nonlinear power amplifier. Detailed information was given about AM/AM response and AM/PM response in chapter 3. It has been mentioned in chapter 3 that there are complex envelope response models widely used in the literature for modelling the nonlinear behaviour of power amplifiers. One of these models was the *Arctan* model. This model has been used in the simulations as the nonlinear power amplifier model. Recall that the Arctan model has 4 parameters: γ_1, γ_2, ζ_1 and ζ_2 . γ_1& γ_2 are complex numbers and ζ_1& ζ_2 are real numbers. Also recall that AM/AM response and AM/PM response of the Arctan model are as

follows:

$$\underbrace{G(|x|)}_{\text{AM/AM response}} = \left|\gamma_1 \arctan\Big(\zeta_1|x|\Big) + \gamma_2 \arctan\Big(\zeta_2|x|\Big)\right| \tag{4.5}$$

$$\underbrace{\theta(|x|)}_{\text{AM/PM response}} = \angle\left(\gamma_1 \arctan\Big(\zeta_1|x|\Big) + \gamma_2 \arctan\Big(\zeta_2|x|\Big)\right) \tag{4.6}$$

where $|x|$ is the amplitude of the input signal. The following values were assigned to the parameters of the Arctan model in the simulations:

$\gamma_1 = 8.00335 - 4.61157i$, $\zeta_1 = 2.26895$, $\gamma_2 = -3.77167 + 12.03758i$, $\zeta_2 = 0.8234$.

For these parameter values, the AM/AM response & AM/PM response & gain of the amplifier model are illustrated in Figure 4.6.

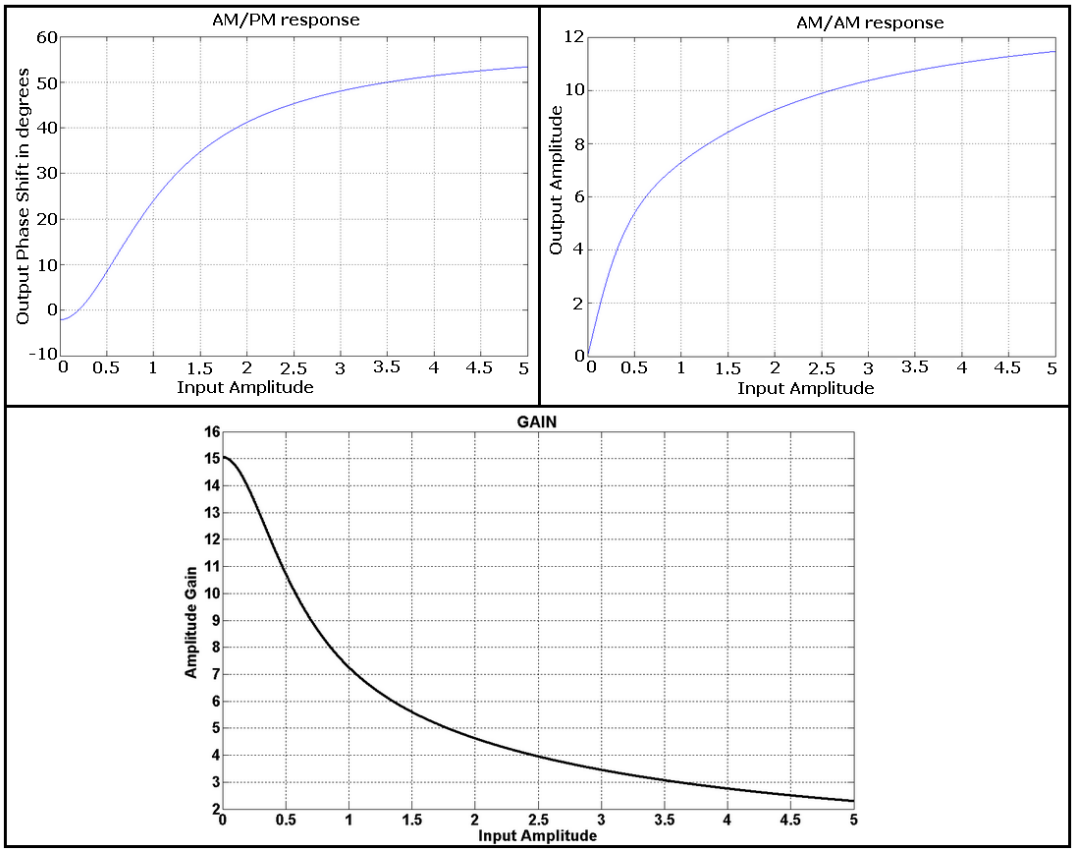


Figure 4.6: AM/AM response & AM/PM response & Gain of the amplifier model used in the simulations

4.1.5 Digital Baseband Predistorter

The function of a predistorter in a communication system is to provide the inverse characteristics of the power amplifier so that the combination of the two will give a linear response. The linear response means a constant gain and no phase shift to the input signal as the input amplitude(power) changes. There are different types of predistorters. One of these types is digital baseband predistorters. Digital baseband predistorters and other predistorter types were discussed in detail in chapter 2 so that discussion won't be repeated here. Two types of digital baseband predistorters were implemented and tested with simulations: **1)** a polar look-up table predistorter **2)** a polar polynomial predistorter. The polar look-up table predistorter is based on the polar look-up table predistorter implemented in [18] and the polar polynomial predistorter is based on the polar polynomial predistorter implemented in [15]. The following subsections discuss these two implemented predistorters.

4.1.5.1 Polar Polynomial Predistorter

The amplitude and phase corrections of a polar polynomial predistorter are implemented by using polynomials. A polar polynomial predistorter has two polynomials with real coefficients. One of these polynomials gives the AM/AM response of the polar polynomial predistorter and the other polynomial gives the AM/PM response of the polar polynomial predistorter. Both of these polynomials are functions of the magnitude of the input signal to the predistorter. If the input signal to the polar polynomial predistorter is denoted by z(z is complex), the AM/AM response of the predistorter is denoted by g_{pre} and the AM/PM

response of the predistorter is denoted by θ_{pre}, g_{pre} and θ_{pre} are given by [15]:

$$\begin{aligned} g_{pre}\Big(|z|\Big) &= a_1|z| + a_2|z|^2 + a_3|z|^3 + \ldots\ldots + a_N|z|^N \\ &= \sum_{k=1}^{N} a_k|z|^k = (\,\overline{V}\,)^T\,\overline{R}_a \qquad (4.7) \\ \theta_{pre}\Big(|z|\Big) &= p_0 + p_1|z| + p_2|z|^2 + p_3|z|^3 + \ldots\ldots + p_N|z|^N \\ &= \sum_{k=0}^{N} p_k|z|^k = (\,\overline{P}\,)^T\,\overline{R}_p \qquad (4.8) \end{aligned}$$

where $\overline{V} = \Big[a_1\ a_2\ a_3 \ldots a_N\Big]^T$, $\overline{R}_a = \Big[\,|z|\ |z|^2\ |z|^3 \ldots |z|^N\Big]^T$,

$\overline{P} = \Big[p_0\ p_1\ p_2\ p_3 \ldots p_N\Big]^T$, $\overline{R}_p = \Big[1\ |z|\ |z|^2\ |z|^3 \ldots |z|^N\Big]^T$. N is the order of AM/AM & AM/PM polynomials, $a_1\ a_2\ a_3 \ldots a_N$ & $p_0\ p_1\ p_2\ p_3 \ldots p_N$ are the coefficients of AM/AM & AM/PM polynomials and V & P are the coefficient vectors of AM/AM & AM/PM polynomials. N is one of the parameters in the simulations. So if the complex input signal to the polar polynomial predistorter is z, the output signal will be $g_{pre}\Big(|z|\Big)\exp\Bigg(j\Big(\angle z + \theta_{pre}\Big(|z|\Big)\Big)\Bigg)$.

As seen in the simulated system model given in Figure 4.1, the power amplifier which is modelled by a complex envelope response(AM/AM & AM/PM responses) comes after the predistorter. For the polar polynomial predistorter to achieve linearity(constant gain and no phase shift as the input amplitude changes), the AM/AM response of the predistorter & amplifier combination must provide a constant gain and the AM/PM response of the predistorter & amplifier combination must provide zero phase shift independent of input amplitude. Mathematically, this condition can be expressed as follows:

$$\begin{aligned} g_{amp}\Bigg(g_{pre}\Big(|z|\Big)\Bigg) &= G_0|z| \qquad (4.9) \\ \theta_{pre}\Big(|z|\Big) + \theta_{amp}\Bigg(g_{pre}\Big(|z|\Big)\Bigg) &= 0 \qquad (4.10) \end{aligned}$$

where z is the complex input signal, G_0 is the desired constant gain, $g_{amp}(.)$ is the AM/AM response of the amplifier and $\theta_{amp}(.)$ is the AM/PM response of the

amplifier. For the polar polynomial predistorter to satisfy the conditions given in (4.9) and (4.10), its coefficients (coefficient vectors V and P) must take the appropriate values. This is achieved at the training phase during simulations. Training is the first phase of the simulations. The other phase is testing. In the training phase, the vectors V and P are updated using the amplitude and phase errors at the amplifier output. Here what is meant by error is the difference between the values that are desired at the amplifier output and the values that are actually observed at the amplifier output. At the start of the training phase, V and P are set such that the predistorter does not change the amplitude or phase of the input signal$\Big($V is set to $[\,1\,\underbrace{0\;0\;0\ldots\ldots0}_{N-1\text{ zeros}}]^T$ and P is set to $[\underbrace{0\;0\;0\;0\ldots\ldots0}_{N+1\text{ zeros}}]^T\Big)$. Then by training they converge to appropriate values step by step. The definitions of the amplitude and phase errors are as follows:

$$\begin{aligned} e_{amp} &= \text{amplitude error} = \underbrace{G_0|z|}_{\text{Desired Amplitude}} - \overbrace{g_{amp}\Big(g_{pre}\Big(|z|\Big)\Big)}^{\text{Observed Amplitude}} \\ &= G_0|z| - g_{amp}\Big((\,\overline{V}\,)^T\,\overline{R}_a\Big) \qquad (4.11) \\ e_{ph} &= \text{phase error} = \underbrace{\angle z}_{\text{Desired Phase}} - \Bigg(\overbrace{\angle z + \theta_{pre}\Big(|z|\Big) + \theta_{amp}\Big(g_{pre}\Big(|z|\Big)\Big)}^{\text{Observed Phase}}\Bigg) \\ &= -(\,\overline{P}\,)^T\,\overline{R}_p - \theta_{amp}\Big((\,\overline{V}\,)^T\,\overline{R}_a\Big) \qquad (4.12) \end{aligned}$$

where G_0 is the desired gain and z is the complex input signal to the predistorter. During the training phase, V and P coefficient vectors are updated for every input sample according to the LMS(least mean squares) algorithm by using amplitude and phase errors. If the k^{th} input sample to the predistorter is $z_k = r_k\,\mathrm{e}^{j\theta_k}$, the update of V and P vectors according to the LMS algorithm for this input is as follows [15]:

$$\overline{V}_{k+1} = \overline{V}_k + \mu_k\,\overline{R}_{a,k}\,g'_{amp}\Big(\overline{V}_k^T\overline{R}_{a,k}\Big)\,e_{amp,k} \qquad (4.13)$$

where $e_{amp,k} = G_0 r_k - g_{amp}\left(\overline{V}_k^T \overline{R}_{a,k}\right)$, μ_k is a positive step size and $g'_{amp}(\cdot)$ denotes the derivative of the function $g_{amp}(\cdot)$. Since the AM/AM response of the amplifier model used in the simulations is a monotonically increasing function, $g'_{amp}(\cdot)$ will always be positive. As a result, to simplify the update equation it can be replaced by a small positive constant and when this is done, the update equation simplifies to the following form [15]:

$$\overline{V}_{k+1} = \overline{V}_k + \mu_V \overline{R}_{a,k}\, e_{amp,k} \tag{4.14}$$

where μ_V is a small positive step size. Likewise a similar update is done for vector P [15]:

$$\overline{P}_{k+1} = \overline{P}_k + \mu_P \overline{R}_{p,k}\, e_{ph,k} \tag{4.15}$$

where μ_P is a small positive step size.
μ_V and μ_P(small positive steps used for updating V and P) are two important parameters in the simulations. They should be chosen small enough to guarantee the stability and convergence of the update algorithm. A detailed analysis of how they should be chosen is provided in [15].

At the end of the training phase, one hopes that the vectors V and P will converge to appropriate values that will linearize the amplifier. Then the testing phase of the simulations comes and the performance of the obtained polar polynomial predistorter is tested with simulations. No update is applied to the predistorter during this phase.

4.1.5.2 Polar Look-up Table Predistorter

In a polar look-up table predistorter, the amplitude correction(AM/AM response) and phase correction(AM/PM response) of the predistorter are stored in a look-up table. Figure 4.7 shows the block diagram of the implemented polar look-up table predistorter. As seen in the figure, it has 3 columns. The first

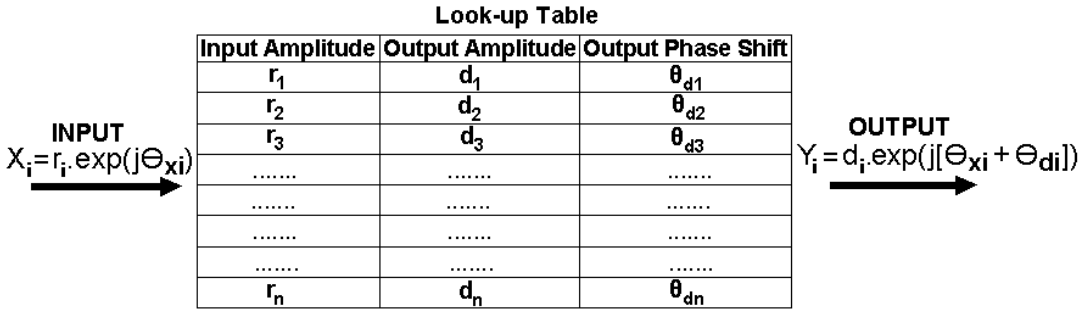


Figure 4.7: Block diagram of the implemented polar look-up table predistorter [18]

column contains the input amplitude values. The second and third columns contain the corresponding output amplitude(AM/AM response) and output phase shift(AM/PM response) values. Like the polar polynomial predistorter, AM/AM response and AM/PM response of the polar look-up table predistorter are functions of the input amplitude. The polar look-up table predistorter has 2 important parameters. These are its size and range. The size parameter determines the number of entries in each column. The range parameter determines the maximum amplitude for which a response is stored in the look-up table. The ratio $\frac{range}{size-1}$ gives the constant amplitude step size used while storing the responses for increasing input amplitude values. The input amplitude levels present in the look-up table are equally spaced. The minimum input amplitude for which a response is stored is equal to 0 and the maximum input amplitude for which a response is stored is equal to range. The indexing of the look-up table is done using the magnitude of the input signal. If the complex input signal to the predistorter is denoted by $z = r\,e^{j\theta}$, there are 3 possible cases:

1. **r > range** : Since the magnitude of the input signal is greater than range, there is no stored response for this input signal. In such cases, the predistorter doesn't change the magnitude or phase of the input signal. The input signal leaves the predistorter unchanged.

2. $\mathbf{r \leq range\ \ and\ \ r * \frac{size-1}{range}\ equals\ an\ integer}$: When these two conditions are satisfied, there is a stored response for the magnitude r. The entries with index $1 + r * \frac{size-1}{range}$ in the AM/AM response and AM/PM response columns give us the response of the predistorter for this input. The magnitude of the output signal is the entry at index $1 + r * \frac{size-1}{range}$ in the AM/AM response column. The phase of the output signal is the sum of the input phase θ and the entry at index $1 + r * \frac{size-1}{range}$ in the AM/PM response column.

3. $\mathbf{r \leq range\ \ and\ \ r * \frac{size-1}{range}\ not\ integer}$: In this case r is between two magnitude values(r_k *and* r_{k+1}) in the table. The response of the predistorter for this case is found by linear interpolation. If the output signal is denoted by $z_{out} = r_{out}\, e^{j\theta_{out}}$, the magnitude of the output signal(AM/AM response) will be given by [18]:

$$r_{out} = d_k + \frac{d_{k+1} - d_k}{r_{k+1} - r_k} * (r - r_k) \tag{4.16}$$

where d_k is the output magnitude corresponding to input magnitude r_k and d_{k+1} is the output magnitude corresponding to input magnitude r_{k+1}. The phase of the output signal will be given by [18]:

$$\theta_{out} = \overbrace{\theta}^{\text{input phase}} + \ \theta_{d_k} + \ \frac{\theta_{d_{k+1}} - \theta_{d_k}}{r_{k+1} - r_k} * (r - r_k) \tag{4.17}$$

where $\theta_{d_{k+1}}$ is the output phase shift corresponding to input magnitude r_{k+1} and θ_{d_k} is the output phase shift corresponding to input magnitude r_k.

Like the polar polynomial predistorter, the polar look-up table predistorter must be trained with the nonlinear characteristic of the amplifier to achieve linearity(constant gain & no phase shift). This is achieved during the training phase of the simulations by updating the table entries using the amplitude and phase errors at the amplifier output. As explained before, what is meant by error

is the difference between the values that are desired at the amplifier output and the values that are actually observed at the amplifier output. At the beginning of the training phase, the magnitude range of the look-up table predistorter is set so that it will cover the magnitude range of the training input signal. Also the table entries are set so that the predistorter is transparent(doesn't change the magnitude or phase of the input signal). Then during the training phase, they converge to appropriate values step by step with the help of updating. Let us denote the i^{th} training input sample by $X_i = |X_i|\mathrm{e}^{j\angle X_i}$. There are two possible cases for $|X_i|$. It can correspond to a magnitude level present in the table or it can be between two magnitude levels present in the table. The updates for these two cases will be different. In the first case, only a single entry in the AM/AM & AM/PM response columns will be updated. In the second case, two entries in the AM/AM & AM/PM response columns will be updated. For the first case, let $|X_i| = r_k$ where r_k is a magnitude level present in the table. The update of the table is as follows for this case [18]:

$$d_{i+1,k} = d_{i,k} + S_a * e_{amp,i} \tag{4.18}$$

$$\theta_{i+1,k} = \theta_{i,k} + S_p * e_{ph,i} \tag{4.19}$$

In (4.18) and (4.19), the index i is the training iteration index and index k is table position index. S_a and S_p are two small update steps. $d_{i,k}$ is the output magnitude(AM/AM response entry in the table) corresponding to input magnitude r_k at the i^{th} training iteration. $\theta_{i,k}$ is the output phase shift(AM/PM response entry in the table) corresponding to input magnitude r_k at the i^{th} training iteration. $e_{amp,i}$ is the magnitude error at the amplifier output at the i^{th} training iteration(corresponding to input X_i) and is given by $e_{amp,i} = G_0|X_i| - g_{amp}(d_{i,k})$ where G_0 is the desired constant gain and $g_{amp}(\cdot)$ is the AM/AM response of the nonlinear amplifier. $e_{ph,i}$ is the phase error at the amplifier output at the i^{th} training iteration(corresponding to input X_i) and is given by $e_{ph,i} = -\theta_{i,k} - g_{ph}(d_{i,k})$ where $g_{ph}(\cdot)$ is the AM/PM response of the nonlinear amplifier. For the second case, let $r_k < |X_i| < r_{k+1}$ where r_k and r_{k+1} are two magnitude levels present

in the table and let Y_i denote the output of the predistorter for the input X_i where Y_i should be computed by using the interpolation formulas given in (4.16) and (4.17). As mentioned before, multiple AM/AM & AM/PM response entries(corresponding to r_k and r_{k+1}) will be updated for this case. The update of these table entries is as follows [18]:

$$d_{i+1,k} = d_{i,k} + S_a * \Delta_{i,k} * e_{amp,i} \tag{4.20}$$

$$\theta_{i+1,k} = \theta_{i,k} + S_p * \Delta_{i,k} * e_{ph,i} \tag{4.21}$$

$$d_{i+1,k+1} = d_{i,k+1} + S_a * \Delta_{i,k+1} * e_{amp,i} \tag{4.22}$$

$$\theta_{i+1,k+1} = \theta_{i,k+1} + S_p * \Delta_{i,k+1} * e_{ph,i} \tag{4.23}$$

In the above equations, the index i is the training iteration index and indices k & k+1 are table position indices. $d_{i,k}$ is the output magnitude(AM/AM response entry in the table) corresponding to input magnitude r_k at the i^{th} training iteration. $d_{i,k+1}$ is the output magnitude(AM/AM response entry in the table) corresponding to input magnitude r_{k+1} at the i^{th} training iteration. $\theta_{i,k}$ is the output phase shift(AM/PM response entry in the table) corresponding to input magnitude r_k at the i^{th} training iteration. $\theta_{i,k+1}$ is the output phase shift(AM/PM response entry in the table) corresponding to input magnitude r_{k+1} at the i^{th} training iteration. $e_{amp,i}$ is the magnitude error at the amplifier output at the i^{th} training iteration(corresponding to input X_i) and is given by $e_{amp,i} = G_0|X_i| - g_{amp}(|Y_i|)$ where G_0 is the desired constant gain, $g_{amp}(\cdot)$ is the AM/AM response of the nonlinear amplifier and Y_i is the output of the predistorter corresponding to input X_i, which is given by :
$|Y_i| = d_{i,k} + \frac{d_{i,k+1} - d_{i,k}}{r_{i,k+1} - r_{i,k}} * \Big(|X_i| - r_k\Big)$ $\angle Y_i = \angle X_i + \theta_{i,k} + \frac{\theta_{i,k+1} - \theta_{i,k}}{r_{k+1} - r_k} * \Big(|X_i| - r_k\Big)$.
$e_{ph,i}$ is the phase error at the amplifier output at the i^{th} training iteration(corresponding to input X_i) and is given by :
$e_{ph,i} = -\left(\theta_{i,k} + \frac{\theta_{i,k+1} - \theta_{i,k}}{r_{k+1} - r_k} * \Big(|X_i| - r_k\Big) + g_{ph}\Big(|Y_i|\Big)\right)$ where $g_{ph}(\cdot)$ is the AM/PM response of the nonlinear amplifier. $\Delta_{i,k}$ and $\Delta_{i,k+1}$ in the equations

are used to weight the updating values. The idea is that the entries corresponding to the magnitude which is closer to the input magnitude get the larger share of magnitude & phase errors. $\Delta_{i,k}$ and $\Delta_{i,k+1}$ are given by [18]:

$$\Delta_{i,k} = \frac{r_{k+1} - |X_i|}{r_{k+1} - r_k} = \frac{r_{k+1} - |X_i|}{\underbrace{range/(size-1)}_{\text{magnitude step in the table}}} \tag{4.24}$$

$$\Delta_{i,k+1} = \frac{|X_i| - r_k}{r_{k+1} - r_k} = \frac{|X_i| - r_k}{\underbrace{range/(size-1)}_{\text{magnitude step in the table}}} \tag{4.25}$$

S_a and S_p(small positive steps used for updating AM/AM response & AM/PM response entries in the table predistorter) are important parameters in the simulations. They correspond to parameters μ_V and μ_P in the polar polynomial predistorter. Like μ_V and μ_P, S_a and S_p should also be chosen small enough to guarantee the stability and convergence of the update algorithm of the table predistorter. A detailed analysis of how they should be chosen can be found in [18].

At the end of the training phase, the entries in the table predistorter converge to appropriate values that will linearize the amplifier. Then the testing phase of the simulations comes and the performance of the obtained polar table predistorter is tested with simulations. No update is applied to the predistorter during this phase.

4.2 Simulations, Results and Discussion

As mentioned many times before, the simulations consist of 2 phases: **Training** and **Testing**.

1) Training Phase : In the training phase, the simulated system model takes the form shown in Figure 4.8. First, a random bit sequence is created. This bit sequence is modulated with QAM(M=16). The obtained sequence is first

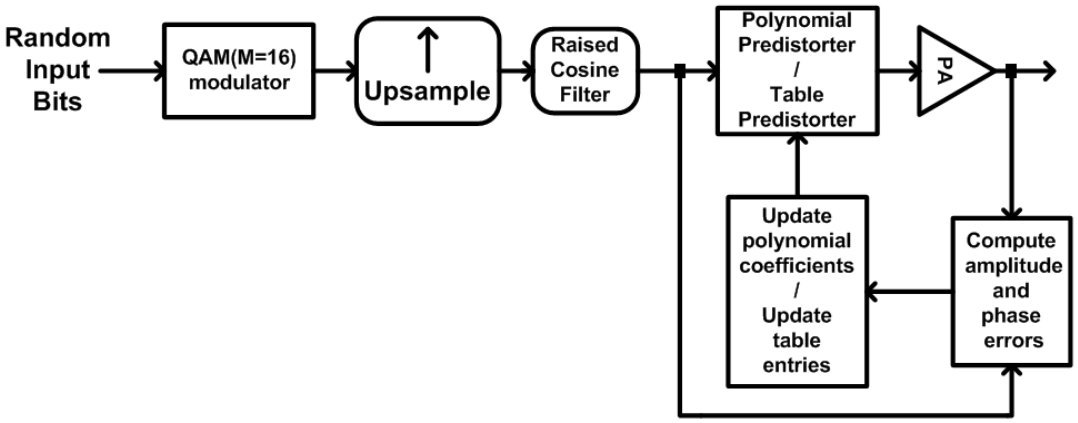


Figure 4.8: System model during training

upsampled and then filtered by a raised cosine filter. The sequence obtained is used to train the predistorter as discussed above.

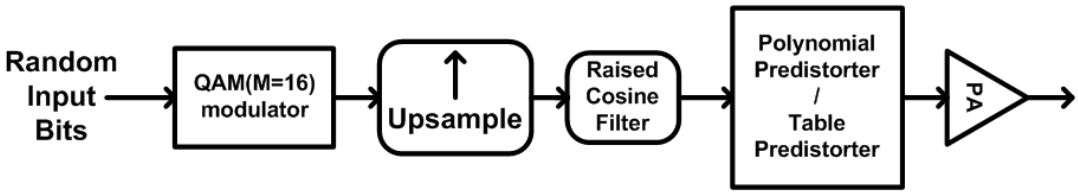


Figure 4.9: System model during testing

2) Testing Phase : After the training phase, the predistorter is tested to see if it achieves linearization. The simulated system model takes the form shown in Figure 4.9 during the testing phase. Like training phase, first a random bit sequence is created. This bit sequence is again modulated with 16-QAM, upsampled and raised cosine filtered just as before. After filtering, the sequence enters the predistorter and then the PA(power amplifier). Since the predistorter has already been trained, it is expected that it will linearize the PA.

In the simulations, the upsampling factor was set to 8. The delay parameter of the raised cosine filter was set to 1000. The roll-off factor of the raised cosine filter was set to 0.5. The desired constant gain of the predistorter-amplifier combination was set to 10. It must be mentioned that the maximum gain that the used amplifier model can provide is 15, which can be observed in Figure 4.6

on page 65. Another point that must be mentioned is that the input signal is normalized before entering the predistorter so that the maximum amplitude will be 1. For this amplitude range, the gain of the amplifier changes between 15 and 7.5 but the aim is to keep it constant at 10 with the help of predistortion.

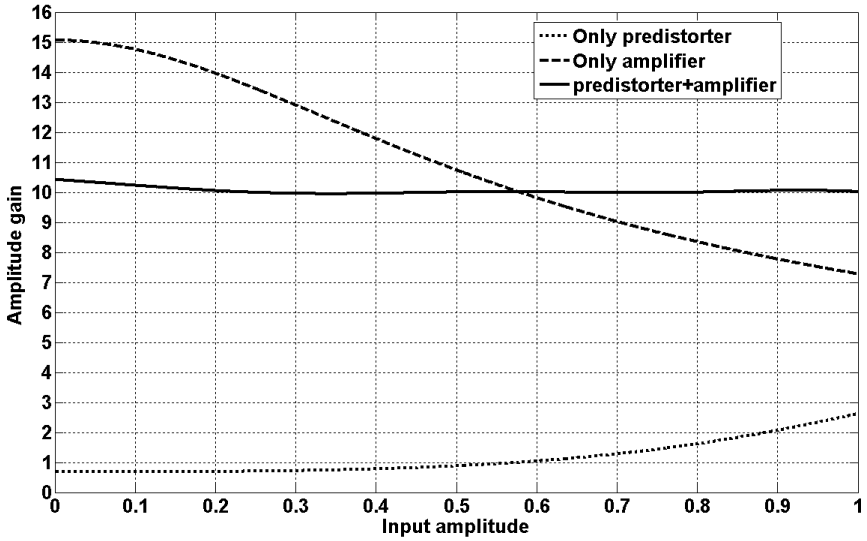


Figure 4.10: Gain of polar polynomial predistorter of order 10, amplifier and polar polynomial predistorter & amplifier combination

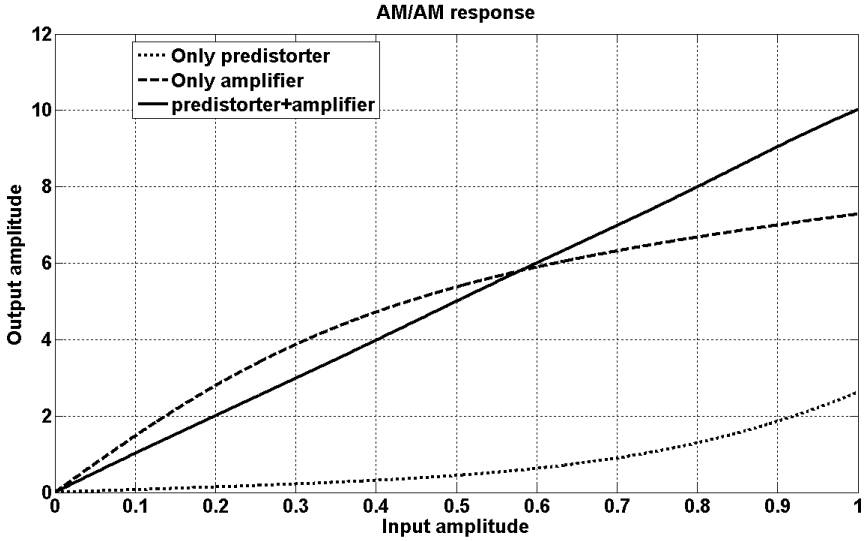


Figure 4.11: AM/AM response of polar polynomial predistorter of order 10, amplifier and polar polynomial predistorter & amplifier combination

Figures 4.10, 4.11 and 4.12 correspond to a polar polynomial predistorter which has amplitude and phase polynomials of order 10. They show the gain

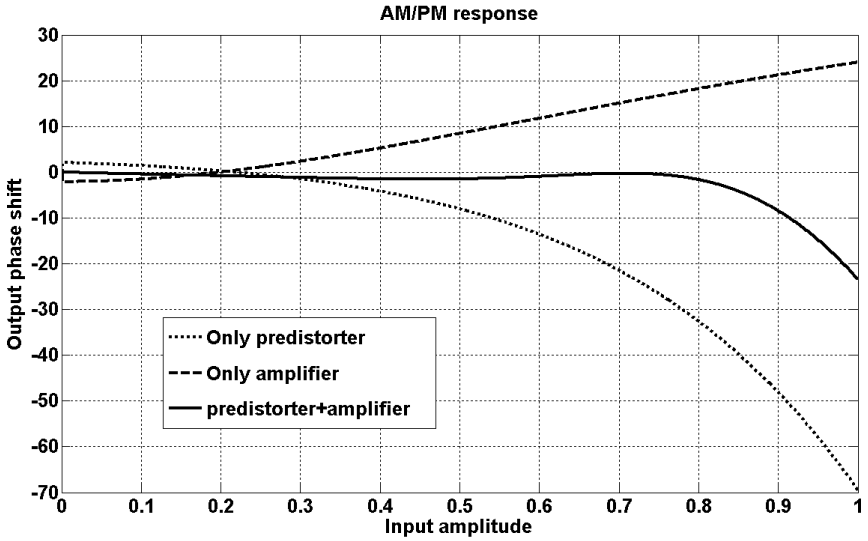


Figure 4.12: AM/PM response of polar polynomial predistorter of order 10, amplifier and polar polynomial predistorter & amplifier combination

& AM/AM response & AM/PM response of the predistorter alone, the amplifier alone and predistorter & amplifier combination. The predistorter has been trained and tested with 100000 16-QAM symbols. The update steps μ_V and μ_P used in the training process are 0.01 and 0.001. These values of μ_V and μ_P were found by trial-and-error method and they provide good convergence characteristics for the update mechanism. As seen in the figures, the polar polynomial predistorter has a pretty good performance. It compensates for the compressive characteristic of the amplifier by providing an expansive characteristic. Without the predistorter, the amplifier has a compressive AM/AM response and a gain that changes between 7.5 and 15 in the input amplitude range. With the predistorter, the gain is fixed to 10. It deviates a little from 10 for small input amplitudes. With the predistorter, the AM/AM response becomes pretty linear. With the predistorter, the AM/PM response is also fixed. It stays approximately constant at 0 for most of the input amplitude range but shows some deviation for large amplitude values. The largest deviation occurs when the input amplitude is 1(which is the biggest possible input amplitude) and is about -23°. The reason for the very small deviation in the AM/AM response for small input amplitudes and the large deviation in the AM/PM response for large input amplitudes is

that there are not enough samples in the input signal for low and high amplitudes and as a result, the predistorter is not trained well for those amplitude values.

Figures 4.13 and 4.14 show the spectral plots for the same case. Figure 4.13

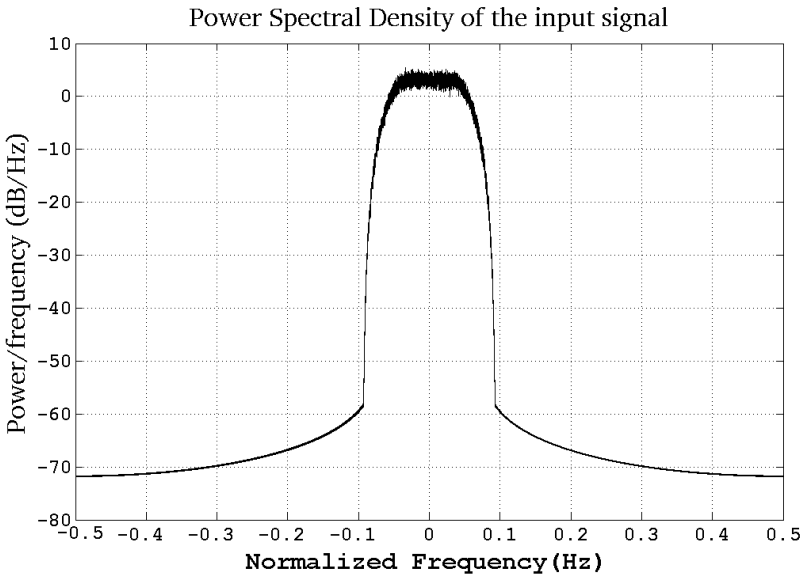


Figure 4.13: Power Spectral Density of the input signal to the polar polynomial predistorter

shows the power spectral density of the input signal to the polar polynomial predistorter. Figure 4.14 shows the power spectral density of the output signal of the amplifier when the polar polynomial predistorter exists and does not exist before the amplifier. As seen in the figures, the amplifier causes both in-band and out-of-band distortion. The out-of-band distortion will cause adjacent channel interference for adjacent channels. The predistorter avoids this to some extent by reducing out-of-band distortion. As observed in Figure 4.14, there is approximately 20 dB reduction in adjacent channel power ratio.

Figure 4.15 shows the bit error rate performance of the designed polar polynomial predistorter under additive white gaussian noise. To calculate BER, the output of the amplifier is passed through an AWGN channel and then demodulated by a 16-QAM demodulator. SNR(signal-to-noise ratio, E_b/N_0) of the AWGN channel is changed between 0 dB and 20 dB and the corresponding BER is calculated for every case. As seen in the figure, when there is no predistorter,

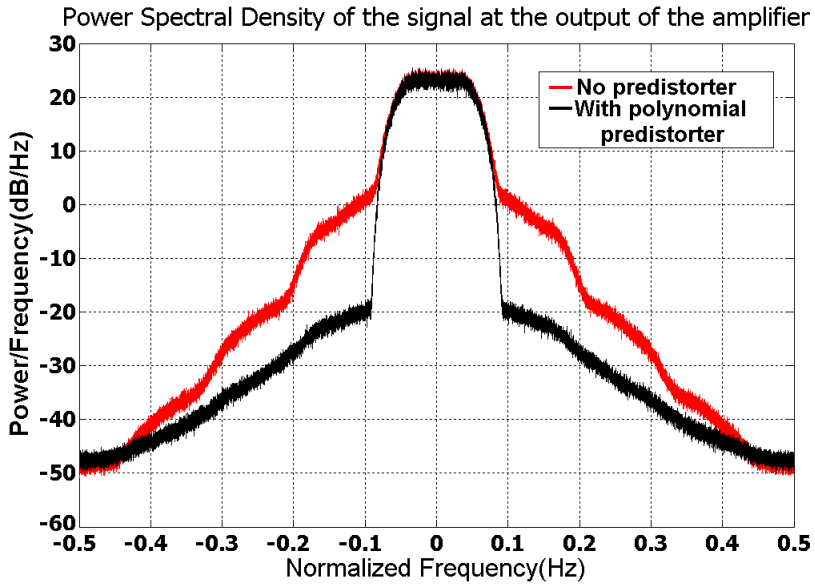


Figure 4.14: Power Spectral Density of the output signal of the amplifier

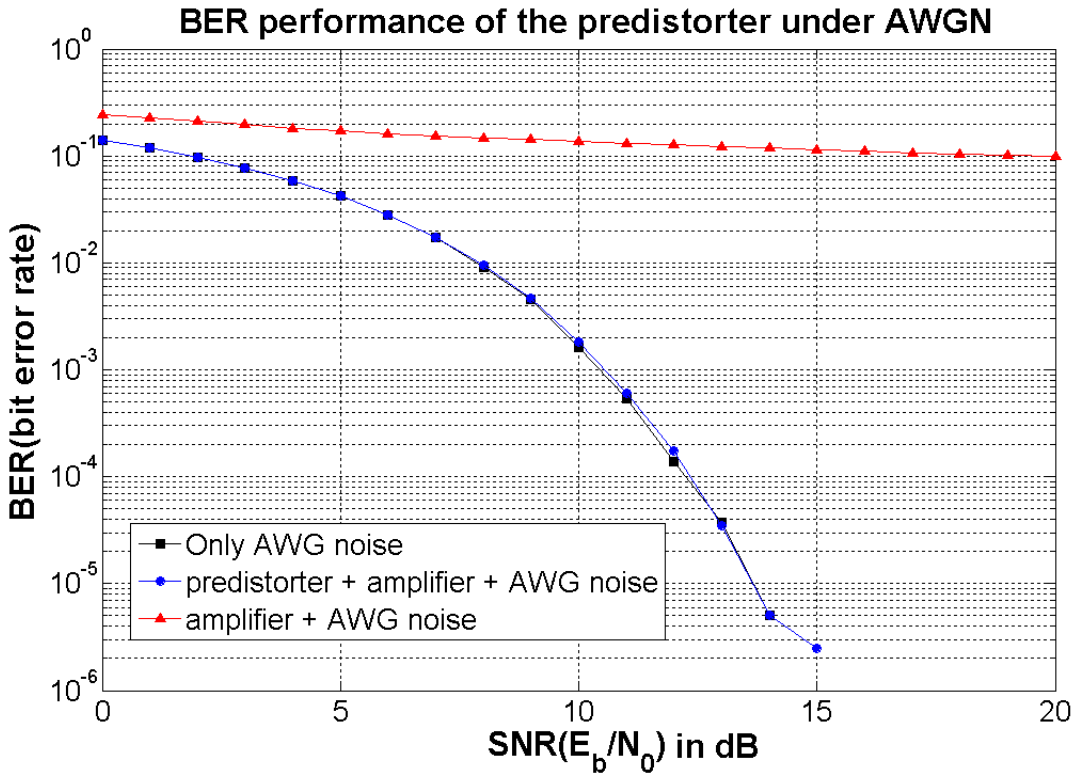


Figure 4.15: BER performance of the polar polynomial predistorter under additive white gaussian noise

the nonlinearity of the amplifier dominates over the noise and becomes the factor that determines BER. For that case, even if SNR increases, BER decreases only a little amount and settles down at a level of 0.09 for SNR = 20 dB. This is the lower limit of BER set by the nonlinear amplifier. When the polar polynomial predistorter is present in the system, it compensates for the nonlinear effects of the amplifier and as a result, the BER equals the theoretical BER under AWGN, which is the square marked plot in Figure 4.15.

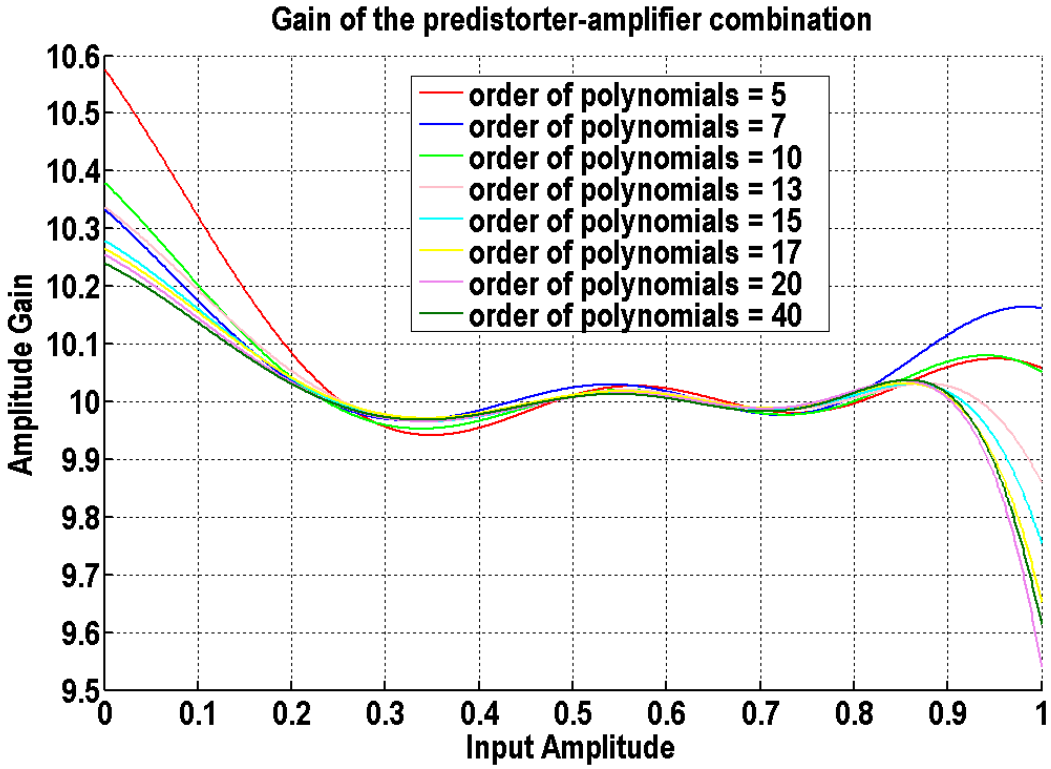


Figure 4.16: Gain of the polar polynomial predistorter-amplifier combination for different polynomial orders

To see the effect of order of AM/AM response & AM/PM response polynomials on the performance of the polar polynomial predistorter, the order of AM/AM response & AM/PM response polynomials of the polar polynomial predistorter was set to 5,7,13,15,17,20 and 40 while keeping the other parameters constant. Figures 4.16 and 4.17 show the gain and AM/PM response of the predistorter-amplifier combination for these polynomial orders. As seen in Figure 4.16, for

mid-range amplitude values all cases show the same performance and they manage to keep the gain constant at the desired value of 10. For low amplitude values, all cases deviate from the desired gain value 10. The deviations are small and it is observed that the deviation decreases when the polynomial order is increased. The maximum deviation corresponds to the *order of polynomials = 5* case, which has a gain deviation of 0.57. For large amplitude values, there is again a small deviation from the desired gain value 10. Some cases show positive gain deviation while others show negative gain deviation for large amplitude values. It seems that increasing the order of polynomials increases the gain deviation for large amplitude values, too. In this case, the maximum gain deviation corresponds to the *order of polynomials = 20* case, which has a gain deviation of 0.45. It can be concluded that the order of polynomials does not have a strong effect on AM/AM performance of the polar polynomial predistorter. Increasing the order beyond a reasonable value does not change and enhance the AM/AM performance much. In terms of AM/PM response, all cases show good performance for low and mid-range amplitude values but there is a great deviation from the ideal phase shift value 0 for large amplitude values. In this case, the best performance corresponds to the largest polynomial order value 40, which has a maximum phase deviation of 9°. Starting with polynomial order 5, increasing the order of polynomials first increases this deviation till order value 10 which has the maximum phase deviation(25°). After this value, increasing the order of polynomials enhances the AM/PM performance, decreases the deviation and the best performance is reached at the maximum polynomial order value 40. So it can be concluded that increasing the order of polynomials enhances the AM/PM performance of the polar polynomial predistorter.

As mentioned before, other than a polar polynomial predistorter, a polar look-up table predistorter was also implemented. Figures 4.18, 4.19 and 4.20 correspond to a polar look-up table predistorter which has a size of 128(128 AM/AM response entries & 128 AM/PM response entries). They show the gain

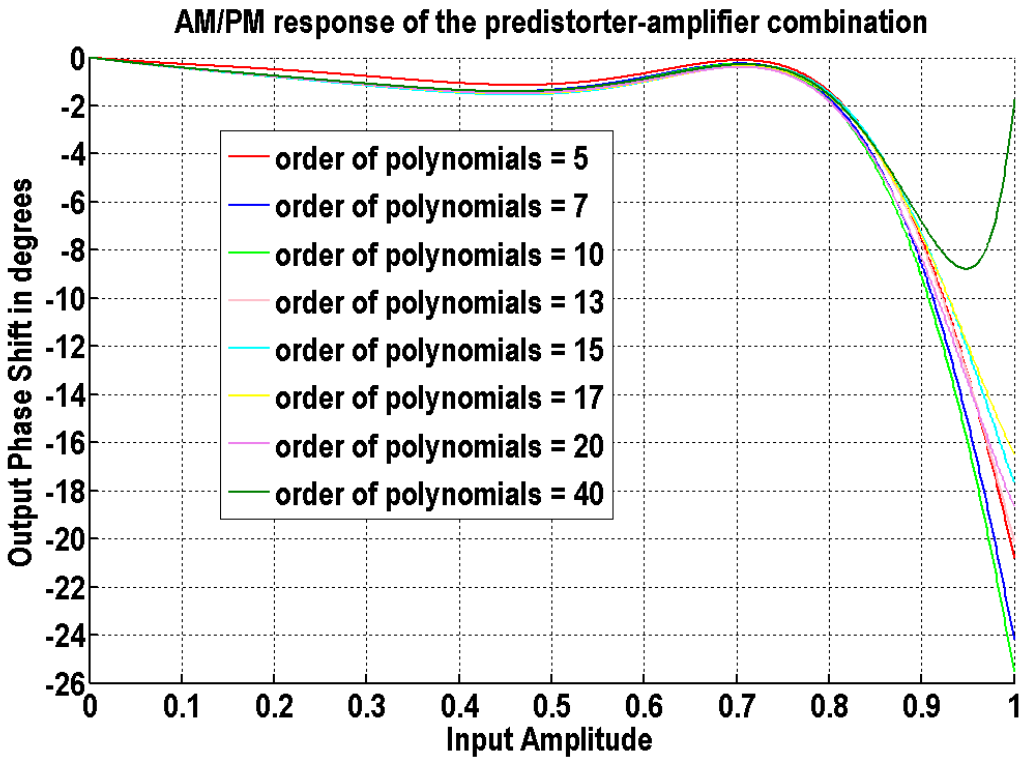


Figure 4.17: AM/PM response of the polar polynomial predistorter-amplifier combination for different polynomial orders

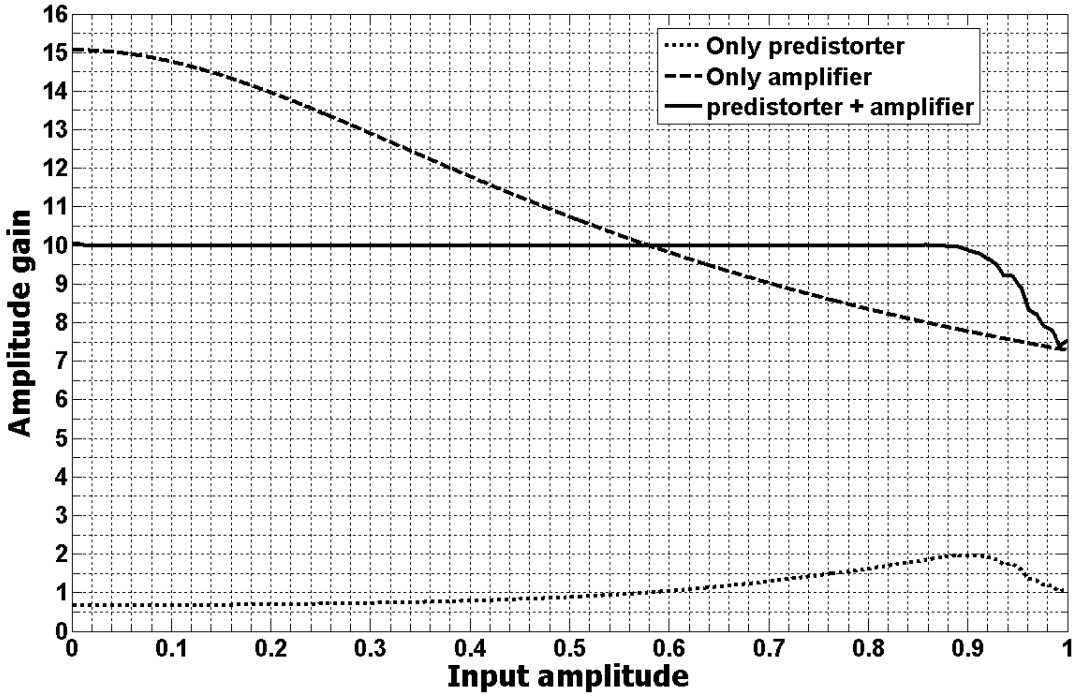


Figure 4.18: Gain of polar look-up table predistorter, amplifier and polar look-up table predistorter & amplifier combination

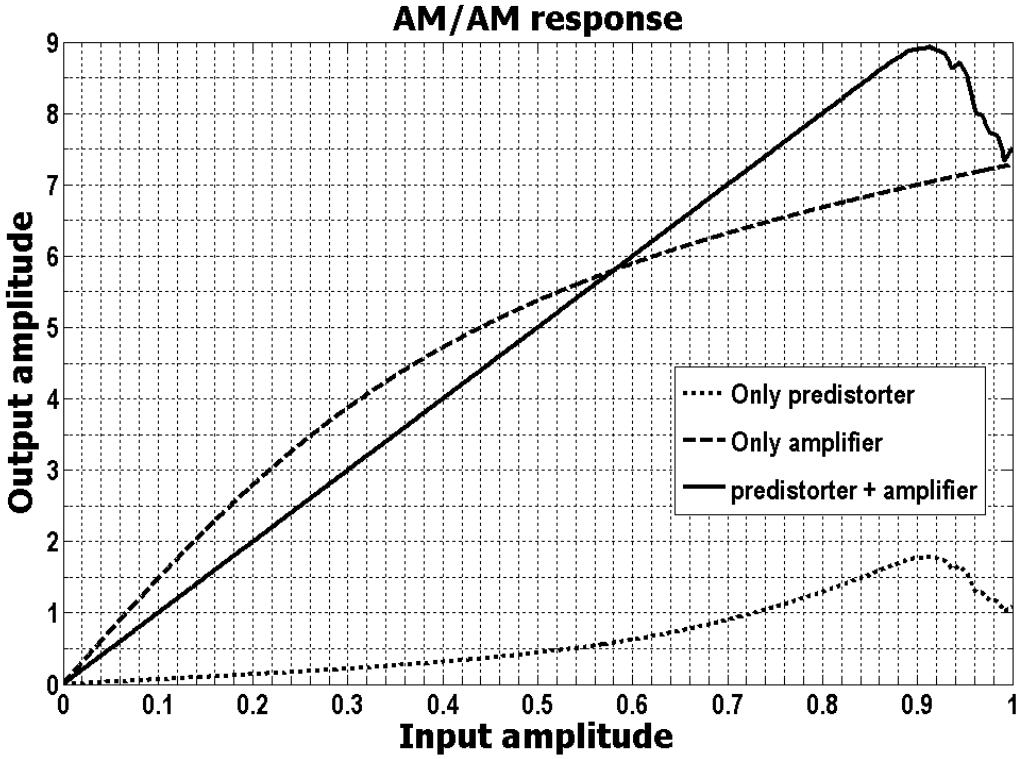


Figure 4.19: AM/AM response of polar look-up table predistorter, amplifier and polar look-up table predistorter & amplifier combination

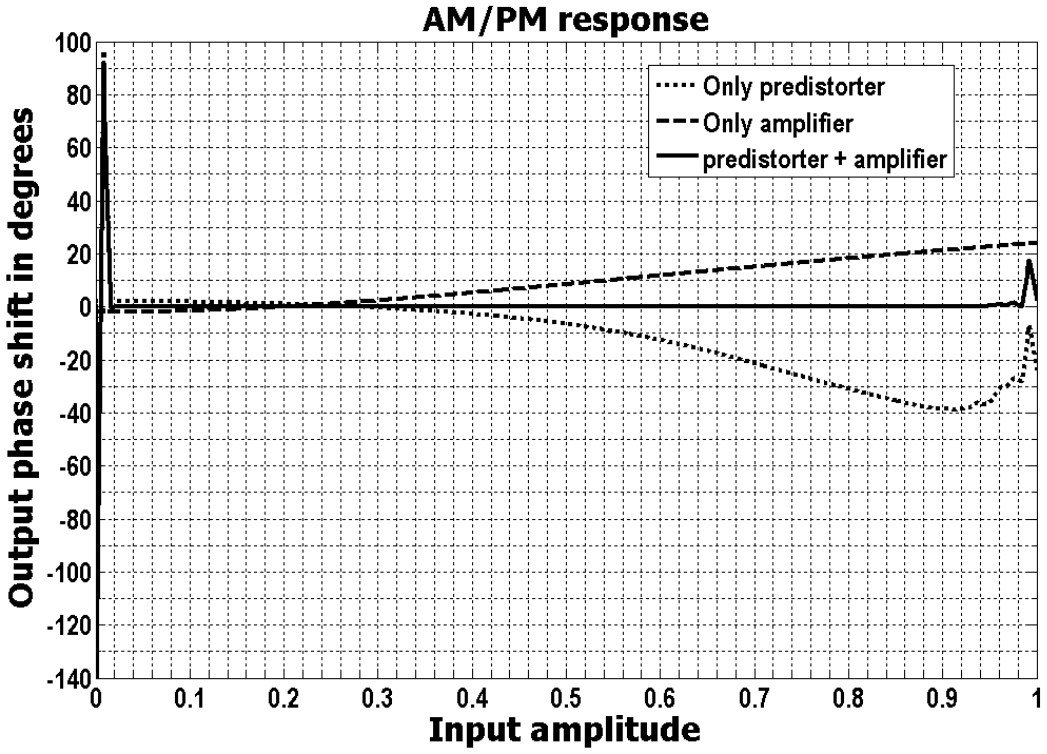


Figure 4.20: AM/PM response of polar look-up table predistorter, amplifier and polar look-up table predistorter & amplifier combination

& AM/AM response & AM/PM response of the predistorter alone, the amplifier alone and predistorter & amplifier combination. The predistorter has been trained and tested with 100000 16-QAM symbols. The update steps S_a and S_p used in the training process are 0.01 and 0.5. These values of S_a and S_p were found by trial-and-error method and they provide good convergence characteristics for the update mechanism. The *range* parameter of the predistorter was set to 1 so the amplitude step used in storing the responses in the look-up table is $\frac{1}{127}$. As seen in the figures, the polar look-up table predistorter has a pretty good performance. It compensates for the compressive characteristic of the amplifier by providing an expansive characteristic. Without the predistorter, the amplifier has a compressive AM/AM response and a gain which changes between 7.5 and 15 in the input amplitude range. With the predistorter, the gain is fixed to 10 except for large input amplitudes. For large input amplitudes, there is a deviation from the desired gain value 10 and from the linear behaviour of AM/AM response. The maximum gain deviation is approximately 2.5. The reason for this behaviour is that there are not enough samples in the input signal for high amplitudes and as a result, the predistorter is not trained well for those amplitude values. As seen in Figure 4.20, the predistorter has also a good AM/PM performance except for low and high amplitude values. It keeps the phase shift constant at 0° except for a small range of low and high amplitude values. For amplitude values smaller than 0.02, there is an unstable behaviour and the predistorter has a very poor AM/PM performance. For amplitude values in the range 0.02-0.94, the predistorter has a perfect AM/PM performance keeping the phase shift constant at 0°. For amplitude values greater than 0.94 upto 1, there is a deviation from the ideal phase shift value 0°. The maximum phase deviation in this range is approximately 20°. The deviation in the AM/PM response for large amplitude values results from poor training but there is no apparent reason for the unstable behaviour observed for small amplitude values.

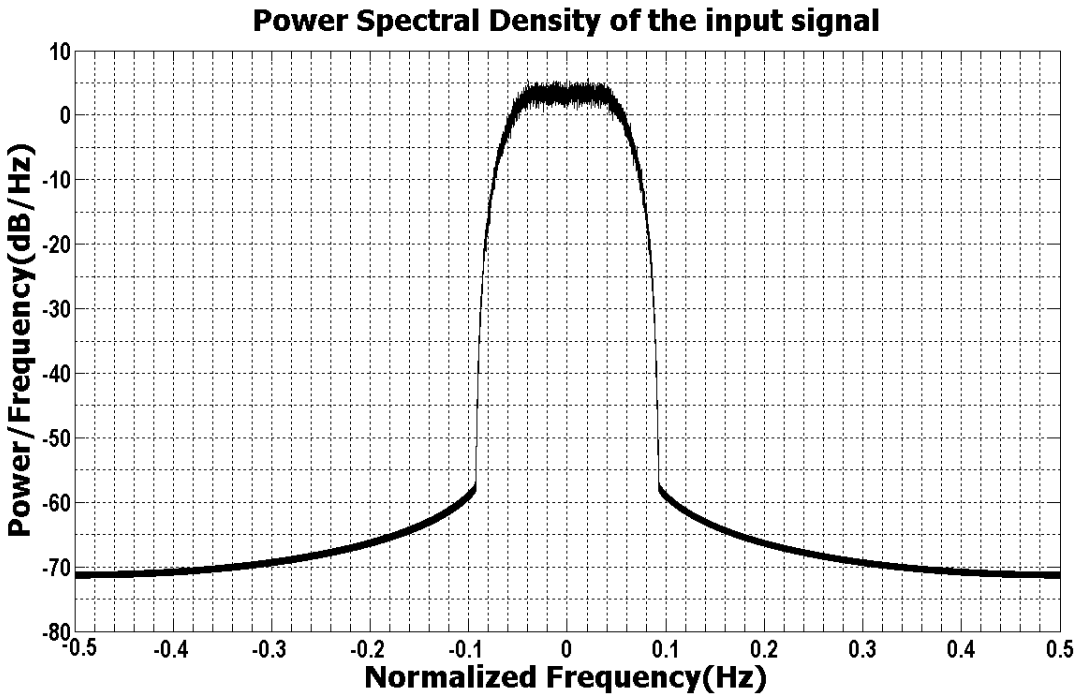


Figure 4.21: Power Spectral Density of the input signal to the polar look-up table predistorter

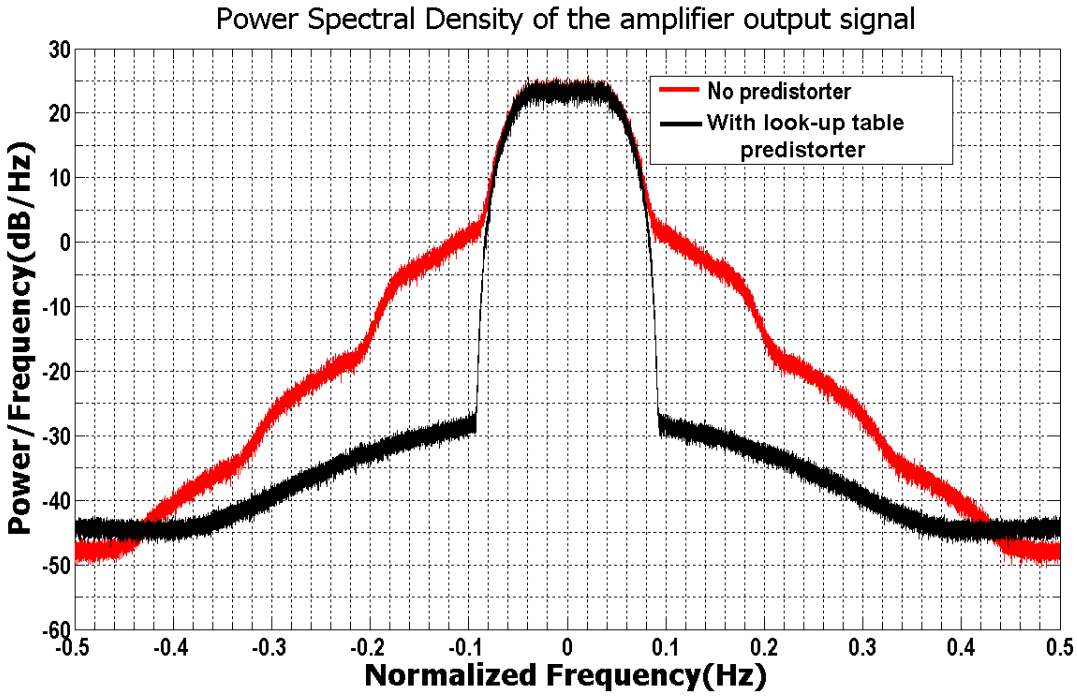


Figure 4.22: Power Spectral Density of the amplifier output signal

Figures 4.21 and 4.22 show the spectral plots corresponding to the polar look-up table predistorter. Figure 4.21 shows the power spectral density of the input signal to the polar look-up table predistorter. Figure 4.22 shows the power spectral density of the amplifier output signal when the polar look-up table predistorter exists and does not exist before the amplifier. As seen in the figures, the power amplifier causes both in-band and out-of-band distortion. The out-of-band distortion will cause adjacent channel interference for adjacent channels. The polar look-up table predistorter avoids this to some extent by reducing out-of-band distortion. As observed in Figure 4.22, there is approximately 25 dB reduction in adjacent channel power ratio. The reduction provided by the polar polynomial predistorter in the adjacent channel power ratio was approximately 20 dB. This means that the performance of the polar look-up table predistorter is better than the performance of the polar polynomial predistorter in terms of out-of-band distortion reduction.

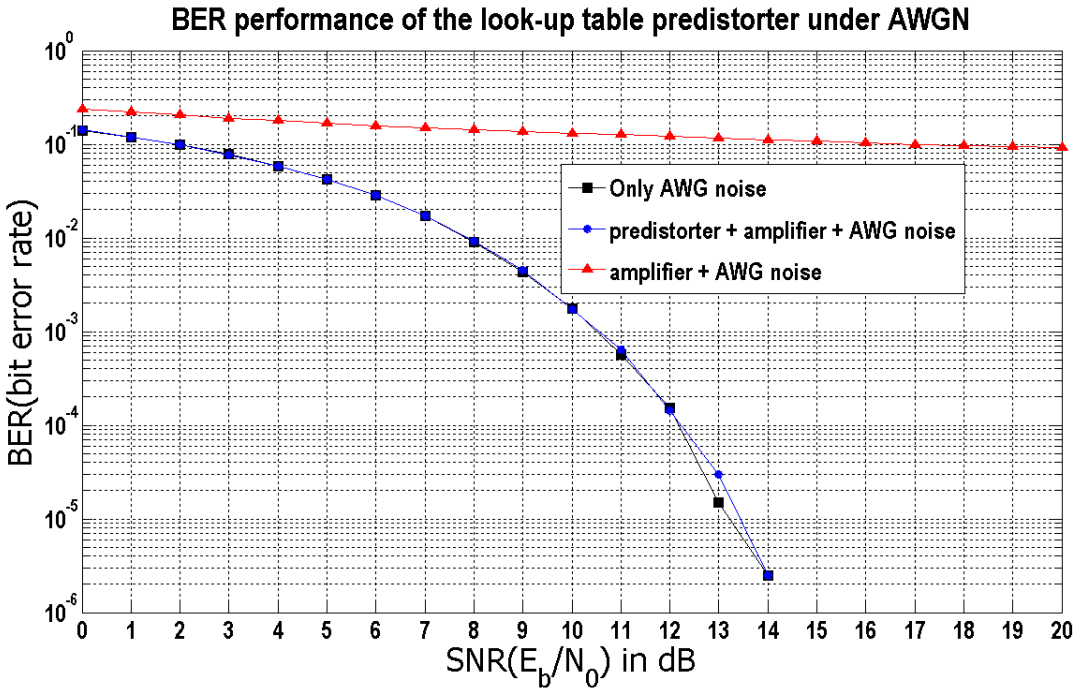


Figure 4.23: BER performance of the polar look-up table predistorter under additive white gaussian noise

Figure 4.23 shows the bit error rate performance of the designed polar look-up table predistorter under additive white gaussian noise. To calculate BER, the output of the amplifier is passed through an AWGN channel and then demodulated by a 16-QAM demodulator. SNR(signal-to-noise ratio, E_b/N_0) of the AWGN channel is changed between 0 dB and 20 dB and the corresponding BER is calculated for every case. As seen in the figure, when the look-up table predistorter is not present in the system, the nonlinearity of the amplifier dominates over the noise and becomes the factor that determines BER. For that case, even if SNR increases, BER decreases only a little amount and settles down at a level of 0.09 for SNR = 20 dB. This is the lower limit of BER set by the nonlinear amplifier. When the polar look-up table predistorter is present in the system, it compensates for the nonlinear effects of the amplifier and as a result, the BER equals the theoretical BER under AWGN, which is the square marked plot in Figure 4.23.

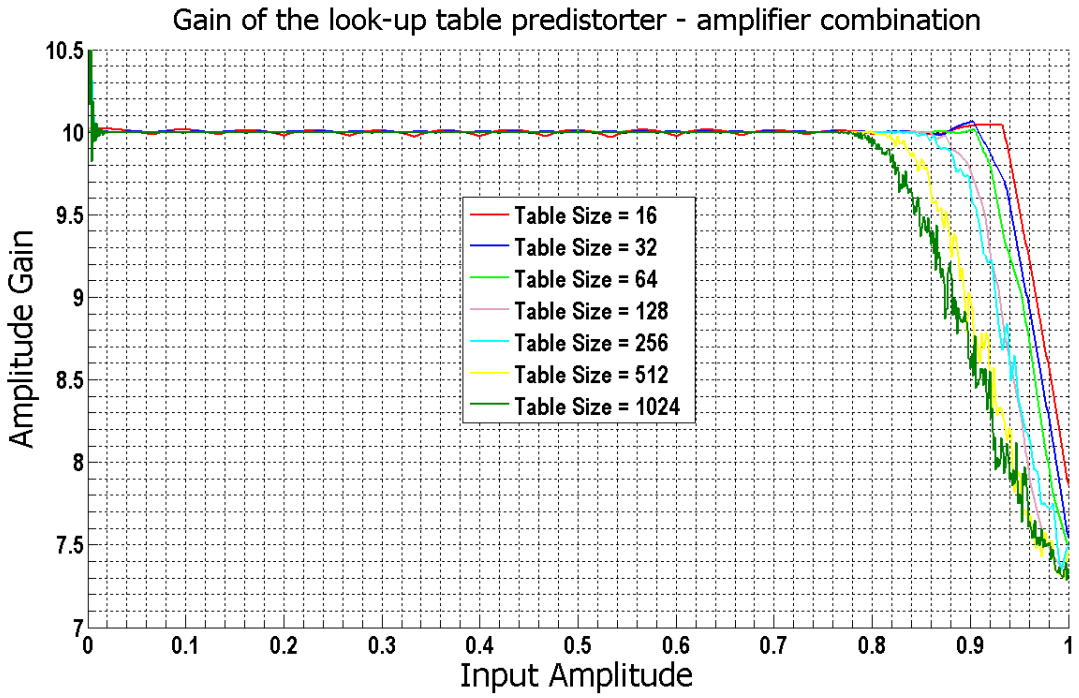


Figure 4.24: Gain of the polar look-up table predistorter-amplifier combination for different table sizes

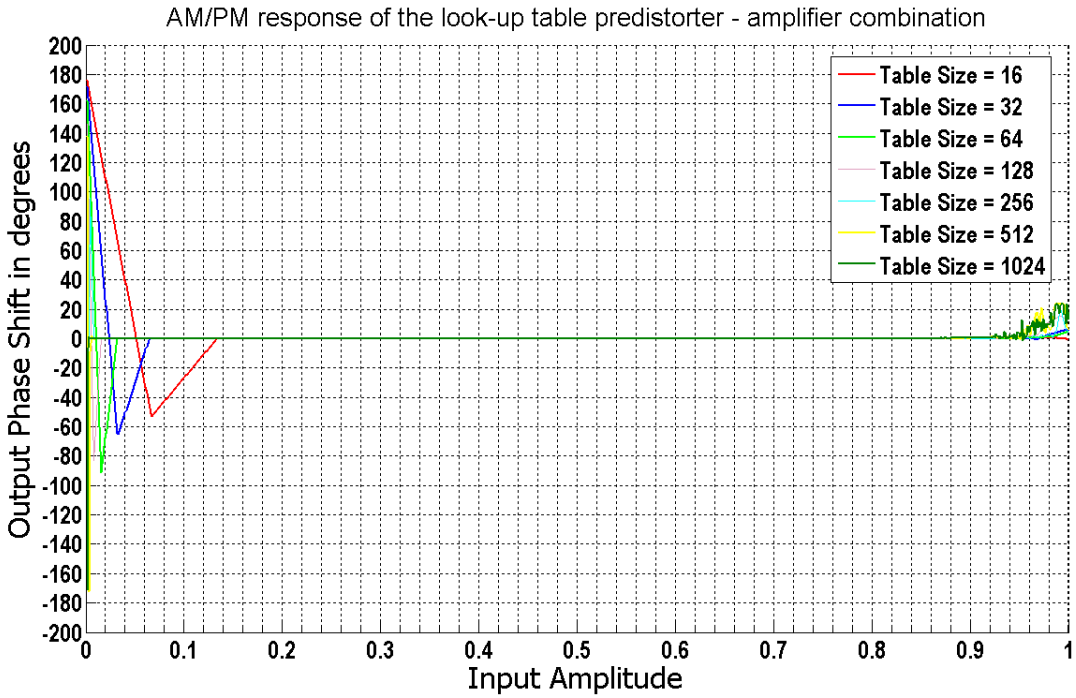


Figure 4.25: AM/PM response of the polar look-up table predistorter-amplifier combination for different table sizes

To see the effect of table size on the performance of the polar look-up table predistorter, table size of the polar look-up table predistorter was set to 16, 32, 64, 256, 512 and 1024 while keeping the other parameters constant. Figures 4.24 and 4.25 show the gain and AM/PM response of the predistorter-amplifier combination for these table sizes. The gain of *Table size = 512* and *Table size = 1024* cases show unstable behaviour for very small amplitude values but this is not observed in Figure 4.24 because the y axis is limited to the range 7-10.5. Other than this, all cases show good performance for small and mid-range amplitude values and keep the gain constant at the desired value 10. For large amplitude values, all cases show deviation from the ideal behaviour. It is observed that the amount of maximum gain deviation increases with increasing table size. It is also observed that the input amplitude at which the deviation from the ideal behaviour starts decreases with increasing table size. It seems that increasing the table size has a negative effect on AM/AM performance. In terms of AM/PM response, all cases show good performance for mid-range amplitude values and

keep the phase shift constant at the ideal value 0°. For large amplitude values, there is a deviation from this ideal behaviour and it is observed that this phase deviation increases with increasing table size. The maximum phase deviation corresponds to *Table size = 1024* case and it has a value of approximately 20°. For small input amplitudes, all cases show unstable behaviour. This unstable behaviour starts at *amplitude = 0* and extends upto a certain amplitude. It is observed that the extent of the unstable behaviour decreases with increasing table size. Increasing the table size has both positive and negative effects on AM/PM performance but the extent of the unstable behaviour is more important than the deviation observed at large amplitudes. So it can be concluded that increasing the table size enhances the AM/PM performance.

The work done with predistortion is not limited to what is described above. The effect of lowpass filtering on the performance of the predistorter was also investigated. In a real communication system, there exists a bandpass IF filter between the mixer and power amplifier stages in transmitting chains. Such a filter is crucial and necessary to suppress out-of-band interference in a real communication system. Therefore a simulation of a communication system ignoring this filter would not be realistic. The effect of this filter is included in the predistorter simulations and how the performance of the predistorter changes is investigated. Since the simulations are carried out in baseband and every element is represented by its baseband equivalent, this bandpass filter is represented as an equivalent baseband lowpass filter in the simulated system model. As in the previous cases, the first phase in the simulations is training. Training is done exactly in the same way as the previous cases and the lowpass filter is not included in the system model during training phase. As in the previous cases, testing phase comes after training but this time there is a difference from the previous cases. There is a lowpass filter between the predistorter and power amplifier. Figure 4.26 shows the simulated system model for this case.

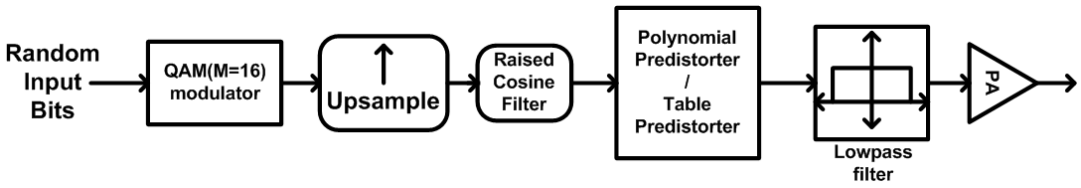


Figure 4.26: Simulated system model including lowpass filter

In the simulations, the lowpass filter is implemented as a FIR filter which has a finite length impulse response. This filter has two parameters which are the length of its impulse response and its cutoff frequency. The length of the impulse response determines how well the filter approximates an ideal lowpass filter. As it increases, the approximation of the ideal lowpass filter behaviour gets better. It also determines the group delay of the lowpass filter, which is given by $\frac{\text{filter impulse response length} - 1}{2}$. In the simulations, this length parameter was set to 1001 and for this value of the filter length, the ideal lowpass filter behaviour is approximated pretty well. The cutoff frequency of the lowpass filter is assigned relative to *sampling frequency/2* and must be in the range $0 < \textit{cutoff frequency} < 1$ where 1 corresponds to *sampling frequency/2*. Figure 4.27 shows the transfer function of the lowpass filter on a normalized frequency axis for the parameter values filter length = 1001, cutoff frequency = 0.2. The interpretation of the normalized frequency axis is also given in the figure. The bandwidth of the lowpass filter must be larger than the bandwidth of the raised cosine filter in the simulations. The ratio of the bandwidth of the lowpass filter to the bandwidth of the raised cosine filter is given by $\frac{\text{cutoff} * \text{upsampling factor}}{1 + \text{rolloff factor}}$ where *cutoff* is the relative cutoff frequency of the lowpass filter, *rolloff factor* is the rolloff factor of the raised cosine filter and *upsampling factor* is the upsampling factor used in the simulations. So for the bandwidth of the lowpass filter to be larger than the bandwidth of the raised cosine filter, *cutoff* should satisfy $\text{cutoff} > \frac{1 + \text{rolloff factor}}{\text{upsampling factor}}$. It is the ratio of filter bandwidths that determines the effect of lowpass filtering on the performance of the predistorter. To see this effect, the ratio of filter bandwidths is changed in the simulations by changing the

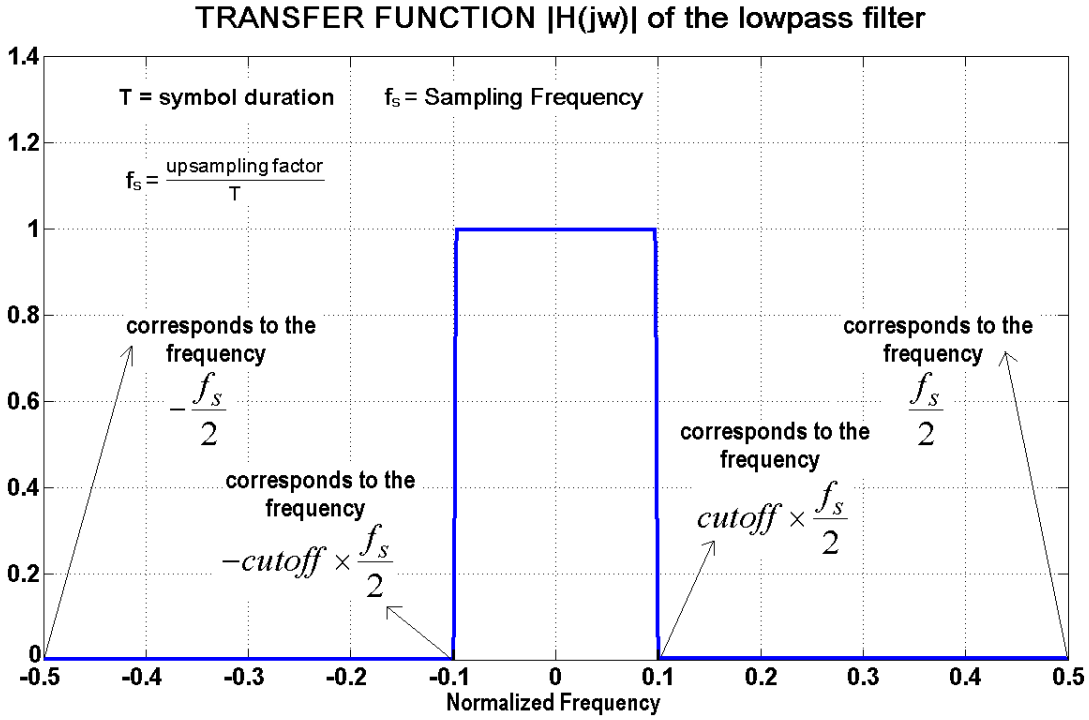


Figure 4.27: Transfer function of the lowpass filter for filter length = 1001, cutoff frequency = 0.2

upsampling factor and the cutoff frequency of the lowpass filter. While changing these two parameters, it is made sure that the bandwidth of the lowpass filter is larger than the bandwidth of the raised cosine filter. The length of the impulse response of the lowpass filter is set to 1001 in all of the simulations. The other simulation parameters are kept the same as in previous cases. It will be good to repeat their values here once again. The delay parameter of the raised cosine filter was set to 1000. The rolloff factor of the raised cosine filter was set to 0.5. The desired gain of the amplifier-predistorter combination was set to 10. In the training and testing phases, 100000 16-QAM symbols were used. The update steps used during training for the polynomial predistorter(μ_V and μ_P) and the look-up table predistorter(S_a and S_p) were also kept the same. μ_V and μ_P were set to 0.01 and 0.001. S_a and S_p were set to 0.01 and 0.5.

The effect of lowpass filtering on the performance of the predistorter is first analyzed in terms of power spectral density. Figure 4.28 corresponds to a polar polynomial predistorter which has amplitude and phase polynomials of order 10.

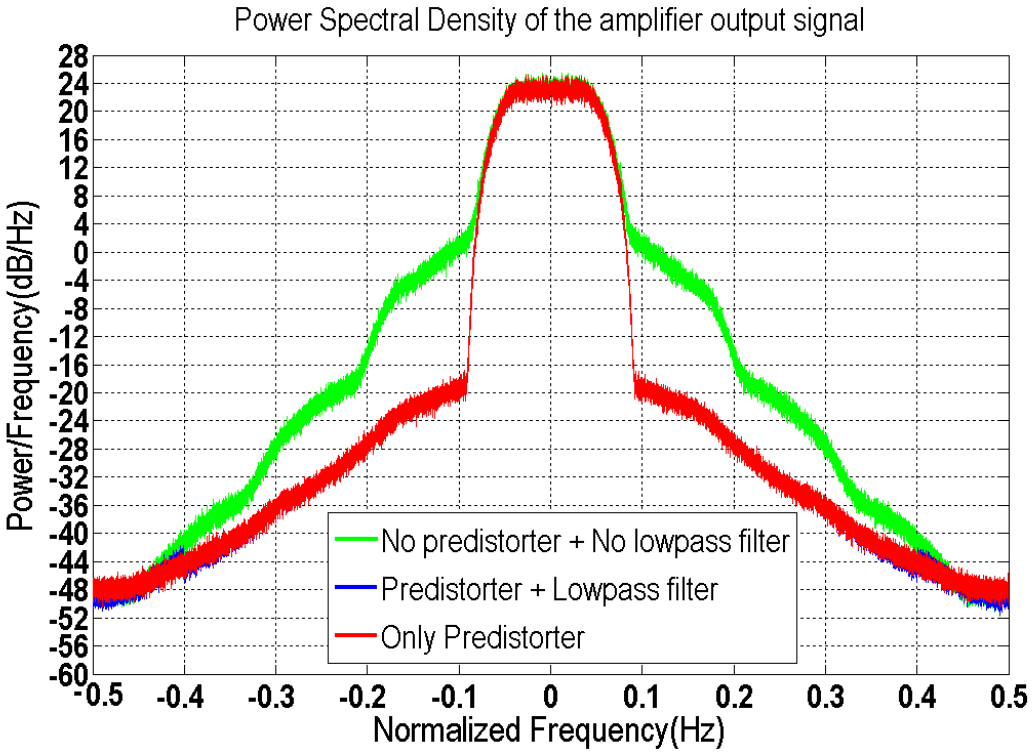


Figure 4.28: Spectral performance of the polar polynomial predistorter which has AM/AM & AM/PM polynomials of order 10 for the case where ratio of filter bandwidths = 4.27

It shows the power spectral density of the amplifier output signal when there is no predistorter & lowpass filter before the amplifier, when there is a predistorter but no lowpass filter before the amplifier and when there is a predistorter & lowpass filter before the amplifier. The cutoff frequency of the lowpass filter is 0.8 and the upsampling factor is 8. So the ratio of filter bandwidths is $\frac{0.8 * 8}{1 + 0.5} = 4.27$. The bandwidth of the lowpass filter is much larger than the bandwidth of the raised cosine filter and as a result, lowpass filtering has no effect on the performance of the polar polynomial predistorter for this case. The blue and red curves almost completely overlap. There is a very small difference between them.

Figure 4.29 shows the spectral performance of the same polynomial predistorter for the case where cutoff frequency of the lowpass filter = 0.6. All the other parameters are kept the same. The ratio of filter bandwidths for this case is $\frac{0.6 * 8}{1 + 0.5} = 3.2$. The effect of the lowpass filter on predistorter performance can be clearly observed in the figure. Blue and red curves overlap up to the cutoff

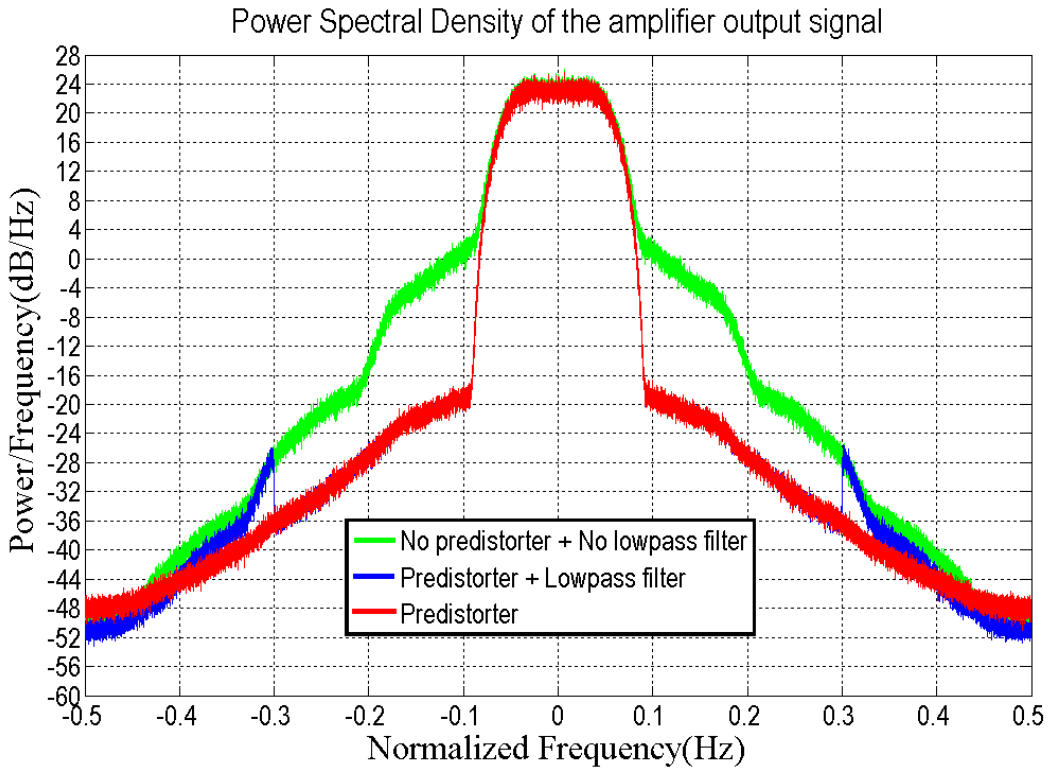


Figure 4.29: Spectral performance of the polar polynomial predistorter which has AM/AM & AM/PM polynomials of order 10 for the case where ratio of filter bandwidths = 3.2

frequency of the lowpass filter but after that point, the blue curve is approximately the same as green curve(no predistorter case). The reason for this is that for that frequency range, the effect of the predistorter is removed by the lowpass filter and as a result, the nonlinear behaviour of the amplifier shows itself in that frequency range. We can also conclude that although the bandwidth ratio is again large like cutoff frequency = 0.8 case, it is not enough for the lowpass filter to have approximately no effect on the performance of the predistorter.

Figure 4.30 shows the spectral performance of the same polynomial predistorter for the case where cutoff frequency of the lowpass filter = 0.4. All the other parameters are kept the same. The ratio of filter bandwidths for this case is $\frac{0.4 * 8}{1 + 0.5} = 2.13$. The effect of the lowpass filter on predistorter performance can be observed in this figure, too. Blue and red curves overlap up to the cutoff frequency of the lowpass filter but after that point, the blue curve is approximately the same as green curve(no predistorter case). The reason for this is that

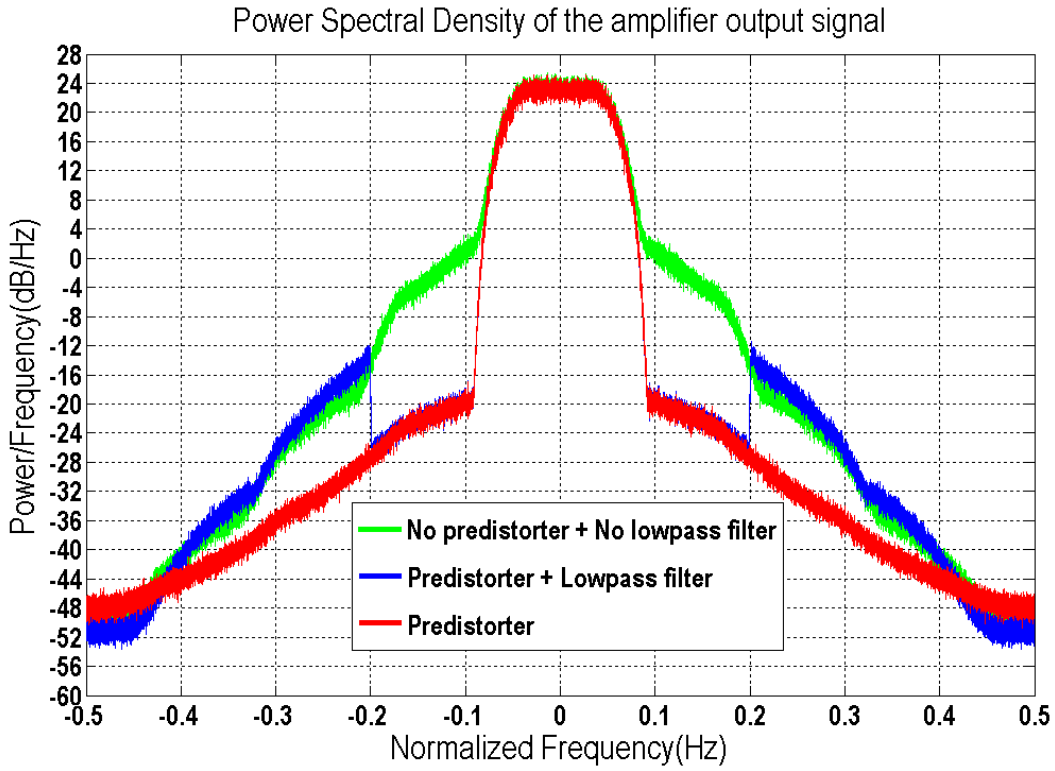


Figure 4.30: Spectral performance of the polar polynomial predistorter which has AM/AM & AM/PM polynomials of order 10 for the case where ratio of filter bandwidths = 2.13

for that frequency range, the effect of the predistorter is removed by the lowpass filter and as a result, the nonlinear behaviour of the amplifier shows itself in that frequency range. As observed from both Figure 4.29 and Figure 4.30, the negative effect of the lowpass filter on the performance of the polar polynomial predistorter increases as the ratio of filter bandwidths decreases.

The effect of lowpass filtering on the performance of the predistorter is also analyzed in terms of AM/AM and AM/PM responses. Figures 4.31 and 4.32 show the AM/AM and AM/PM performance of the same polar polynomial predistorter for the case where cutoff frequency of the lowpass filter = 0.8, upsampling factor = 8 and desired constant gain = 10. For these parameter values, ratio of filter bandwidths is 4.27. As seen in the figures, lowpass filtering degrades the performance of the predistorter and causes a deviation of gain & phase shift from the case where there is no lowpass filter after the predistorter. It is observed that the deviation of gain & phase shift decreases as the input amplitude increases.

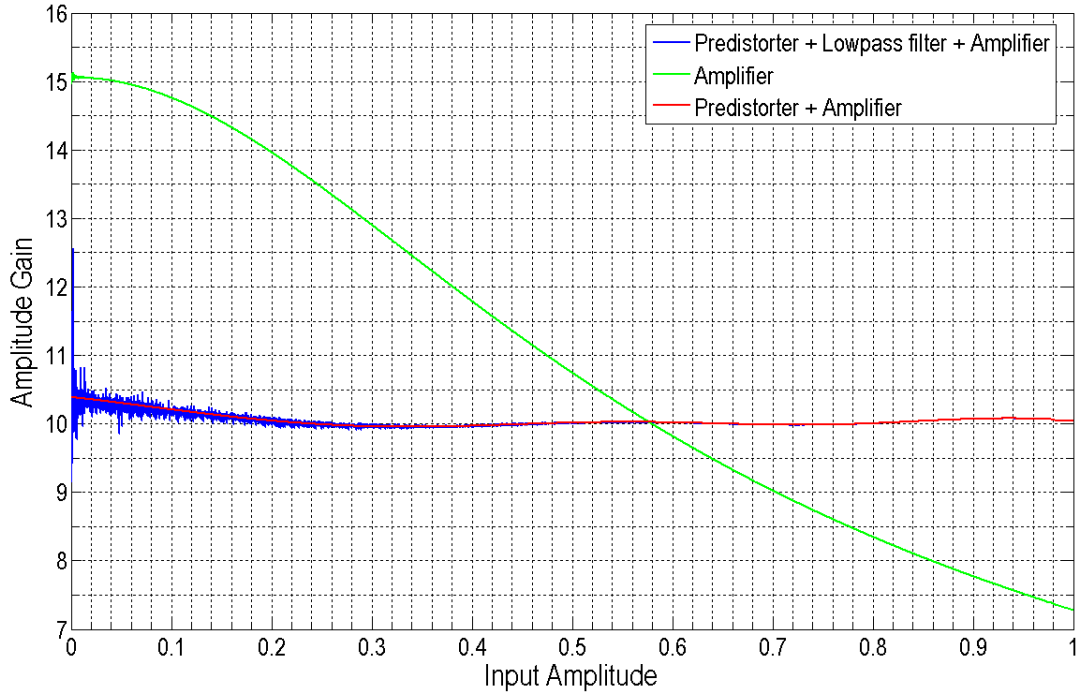


Figure 4.31: AM/AM performance of the polar polynomial predistorter which has AM/AM & AM/PM polynomials of order 10 for the case where ratio of filter bandwidths = 4.27

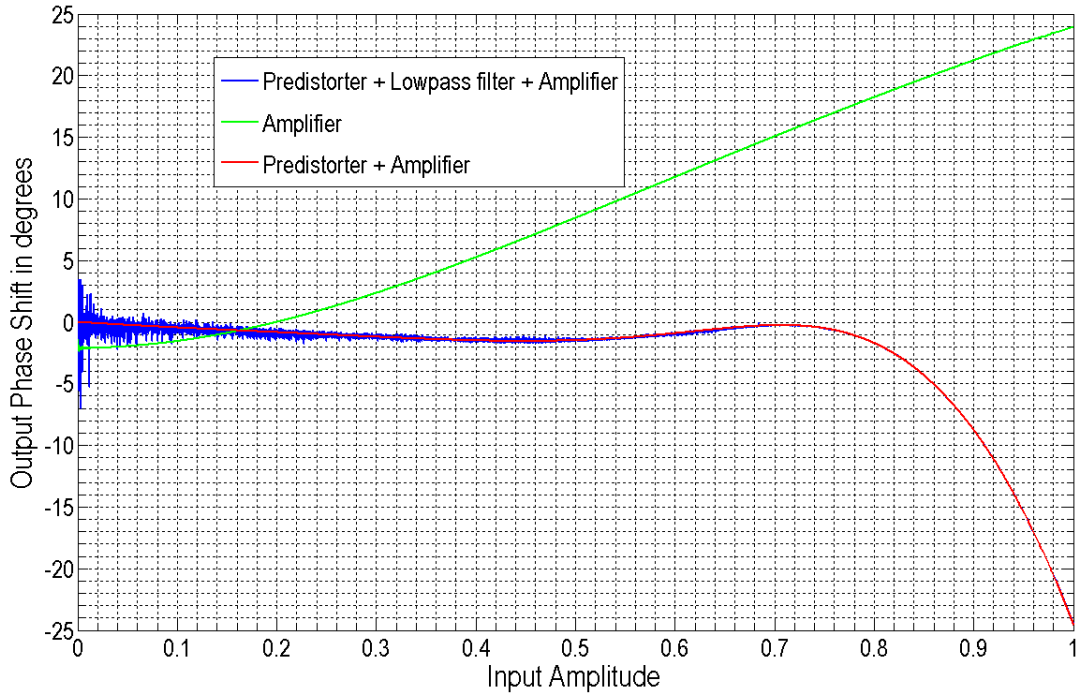


Figure 4.32: AM/PM performance of the polar polynomial predistorter which has AM/AM & AM/PM polynomials of order 10 for the case where ratio of filter bandwidths = 4.27

For large amplitude values, the existence of the lowpass filter doesn't alter the gain or phase shift so if the input amplitude is large, lowpass filtering doesn't affect the performance of the predistorter at all.

Figures 4.33 and 4.34 show the AM/AM and AM/PM performance of the

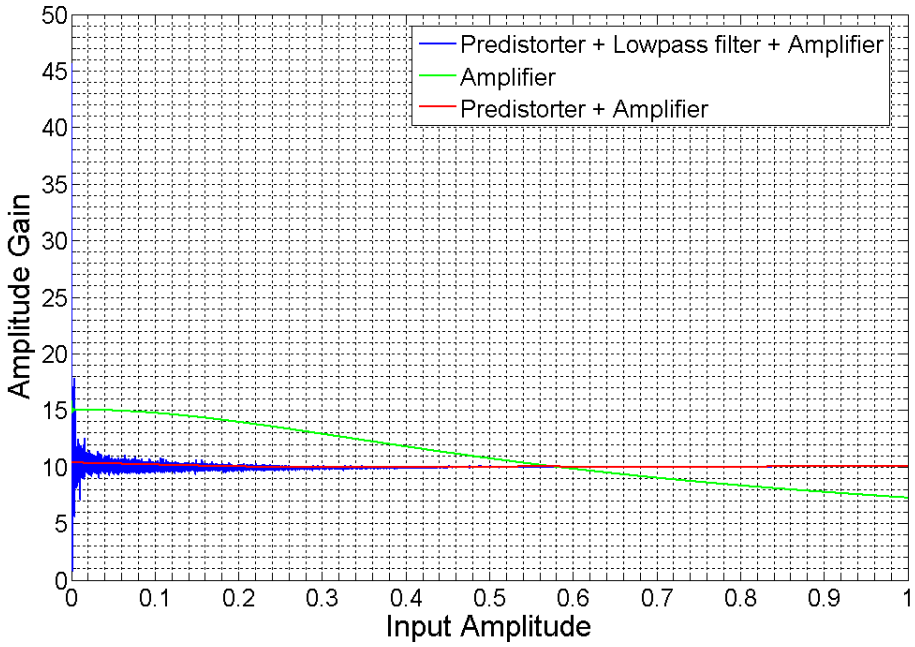


Figure 4.33: AM/AM performance of the polar polynomial predistorter which has AM/AM & AM/PM polynomials of order 10 for the case where ratio of filter bandwidths = 3.2

same polar polynomial predistorter for the case where ratio of filter bandwidths = 3.2(upsampling factor = 8, cutoff frequency of the lowpass filter = 0.6, desired constant gain = 10). Like the previous case, lowpass filtering degrades the performance of the predistorter and causes a deviation of gain & phase shift from the case where there is no lowpass filter after the predistorter. But this time the deviations are larger because the ratio of filter bandwidths is smaller. The decrease in the deviations as the input amplitude increases can be observed here, too.

Figures 4.35 and 4.36 show the AM/AM and AM/PM performance of the same polar polynomial predistorter for the case where ratio of filter bandwidths

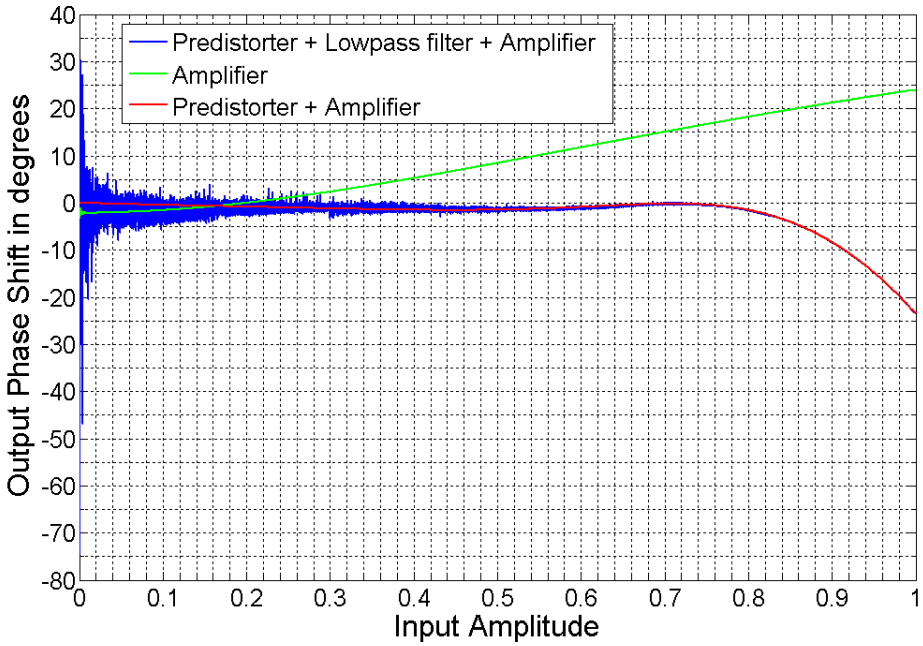


Figure 4.34: AM/PM performance of the polar polynomial predistorter which has AM/AM & AM/PM polynomials of order 10 for the case where ratio of filter bandwidths = 3.2

= 2.13(upsampling factor = 8, cutoff frequency of the lowpass filter = 0.4, desired constant gain = 10). Similar behaviour is observed like the previous two cases. The deviations in the gain & phase shift due to lowpass filtering are larger than the other two cases because the ratio of filter bandwidths is smaller. So the lowpass filtered predistorter has the worst performance for this case among the mentioned three cases. Using these three cases, it can be concluded that the performance of the polar polynomial predistorter gets worse as the ratio of filter bandwidths decreases.

The effect of lowpass filtering on the performance of the predistorter is also evaluated in terms of BER performance under AWGN. Figure 4.37 shows the BER performance of the same polar polynomial predistorter under AWGN when there is a lowpass filter after the predistorter. On the figure, you can see the BER performance for different values of $\frac{\text{the bandwidth of lowpass filter}}{\text{the bandwidth of raised cosine filter}}$. To calculate BER, the output of the amplifier is passed through an AWGN channel and then demodulated by a 16-QAM demodulator. SNR(signal-to-noise ratio,

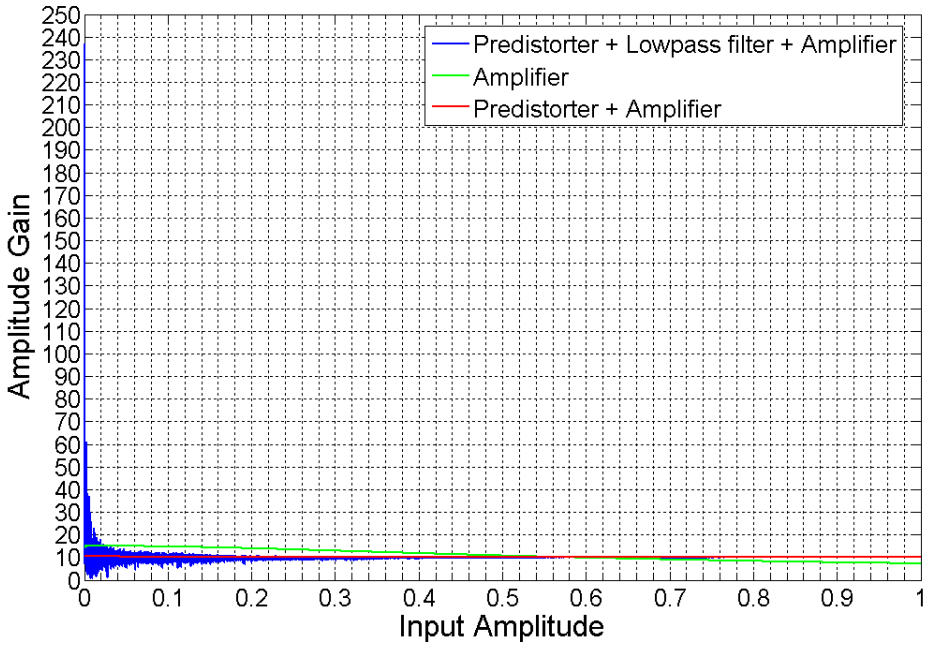


Figure 4.35: AM/AM performance of the polar polynomial predistorter which has AM/AM & AM/PM polynomials of order 10 for the case where ratio of filter bandwidths = 2.13

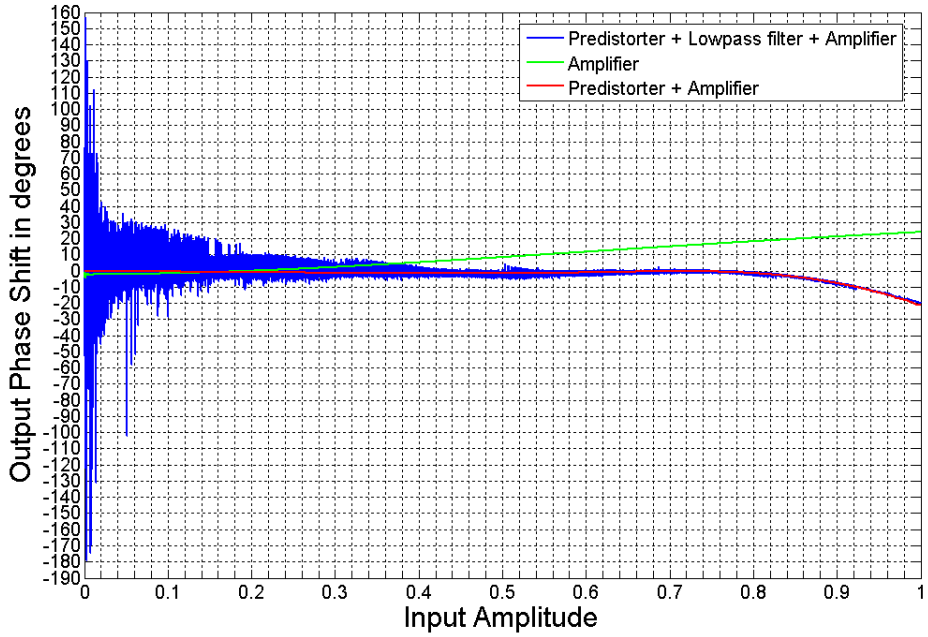


Figure 4.36: AM/PM performance of the polar polynomial predistorter which has AM/AM & AM/PM polynomials of order 10 for the case where ratio of filter bandwidths = 2.13

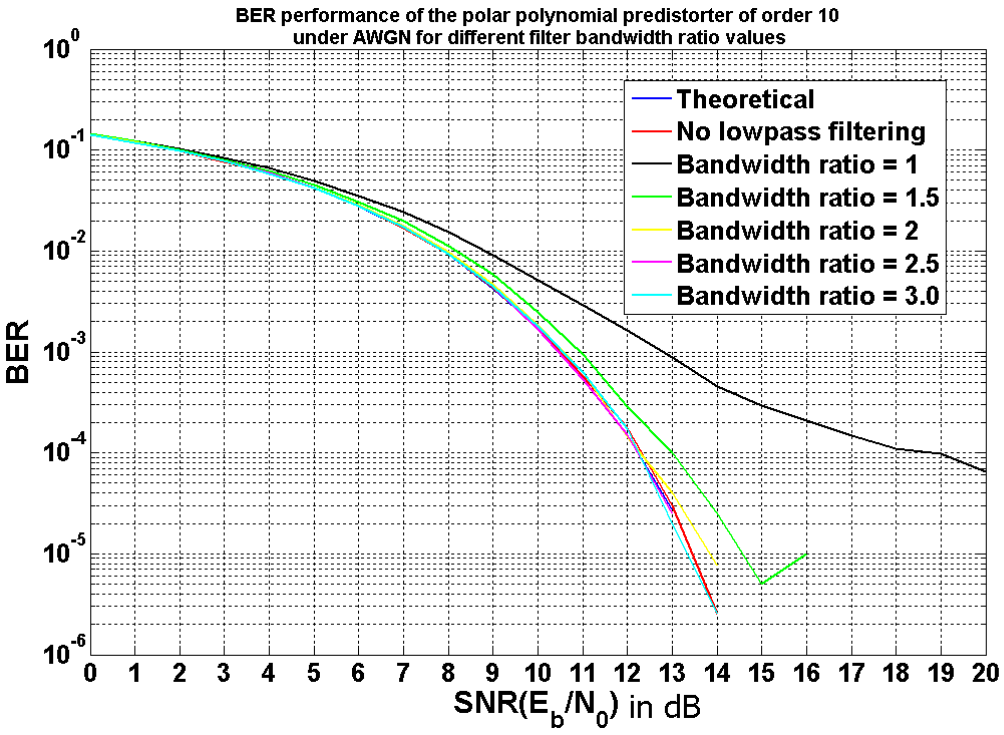


Figure 4.37: BER performance of the polar polynomial predistorter of order 10 under AWGN for different filter bandwidth ratio values

E_b/N_0) of the AWGN channel is changed between 0 dB and 20 dB and the corresponding BER is calculated for every case. As seen in the figure, when there is no lowpass filtering(red curve), the BER equals the theoretical BER under AWGN(blue curve). Lowpass filtering degrades the BER performance. It is observed that as the ratio of filter bandwidths increases, the effect of lowpass filtering decreases and the predistorter converges to its ideal performance. As seen in the figure, for ratio of filter bandwidths = 2 or beyond, the lowpass filter has approximately no effect on BER. Figure 4.38 shows the BER performance of the same polar polynomial predistorter as a function of ratio of filter bandwidths for $E_b/N_0 = 10\,dB$. This figure also proves the statement that for ratio of filter bandwidths = 2 or beyond, the lowpass filter has approximately no effect on BER.

The effect of lowpass filtering on the performance of the polar look-up table predistorter was also investigated. This effect is first analyzed in terms of power

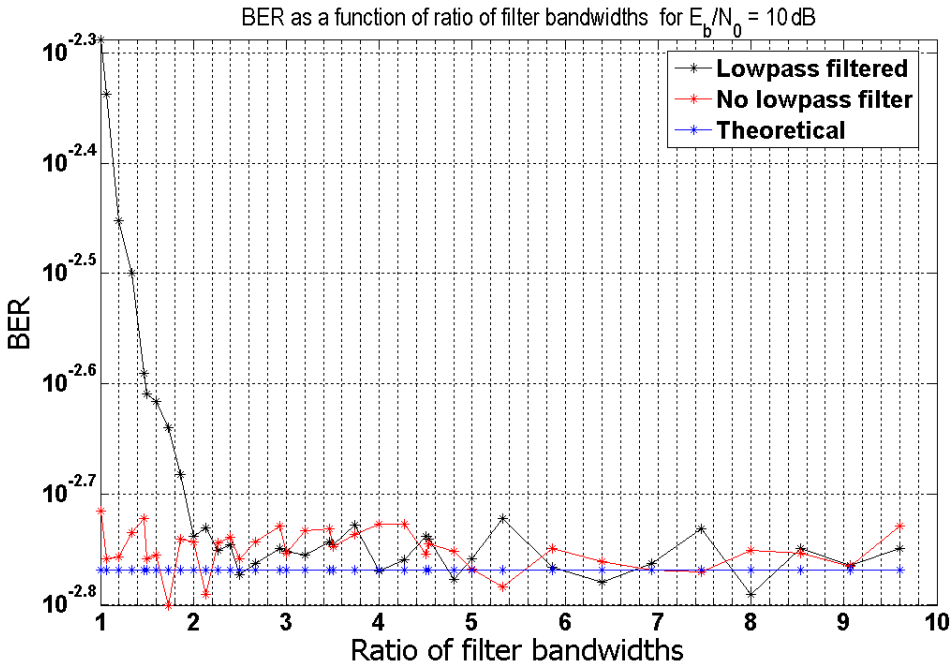


Figure 4.38: BER performance of the polar polynomial predistorter of order 10 as a function of ratio of filter bandwidths for $E_b/N_0 = 10\,dB$

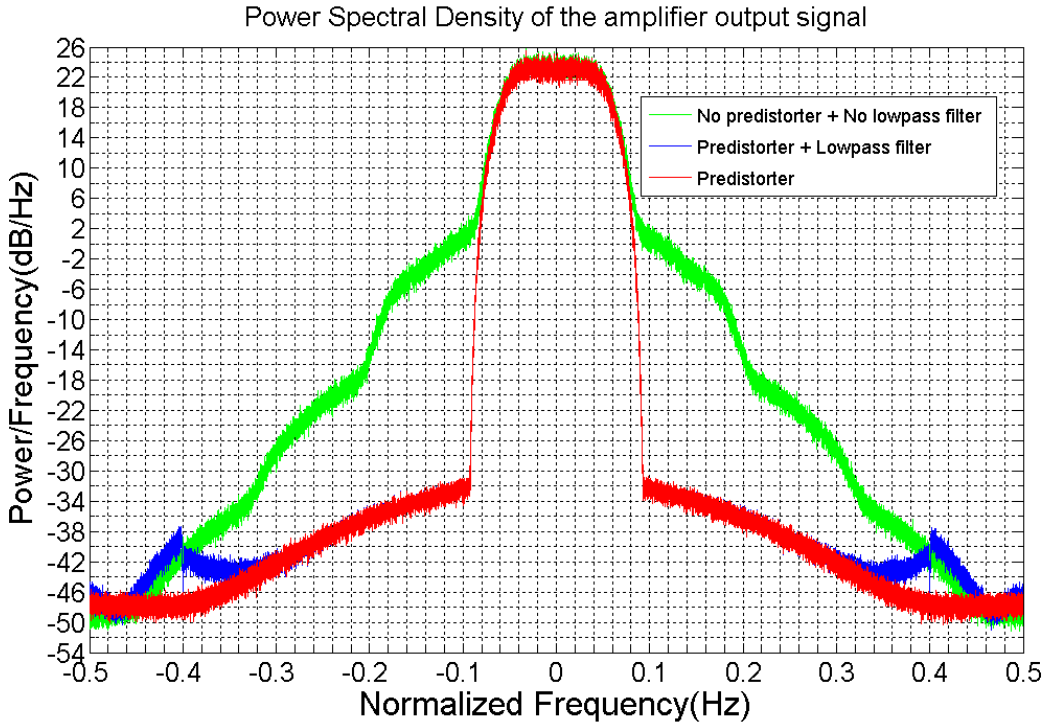


Figure 4.39: Spectral performance of the polar look-up table predistorter which has a table size of 128 for the case where ratio of filter bandwidths = 4.27

spectral density. Figure 4.39 corresponds to a polar look-up table predistorter which has a table size of 128. It shows the power spectral density of the amplifier output signal when there is no predistorter & lowpass filter before the amplifier, when there is a predistorter but no lowpass filter before the amplifier and when there is a predistorter & lowpass filter before the amplifier. The ratio of filter bandwidths is 4.27(upsampling factor = 8, cutoff frequency of the lowpass filter = 0.8). In the corresponding case, polynomial predistorter was not affected by lowpass filtering for this ratio of filter bandwidths but the look-up table predistorter is affected. Also the distortion in the spectrum due to lowpass filtering does not start at the cutoff point of the lowpass filter. It starts before that point. This is another difference from the polynomial predistorter cases. The distortion beyond the cutoff point is normal because for that frequency range, the effect of the polar look-up table predistorter is removed by the lowpass filter and as a result, the nonlinear behaviour of the amplifier shows itself in that frequency range.

Figure 4.40 shows the spectral performance of the same polar look-up table predistorter for the case where ratio of filter bandwidths = 3.2(upsampling factor = 8, cutoff frequency of the lowpass filter = 0.6). Like the previous case, the distortion in the spectrum due to lowpass filtering begins before the cutoff frequency of the lowpass filter. As mentioned before, this is a different behaviour from the polynomial predistorter because for the polynomial predistorter, the distortion in the spectrum due to lowpass filtering begins at the cutoff frequency. After the cutoff frequency, the blue curve(curve corresponding to the lowpass filtered predistorter case) follows the green curve(curve corresponding to the no predistorter case) because for that frequency range, the effect of the polar look-up table predistorter is removed by the lowpass filter and as a result, the nonlinear behaviour of the amplifier shows itself in that frequency range.

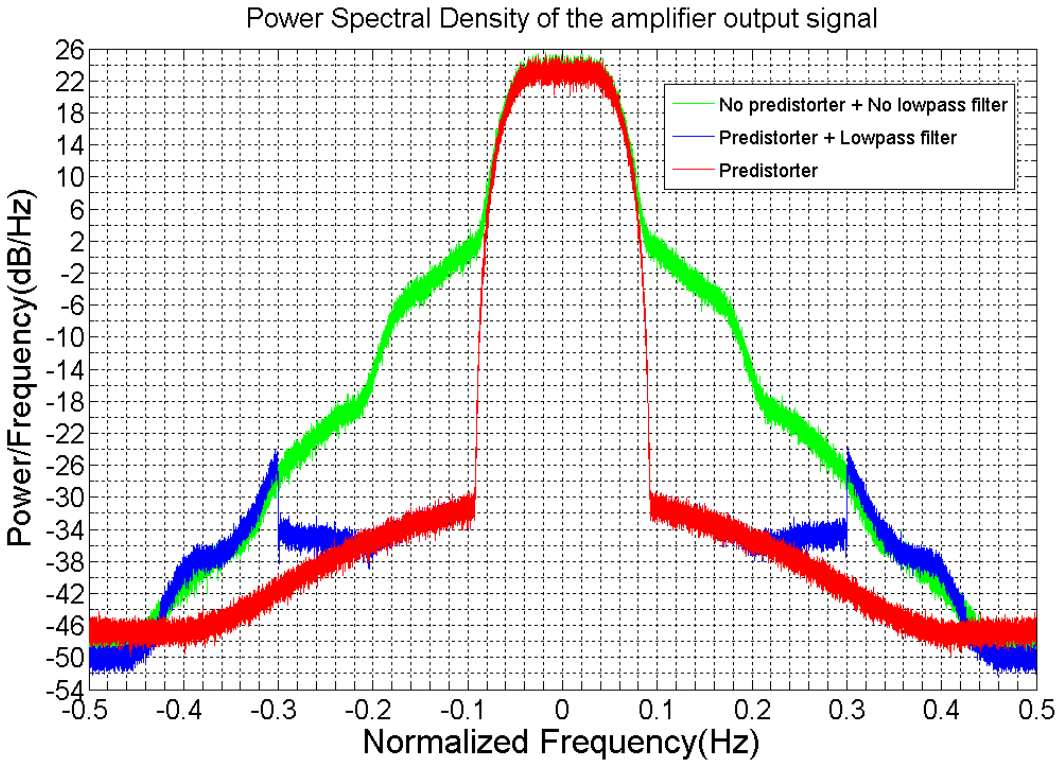


Figure 4.40: Spectral performance of the polar look-up table predistorter which has a table size of 128 for the case where ratio of filter bandwidths = 3.2

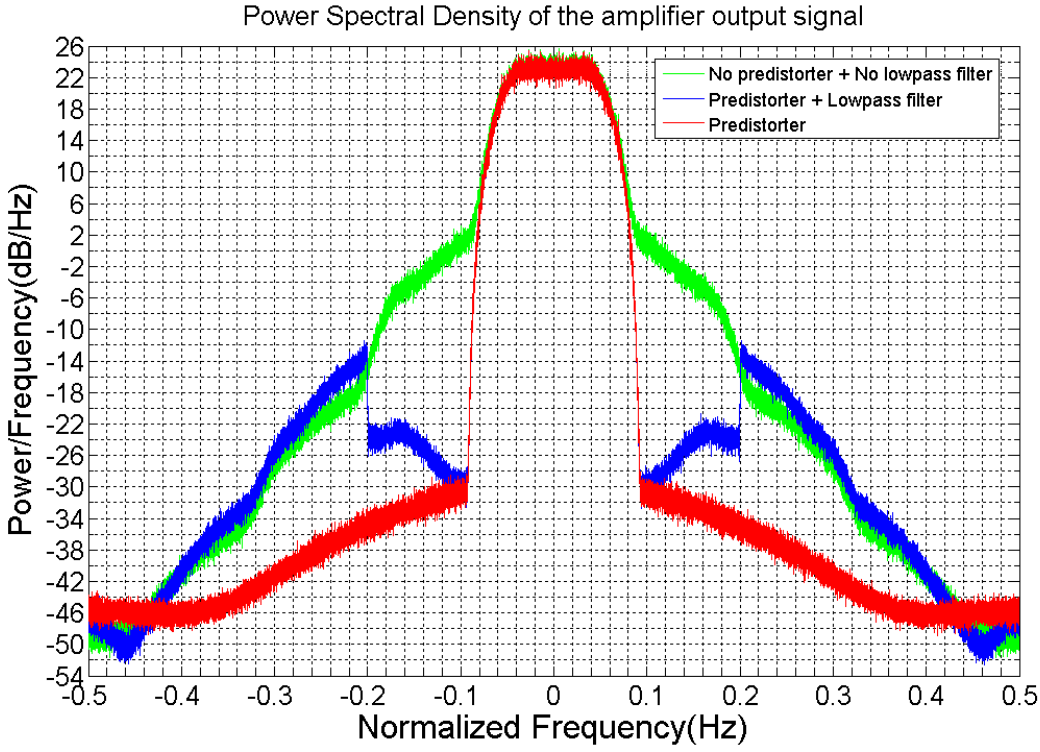


Figure 4.41: Spectral performance of the polar look-up table predistorter which has a table size of 128 for the case where ratio of filter bandwidths = 2.13

Figure 4.41 shows the spectral performance of the same polar look-up table predistorter for the case where ratio of filter bandwidths = 2.13(upsampling factor = 8, cutoff frequency of the lowpass filter = 0.4). Like the other two cases, lowpass filter kills the effect of the polar look-up table predistorter after the cutoff frequency and as a result, the blue curve follows the green curve after that frequency. From these figures, it can be concluded that the polar look-up table predistorter is more negatively affected by lowpass filtering than polar polynomial predistorter.

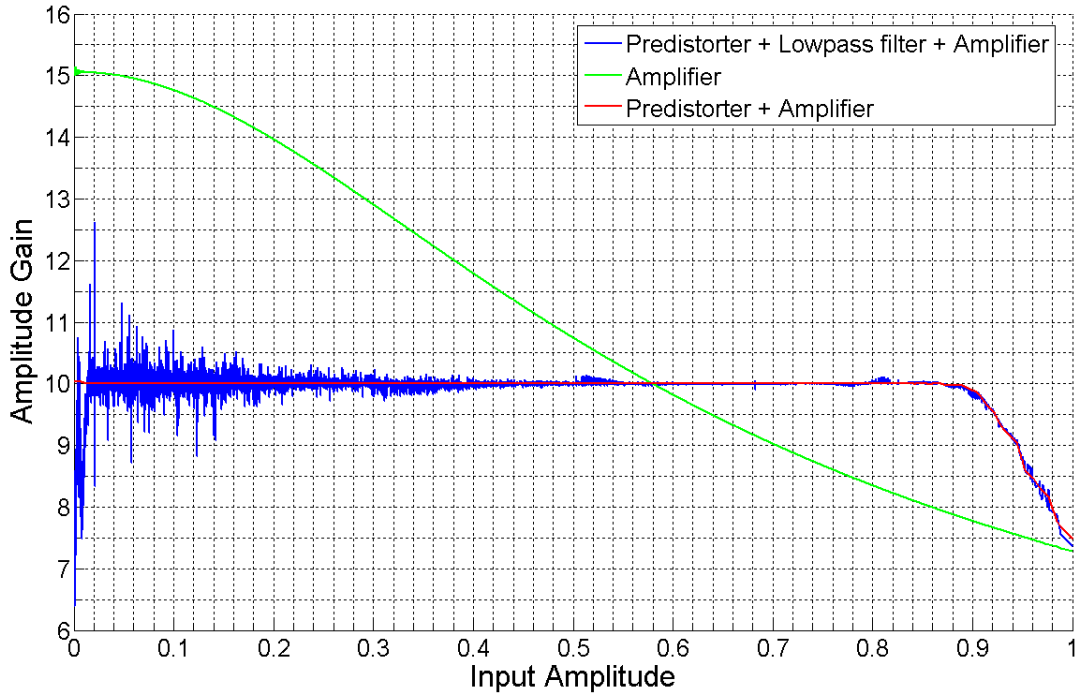


Figure 4.42: AM/AM performance of the polar look-up table predistorter which has a table size of 128 for the case where ratio of filter bandwidths = 4.27

The effect of lowpass filtering on the performance of the polar look-up table predistorter is also analyzed in terms of AM/AM and AM/PM responses. Figures 4.42 and 4.43 show the AM/AM and AM/PM performance of the same polar look-up table predistorter for the case where ratio of filter bandwidths = 4.27(upsampling factor = 8, cutoff frequency of the lowpass filter = 0.8, desired constant gain = 10). As seen in the figures, lowpass filtering degrades the performance of the predistorter and causes a deviation of gain & phase shift from the case where

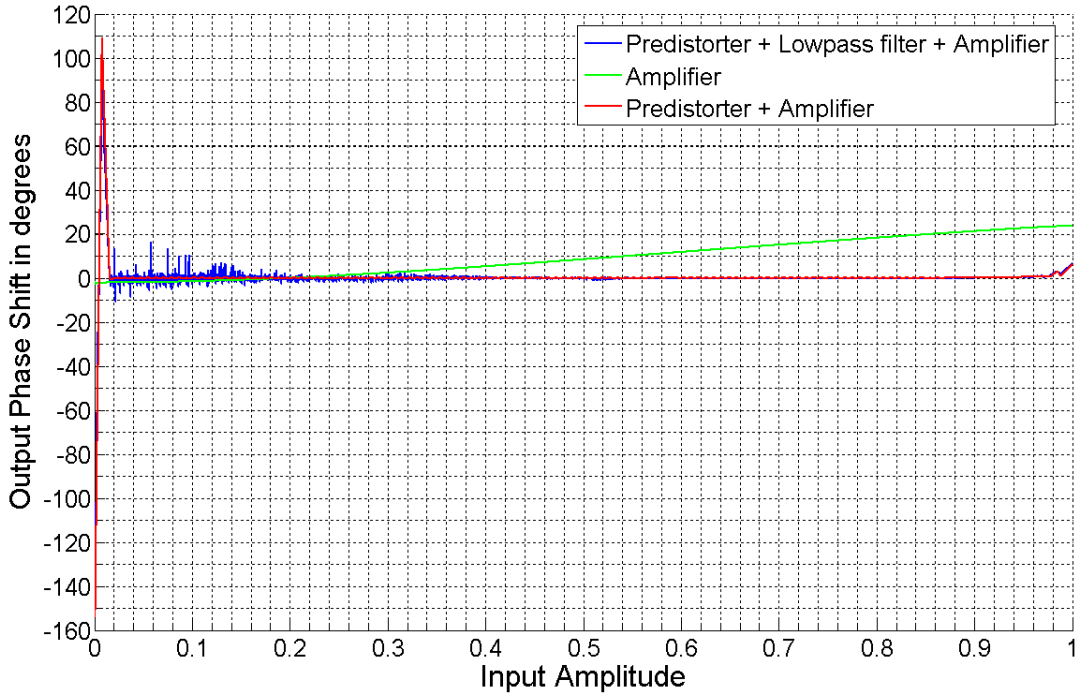


Figure 4.43: AM/PM performance of the polar look-up table predistorter which has a table size of 128 for the case where ratio of filter bandwidths = 4.27

there is no lowpass filter after the predistorter. It is observed that the deviation of gain & phase shift decreases as the input amplitude increases. Another observation is that these deviations are larger than the deviations that occur in the polar polynomial predistorter for the same ratio of filter bandwidths. This supports the statement that polar look-up table predistorter is more negatively affected by lowpass filtering than polar polynomial predistorter.

Figures 4.44 and 4.45 show the AM/AM and AM/PM performance of the same polar look-up table predistorter for the case where ratio of filter bandwidths = 3.2(upsampling factor = 8, cutoff frequency of the lowpass filter = 0.6, desired constant gain = 10). Similar behaviour is observed like the previous case. The deviations in the gain and phase shift caused by lowpass filtering are larger than the previous case because the ratio of bandwidths is smaller and as a result, the negative effect of lowpass filtering on the performance of the predistorter increases. Like the previous case, the deviations decrease as the input amplitude increases.

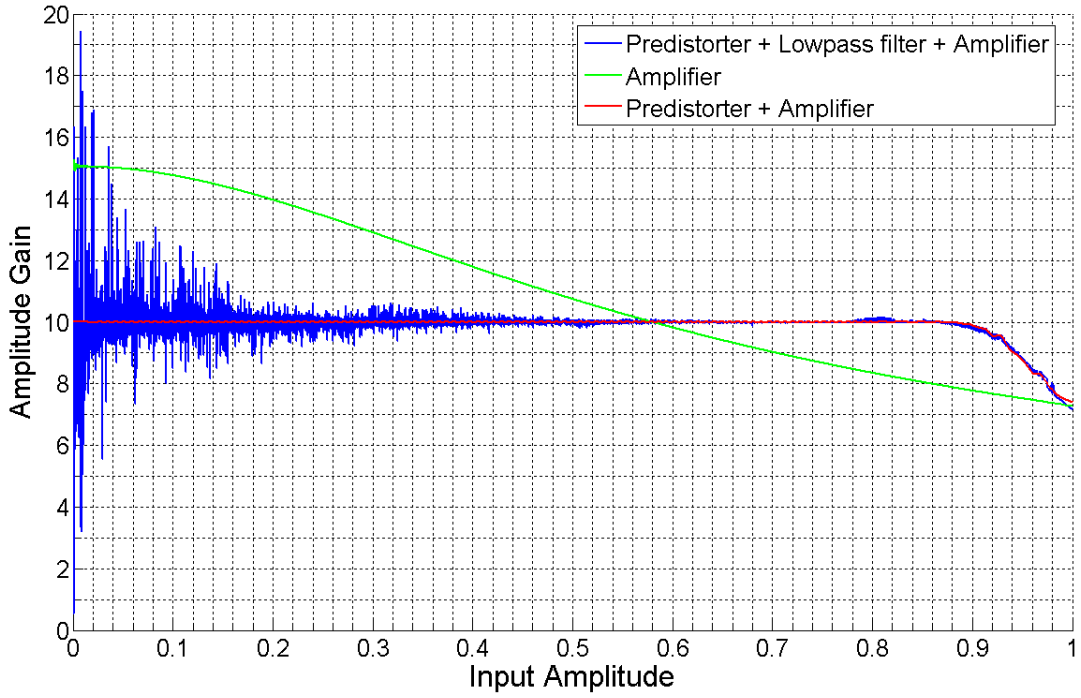


Figure 4.44: AM/AM performance of the polar look-up table predistorter which has a table size of 128 for the case where ratio of filter bandwidths = 3.2

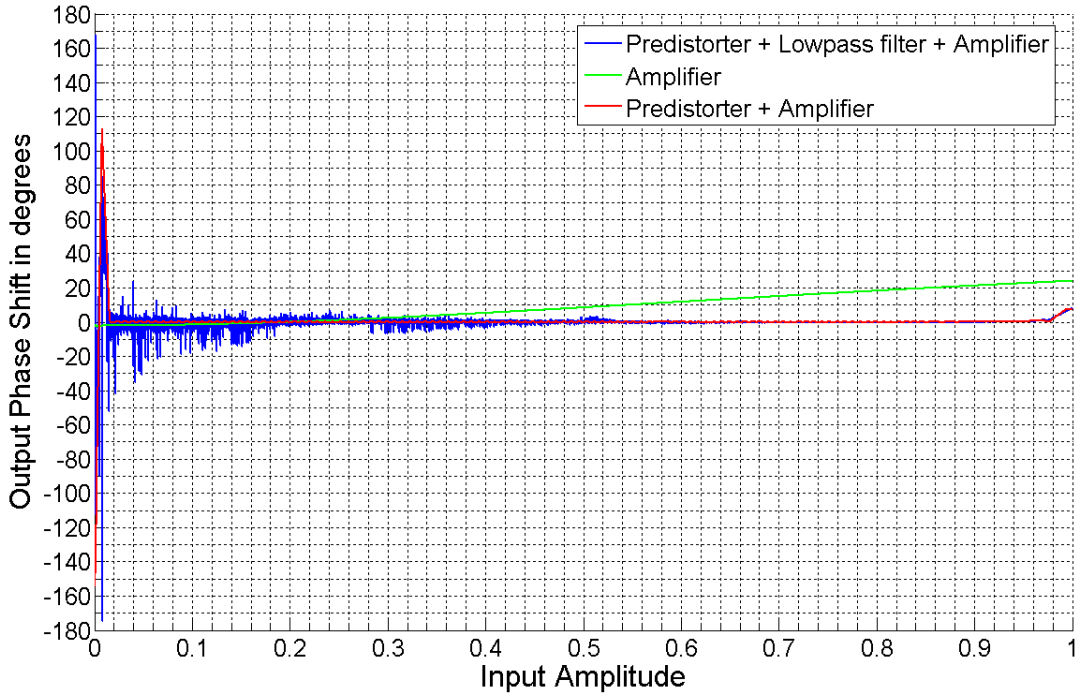


Figure 4.45: AM/PM performance of the polar look-up table predistorter which has a table size of 128 for the case where ratio of filter bandwidths = 3.2

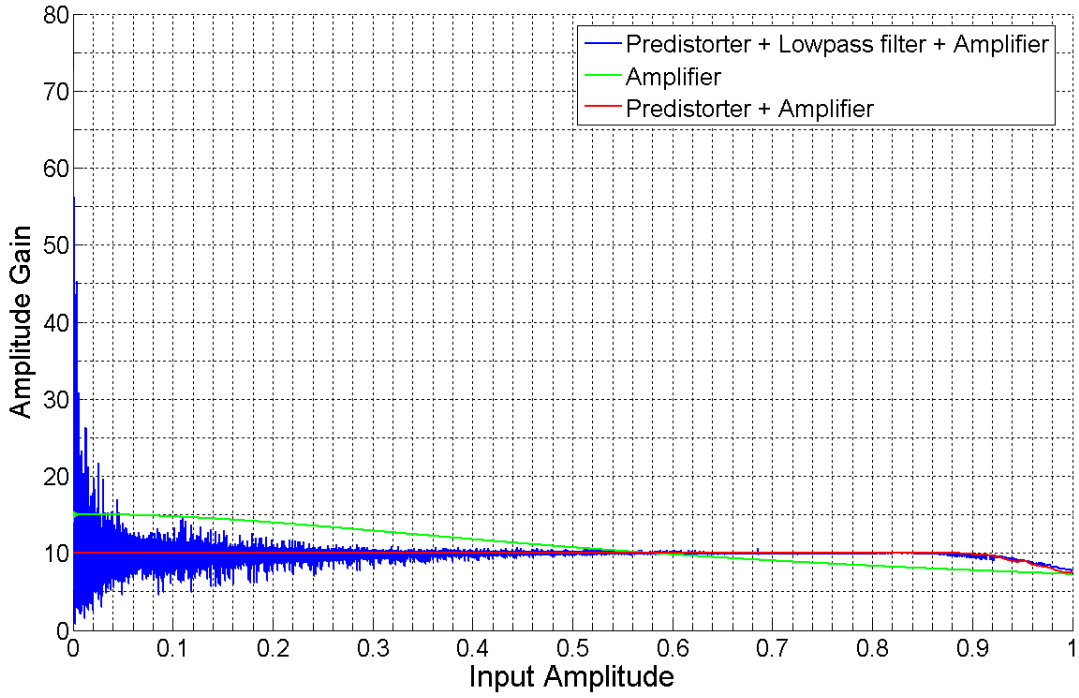


Figure 4.46: AM/AM performance of the polar look-up table predistorter which has a table size of 128 for the case where ratio of filter bandwidths = 2.13

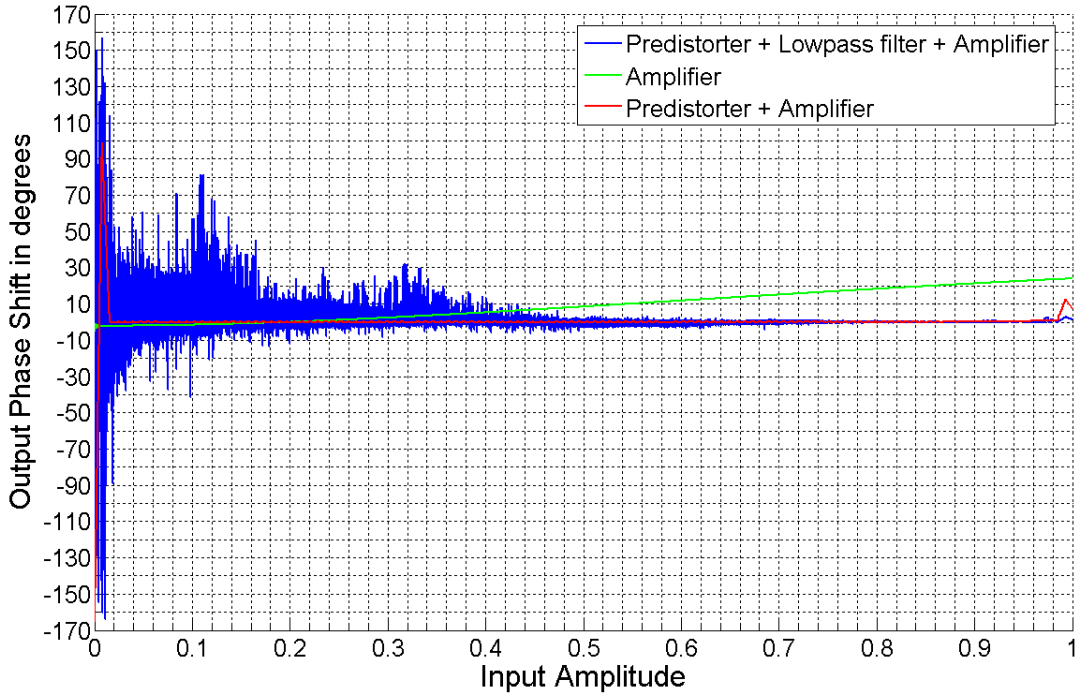


Figure 4.47: AM/PM performance of the polar look-up table predistorter which has a table size of 128 for the case where ratio of filter bandwidths = 2.13

Figures 4.46 and 4.47 show the AM/AM and AM/PM performance of the same polar look-up table predistorter for the case where ratio of filter bandwidths = 2.13(upsampling factor = 8, cutoff frequency of the lowpass filter = 0.4, desired constant gain = 10). Similar behaviour is observed like the previous two cases. The deviations in the gain and phase shift caused by lowpass filtering are larger than the previous two cases because the ratio of bandwidths is smaller and as a result, the negative effect of lowpass filtering on the performance of the predistorter increases. Like the previous two cases, the deviations decrease as the input amplitude increases.

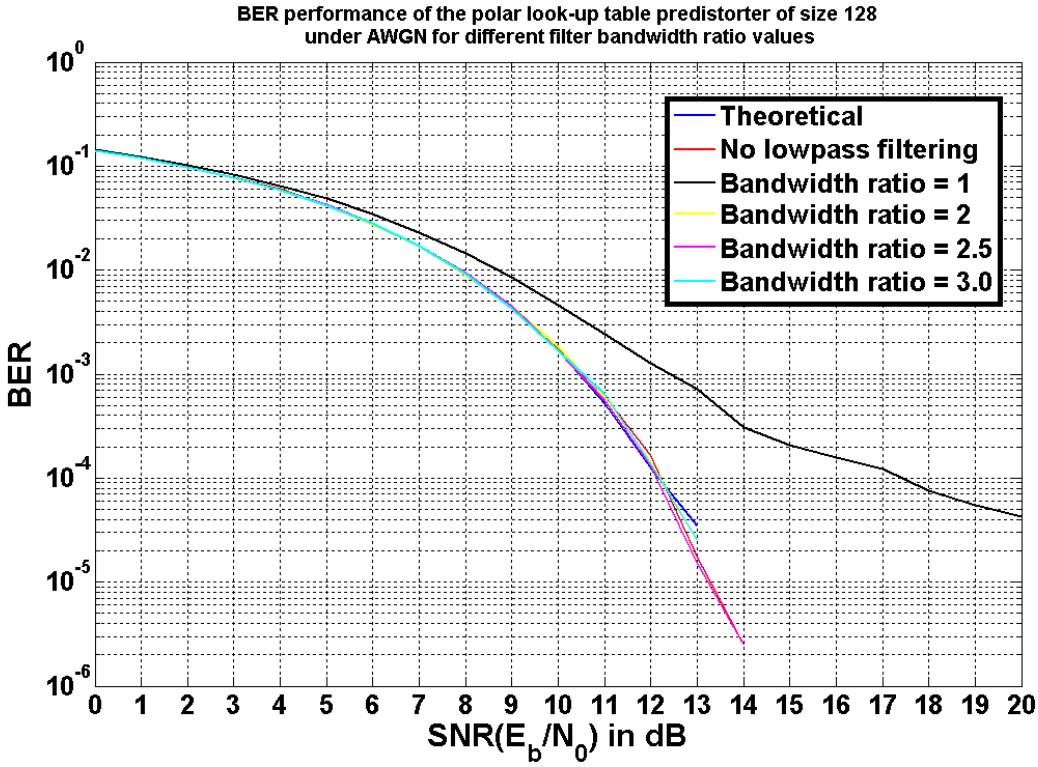


Figure 4.48: BER performance of the polar look-up table predistorter of size 128 under AWGN for different filter bandwidth ratio values

The effect of lowpass filtering on the performance of the look-up table predistorter is also evaluated in terms of BER performance under AWGN. Figure 4.48 shows the BER performance of the same polar look-up table predistorter under AWGN when there is a lowpass filter after

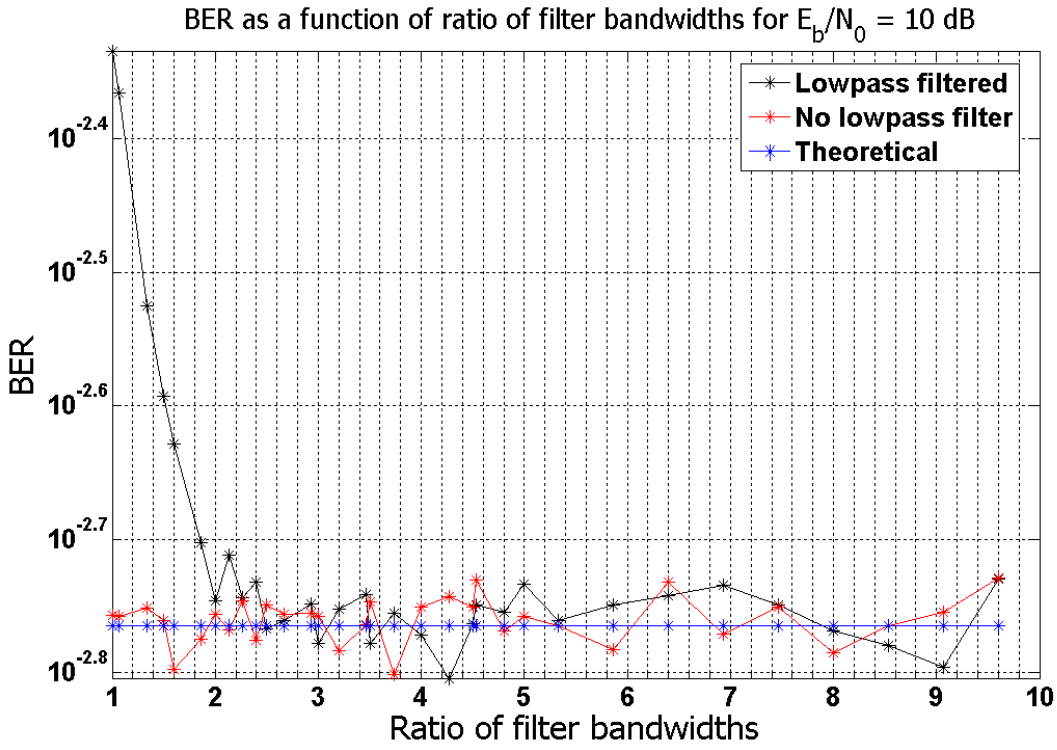


Figure 4.49: BER performance of the polar look-up table predistorter of size 128 as a function of ratio of filter bandwidths for $E_b/N_0 = 10\,dB$

the predistorter. On the figure, you can see the BER performance for different values of $\frac{\text{the bandwidth of lowpass filter}}{\text{the bandwidth of raised cosine filter}}$. To calculate BER, the output of the amplifier is passed through an AWGN channel and then demodulated by a 16-QAM demodulator. SNR(signal-to-noise ratio, E_b/N_0) of the AWGN channel is changed between 0 dB and 20 dB and the corresponding BER is calculated for every case. As seen in the figure, when there is no lowpass filtering(red curve), the BER equals the theoretical BER under AWGN(blue curve). Lowpass filtering degrades the BER performance. It is observed that as the ratio of filter bandwidths increases, the effect of lowpass filtering decreases and the predistorter converges to its ideal performance in terms of BER. As seen in the figure, for ratio of filter bandwidths = 2 or beyond, the lowpass filter has approximately no effect on BER. Figure 4.49 shows the BER performance of the same polar look-up table predistorter as a function of ratio of filter bandwidths for $E_b/N_0 = 10\,dB$. In the figure, it is observed that for ratio of filter bandwidths =

2 or larger, the lowpass filtered case(black curve) is approximately the same as the theoretical case(blue curve). So this figure also supports the statement that for ratio of filter bandwidths = 2 or beyond, the lowpass filter has approximately no effect on BER.

Chapter 5

Summary, Conclusions and Future Work

In this thesis, a polar polynomial predistorter and a polar look-up table predistorter was implemented and tested with simulations in sofware. The implementation and testing was done by using IT++ which is a C++ library of mathematical, signal processing, speech processing, and communications classes and functions. In the simulations, a baseband system model was used. The simulated system model consists of a 16-QAM modulator, an upsampler, a raised cosine filter, the predistorter and a baseband behavioural amplifier model. The amplifier model used is ARCTAN model. This model represents the AM/AM response and AM/PM response of the amplifier by arctan function. The details of the model was described in chapter 3. The AM/AM and AM/PM corrections of the polar polynomial predistorter are two polynomial functions. These two polynomial functions have the same order. They are functions of the input amplitude. The AM/AM and AM/PM corrections of the look-up table are stored in a table. In the table, every AM/AM and AM/PM response value corresponds to a certain input amplitude. These amplitudes and the amplitude step used

while storing the responses are determined by the size of the table. In the simulations, the order of the polynomials of the polynomial predistorter was set to 10 and the size of the table of the look-up table predistorter was set to 128. The simulations done with the predistorters consisted of two phases: Training and testing. In the training phase, the predistorters were updated by using the differences between the desired amplitude & phase values at the amplifier output and the observed amplitude & phase values at the amplifier output. The details of the training process was described in chapter 4. By training, the coefficients of the polynomial predistorter and the entries of the look-up table predistorter converged to approriate values to linearize the amplifier. In the testing phase of the simulations, the performance of the designed predistorters were tested. The performance was evaluated in terms of adjacent channel power ratio, AM/AM & AM/PM responses and BER under AWGN. The predistorters showed good performance in the simulations. The polar polynomial predistorter achieved 20 dB reduction and the polar look-up table predistorter achieved 25 dB reduction in adjacent channel power ratio. The AM/AM & AM/PM response performance of the predistorters were also good. For the polynomial predistorter, there were very small deviations from the desired constant gain for small input amplitude values. The AM/PM performance of the polynomial predistorter was good for small and mid-range input amplitude values but there was a large deviation from the ideal phase shift value 0 for large input amplitudes. This is due to the fact that there weren't enough samples in the training signal with large amplitude values to train the polynomial predistorter. The AM/AM performance of the look-up table predistorter was good except for large input amplitude values. For large input amplitude values, there was a deviation from the desired constant gain. This behaviour can also be explained with the same reasoning mentioned for the polynomial predistorter. The AM/PM response of the look-up table predistorter-amplifier combination showed unstable behaviour for very small amplitude values, which can't be explained. Other than that, the AM/PM

performance was good upto large input amplitudes. For large input amplitudes, there was a large deviation from the ideal phase shift value 0. The predistorters also showed good BER performance under AWGN. They removed the effects of amplifier nonlinearity on BER. In the simulations, the effect of polynomial order and table size on the performance of the predistorters were also investigated. The simulation results showed that increasing the polynomial order does not improve the AM/AM performance of the polynomial predistorter but improves its AM/PM performance. For the look-up table predistorter, increasing the table size had a negative effect on the AM/AM performance but it improved the AM/PM performance. The work done with predistortion is not limited to what is described above. The effect of lowpass filtering on the performance of the predistorters was also investigated. This lowpass filter models the bandpass IF filter which is between the mixer and power amplifier stages in transmitting chains and which is crucial and necessary to suppress out-of-band interference in a real communication system. The lowpass filter was placed between the predistorters and amplifier in the system model. The cutoff frequency of the lowpass filter was changed and its effect on the performance of the predistorters was investigated. While choosing the cutoff frequency of the lowpass filter, it was made sure that its bandwidth was larger than the bandwidth of the raised cosine filter in the system model. Interesting results were obtained in the simulations. It was seen that beyond the cutoff frequency of the lowpass filter, the spectrum of the predistorted and lowpass filtered amplifier output signal followed the spectrum of the amplifier output signal which was neither predistorted nor lowpass filtered. The reason for this is that for that frequency range, the positive effect of the predistorters is removed by the lowpass filter and as a result, the nonlinear behaviour of the amplifier shows itself in that frequency range. The lowpass filter also caused degradations in the AM/AM and AM/PM performances of the predistorters and this degradation increased as the bandwidth of the lowpass filter

decreased. The effect of the lowpass filter on BER performance of the predistorters under AWGN was also investigated. It was observed that when the ratio of the bandwidth of the lowpass filter to the bandwidth of the raised cosine filter exceeds 2, the lowpass filter has approximately no effect on BER for both of the predistorters.

As a future work, the orders of the AM/AM response and AM/PM response polynomials of the polar polynomial predistorter can be made different. This would be good because from the simulations, it seems that the order of the polynomial that will cancel AM/PM distortion should be larger than the order of the polynomial that will cancel AM/AM distortion. Another possible future work is to implement the polynomial predistorter and look-up table predistorter in hardware by using FPGA and DSP chips and to test the performance of the implemented predistorters by using a real power amplifier.

APPENDIX A

16-QAM-OFDM System Performance in the Presence of Adjacent Channel Interference Caused by Amplifier Nonlinearity

A.1 Introduction

OFDM(orthogonal frequency division multiplexing) has been employed in many wireless applications such as digital audio and video broadcasting, interactive video services distribution, broadband wireless local area networks [21]. It has also been employed for fixed-wire applications in the asynchronous digital subscriber line(ADSL) and high-bit-rate DSL(HDSL) systems [22]. The reason for the popularity of OFDM is its efficient use of the available bandwidth, the high

data rates it allows and its ability to combat selective fading. Selective fading effects on OFDM can be efficiently reduced without the need of expensive time-domain equalization, by inserting a cyclic prefix and by using error correcting codes [21]. Another advantage of OFDM is that it can be easily and efficiently obtained and detected by using fast Fourier transform(FFT) and inverse FFT(IFFT) [21]. Due to its promising properties, it is currently being considered the most promising transmission technique to support future wireless multimedia communications in frequency-selective channels [22].

Due to the large number of subcarriers, OFDM signal has a large dynamic signal range(large envelope fluctuations) [23]. Due to its large dynamic range, OFDM is very sensitive to the nonlinear distortion generated by the high-power amplifier(HPA) at the transmitter end. Normally this nonlinear distortion can be avoided by backing off the amplifier, that means forcing the amplifier to work in its linear region [23]. Unfortunately this would not result in a very power efficient operation of the amplifier, which is especially important in the case of cellular and satellite applications [23]. Therefore, for power efficient operation the amplifier must be operated in its nonlinear region close to saturation resulting in nonlinear distortion. The nonlinear distortion of the amplifier causes interference both inside and outside the signal bandwidth of the OFDM signal [21]. The in-band distortion component causes a degradation of the system bit-error rate(BER), whereas the out-of-band distortion component affects adjacent frequency bands and causes adjacent channel interference [21]. The out-of-band distortion is not a problem when there is a single transmitter but when there are multiple transmitters that are operating at close center frequencies(adjacent channels), the out-of-band distortion due to one transmitter will affect the adjacent transmitter(adjacent channel) and cause adjacent channel interference for it. The effect of this adjacent channel interference will depend on the frequency spacing between the channels.

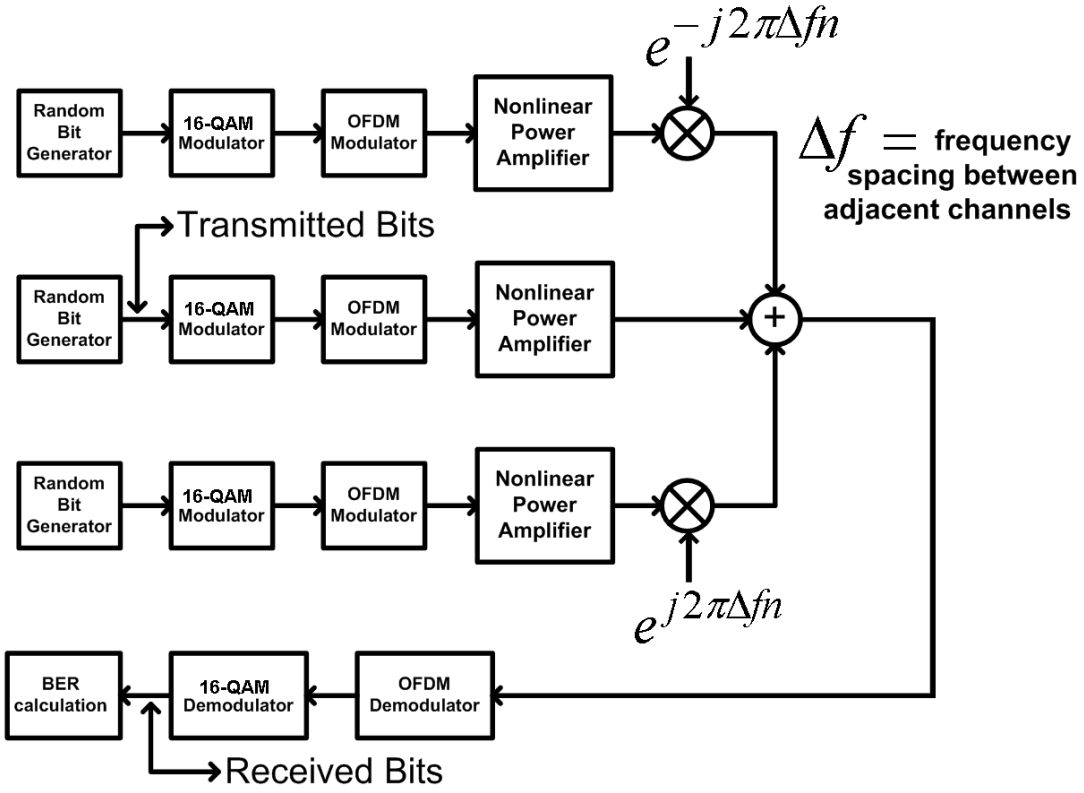


Figure A.1: Simulated baseband system model

This chapter focuses on the effect of adjacent channel interference caused by amplifier nonlinearity on the performance of a 16-QAM-OFDM system. For this purpose, a three transmitter system whose block diagram is shown in Figure A.1 is simulated using IT++. The transmitters operate at adjacent channels and have equal frequency spacing. They employ identical nonlinear power amplifiers at their ends. These nonlinear power amplifiers produce both in-band and out-of-band distortion. The out-of-band distortion introduced by the power amplifiers causes adjacent channel interference. The transmitter operating at the middle channel faces adjacent channel interference resulting from the two adjacent channels at which the other two transmitters operate. This is illustrated in Figure A.2. The performance criterion is the bit-error-rate(BER) of the transmitter operating at the middle channel. The parameters frequency spacing between the

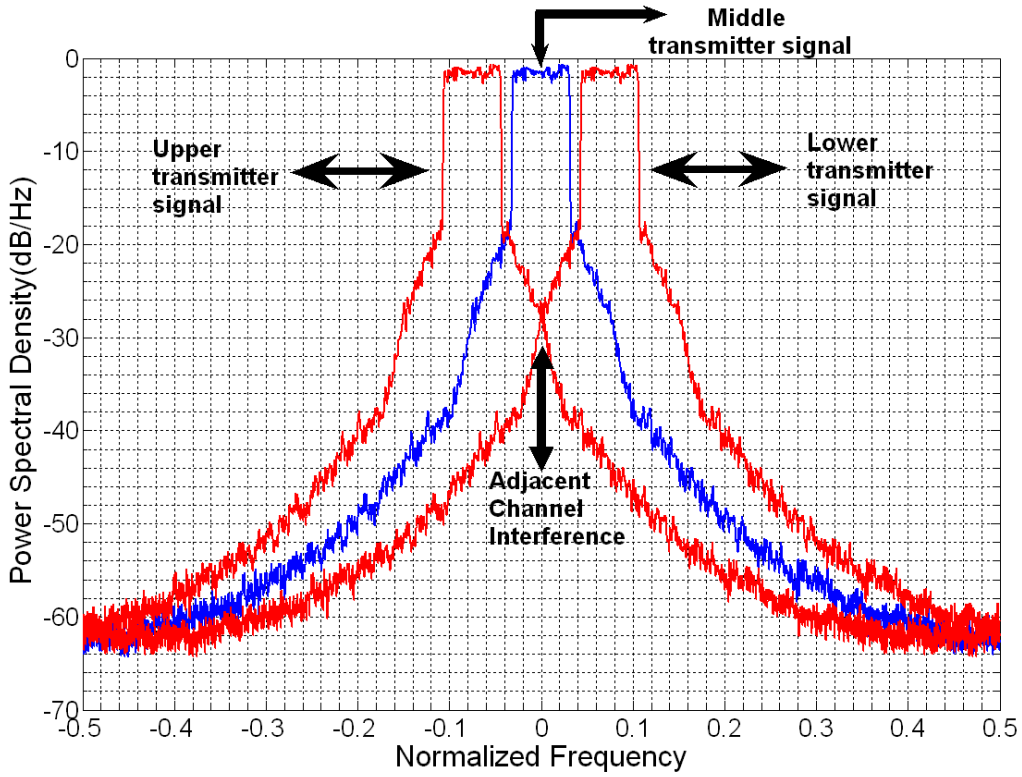


Figure A.2: Adjacent Channel Interference faced by the middle channel

channels, input backoff of the power amplifiers and the ratio of average transmitted powers of the transmitters are changed and their effects on BER are observed.

The organization of this chapter is as follows. Section II describes the simulated system model. In section III, the simulations done are described and their results and the analysis of the results are presented. Finally conclusions are drawn in section IV.

A.2 Simulated System Model

The simulated system model is shown in Figure A.1. This is a baseband equivalent system. Every element is represented by their baseband equivalents. As mentioned before, there are three transmitters in the system. They operate at

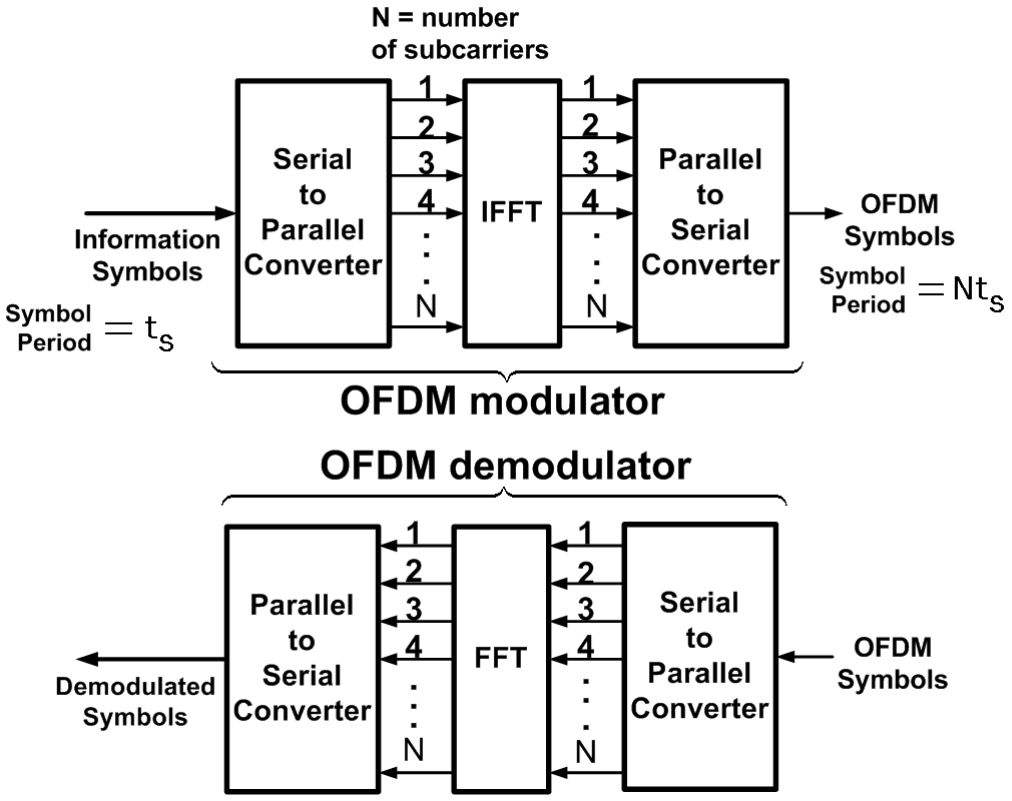


Figure A.3: OFDM modulator and demodulator block diagram

adjacent channels which are equally spaced in frequency. Δf is the frequency spacing between the adjacent channels. In the following subsections, different parts of the system model are described.

A.2.1 OFDM modulator and demodulator

Figure A.3 shows the block diagram of the OFDM modulator and demodulator. As seen in the figure, the modulation and demodulation processes are efficiently implemented through the fast Fourier transform (FFT) algorithm [22].

Let $R_s = 1/t_s$ denote the symbol rate of the information symbols to be transmitted and N denote the number of subcarriers of OFDM. The symbol period of the OFDM signal is $T = Nt_s = N/R_s$. The complex envelope of the OFDM symbol which is transmitted in the time interval $[iT, (i+1)T]$ is given

by [22]

$$s(t) = \sum_{k=0}^{N-1} a_k e^{j2\pi f_k t}, \qquad iT \leq t \leq (i+1)T \tag{A.1}$$

where $f_k = k/T = kR_s/N$ is the k^{th} subcarrier frequency and $a_0, a_1, \ldots, a_{N-1}$ are the information symbols to be transmitted in the time interval $[iT, (i+1)T]$. Since 16-QAM modulation is used, a_k can take one of the values from the alphabet [22] $a_k \, \epsilon \left\{ \frac{1}{\sqrt{10}} \Big([2m-5] + j[2n-5] \Big);\, m, n = 1, 2, 3, 4 \right\}$ with equal probability. (The scaling by $\frac{1}{\sqrt{10}}$ is done to make the average energy of the constellation equal to 1.)

In the simulations, the transmitted OFDM symbol s(t) in the time interval $[iT, (i+1)T]$ is represented by N samples $s_n = s(t)\big|_{t = iT + nt_s} = s(t)\big|_{t = iT + (n/N)T}$, $n = 0, 1, 2, \ldots, N-1$. The samples s_n are given by [22]

$$s_n = \sum_{k=0}^{N-1} a_k e^{j\frac{2\pi}{N} k\, n}, \quad n = 0, 1, 2, \ldots, N-1 \tag{A.2}$$

which corresponds to the IFFT of the information symbols $a_k (k = 0, 1, 2, \ldots, N-1)$. This exactly describes what is done by the OFDM modulator. In each time interval of length T, the vector of N incoming information symbols is transformed by IFFT to a vector of length N, which contains the samples of the baseband OFDM symbol. Oversampling may also be necessary. When there is oversampling, the number of samples s_n increases from N to $N\alpha$ where α is the oversampling factor. In this case, s_n are t_s/α spaced in time and computed by taking $N\alpha$ point IFFT of the N information symbols a_k. So with oversampling (A.2) is modified to

$$s_n = \sum_{k=0}^{N-1} a_k e^{j\frac{2\pi}{N\alpha} k\, n}, \quad n = 0, 1, 2, \ldots, N\alpha - 1. \tag{A.3}$$

The OFDM demodulator implements the inverse process. It computes the FFT of the t_s spaced signal samples to obtain the information symbols transmitted. Similar to the OFDM modulator, in each time interval of length T, the vector of N received signal samples(which are t_s spaced in time) is transformed by FFT

to a vector of length N, which contains the demodulated information symbols. In mathematical terms, if $r_m(m = 0, 1, 2, \ldots, N-1)$ denotes the received signal samples in a duration of T, the corresponding demodulated information symbols denoted as b_k are given by [22]

$$b_k = \frac{1}{N} \sum_{m=0}^{N-1} r_m e^{-j\frac{2\pi}{N} k\, m}, \quad k = 0, 1, 2, \ldots, N-1. \tag{A.4}$$

Since there is nonlinearity in the system, the demodulated information symbols b_k will differ from the transmitted information symbols a_k. If oversampling is applied, the number of received signal samples r_m in a duration of T increases from N to $N\alpha$ where α is the oversampling factor and (A.4) is modified to

$$b_k = \frac{1}{N\alpha} \sum_{m=0}^{N\alpha-1} r_m e^{-j\frac{2\pi}{N\alpha} k\, m}, \; k = 0, 1, 2, \ldots, N-1. \tag{A.5}$$

A.2.2 Nonlinear Power Amplifier

The modelling of nonlinear behaviour of power amplifiers was discussed in detail in chapter 3. Since the simulated system model is a baseband model, a baseband model is needed for the power amplifier in the simulations. For this purpose, the complex envelope response(AM/AM response and AM/PM response) which is a baseband behavioural model is used in the simulations to model the nonlinear power amplifier. Detailed information was given about AM/AM response and AM/PM response in chapter 3. It has been mentioned in chapter 3 that there are complex envelope response models widely used in the literature for modelling the nonlinear behaviour of power amplifiers. Several of these models were Saleh model, Rapp model and third order polynomial model. These three models were used in the simulations as the nonlinear power amplifier with the following parameter values:

Saleh model: $\alpha_a = 1, \beta_a = \beta_p = 0.1, \alpha_p = \dfrac{\pi}{60}$

Rapp model: $v = 1, A_0 = 1, p = 2$

Third order polynomial model: $c_1 = 1, A_{inIP3} = \sqrt{10}$

There is an important parameter called IBO(input backoff) in the simulations. This parameter determines the nonlinear power amplifier operating point. It is defined as $IBO_{dB} = 10\log_{10}\left(\frac{A_{ref}^2}{P_{in}}\right)$ where A_{ref} is a reference input amplitude level and P_{in} is the average power of the input signal. A_{ref} is generally taken as the input amplitude at which amplifier saturates but in the simulations it was taken as the input amplitude at the 1 dB compression point. The parameter IBO determines the level of nonlinear distortion introduced by the power amplifier. As IBO decreases, the nonlinear distortion introduced by the power amplifier increases. The increase of IBO results in the reduction of the nonlinear distortion of the power amplifier. In the simulations, the IBO parameter is set by scaling the input signal to the power amplifier with a suitable constant so that the average power of the input signal P_{in} will give the desired IBO according to the equation $IBO_{dB} = 10\log_{10}\left(\frac{A_{ref}^2}{P_{in}}\right)$ where A_{ref} is the input amplitude at the 1 dB compression point of the power amplifier. Also in the simulations, the same IBO value is applied to 3 amplifiers in the simulated system model.

A.3 Simulations, Results and Discussion

As mentioned before, the baseband system model given in Figure A.1 was used in the simulations. In every simulation, one million bits were used. In the system model, the number of carriers of OFDM was set to 1024 and the oversampling factor applied to the OFDM signal was set to 16. Identical power amplifiers were used at each of the three transmitters. As explained in section A.2.2, Saleh model, Rapp model and third order polynomial model were used as the nonlinear power amplifier in the simulations. The values assigned to the parameters of these models in the simulations were given in section A.2.2. The nonlinear power amplifier has another important parameter which is IBO. IBO was assigned values in the range 0 dB-10 dB in the simulations. The IBO parameters

of the 3 identical amplifiers in the system model were set to same values. Another important parameter in the simulations is the frequency spacing between adjacent channels which is denoted by Δf. It is set by multiplying the upper and lower transmitter signals by $e^{-j2\pi\Delta fn}$ and $e^{j2\pi\Delta fn}$. It is defined relative to the bandwidth of the middle channel. It was changed between 2*bandwidth of middle channel and 6*bandwidth of middle channel in the simulations. There is one thing that must be mentioned here. Since the middle transmitter signal is a baseband signal, its bandwidth is equal to the half of its spectral width. So 2*bandwidth of middle channel actually equals the spectral width of the middle transmitter signal. Since the upper and lower transmitter signals are shifted in frequency, they are bandpass signals. Their bandwidths are equal to their spectral widths. Also the spectral widths of all transmitter signals are equal. So 2*bandwidth of middle channel is actually equal to spectral widths of all transmitter signals. The ratio of average transmitted powers of the transmitters is another important parameter in the simulations. To set this parameter, the average transmitted power of the middle transmitter was left unchanged but at the same time the average transmitted powers of the lower and upper transmitters were scaled by the same appropriate constant so that the ratios of their individual average transmitted powers to the average transmitted power of the middle transmitter were set to the desired value of ratio of average transmitted powers of the transmitters. In the simulations, this parameter was assigned the values 0 dB, 3 dB, 6 dB, 9 dB, 12 dB, 15 dB, 20 dB, 25 dB and 30 dB. To make it more clear, when this parameter takes the value 30 dB, this means that the average transmitted powers of upper and lower transmitters are 30 dB larger than the average transmitted power of the middle transmitter.

In the simulations, the parameters frequency spacing between the channels, input backoff of the power amplifiers and the ratio of average transmitted powers of the transmitters were changed and their effects on BER of the middle transmitter were observed. These parameters took the values given in the above

paragraph during the simulations. Before proceeding to the simulation results, one thing must be mentioned about the BER plots that will be given as simulation results. In the BER plots, you will see labels like " only in-band distortion ", " in-band distortion + adjacent channel interference ", " only adjacent channel interference ". " only in-band distortion " means that the middle transmitter signal is amplified nonlinearly by the nonlinear power amplifier and the upper transmitter signal and the lower transmitter signal are not added to the middle transmitter signal. In this case, the middle transmitter signal will only face in-band distortion caused by its nonlinear amplifier. " in-band distortion + adjacent channel interference " means that all of the transmitter signals are amplified nonlinearly by the same nonlinear amplifier model and as a result, the middle transmitter signal faces both in-band distortion caused by its nonlinear amplifier and adjacent channel interference caused by the nonlinear amplification of the upper and lower transmitter signals. " only adjacent channel interference " means that the middle transmitter signal is amplified linearly but the upper and lower transmitter signals are amplified nonlinearly by the same nonlinear amplifier model and as a result, the middle transmitter signal faces adjacent channel interference caused by nonlinear amplification of the upper and lower transmitter signals.

Now the simulation results will be provided. Only the results corresponding to Rapp model will be provided. The other amplifier models(Saleh model and third order polynomial model) show similar results to Rapp model. The effect of different parameters on BER are the same for different amplifier models. Only the BER levels are different. So there is no need to provide the results for all amplifier models. Figure A.4 shows BER of the middle transmitter as a function of channel spacing for different average transmitted power ratio values. IBO is equal to 0 dB for all of the plots in the figure and this is the worst case for BER in terms of IBO. Average transmitted power ratio means the ratio of average transmitted powers of upper and lower transmitters to the average transmitted

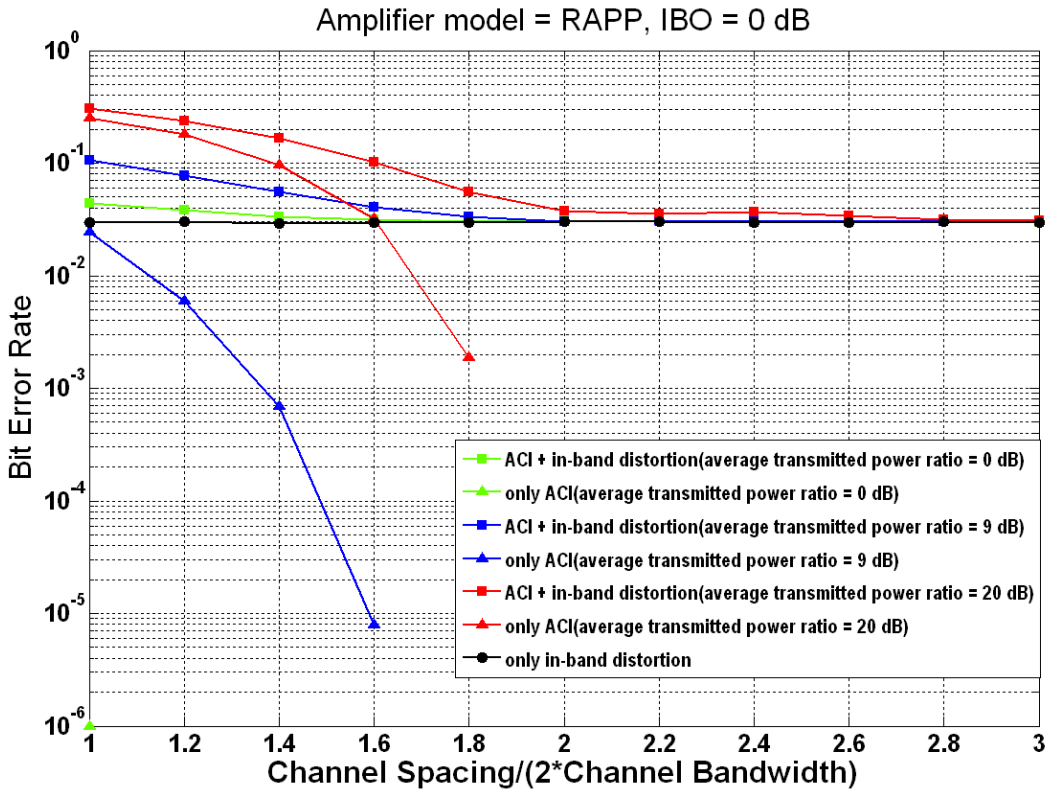


Figure A.4: BER of the middle transmitter as a function of channel spacing for different average transmitted power ratio values where amplifier model = Rapp model, IBO = 0 dB

power of middle transmitter. In this figure and in the other figures that will be provided, ACI stands for adjacent channel interference. As seen in the figure, the effect of in-band distortion on BER is independent of channel spacing and average transmitted power ratio. ACI does not have a strong effect on BER for small average transmitted power ratio values. As average transmitted power ratio value increases, ACI increases and as a result, its effect on BER increases. Another observation is that as channel spacing(frequency spacing between adjacent channels) increases, the effect of ACI on BER diminishes. It is seen that when there is only ACI present on the signal, the BER becomes zero after a certain value of channel spacing. As expected, this certain value of channel spacing after which the effect of ACI on BER completely diminishes increases as the average transmitted power ratio value increases. A similar situation is also observed in " in-band distortion + ACI " cases. Their BER values decrease as channel spacing

increases. After a certain value of channel spacing, which increases as average transmitted power ratio value increases, the effect of ACI on BER completely diminishes and as a result the BER values of " in-band distortion + ACI " cases converge to the BER value of " only in-band distortion " case. The BER values of " in-band distortion + ACI " cases increase as average transmitted power ratio value increases, which is expected because as average transmitted power ratio value increases, ACI increases. It is evident from Figure A.4 that it is the in-band distortion that determines BER, not ACI when interfering channels have the same average power but as the average powers of upper and lower adjacent channels that interfere with the middle channel become larger than the average power of middle channel, the effect of ACI on BER increases and ACI starts to become the dominant factor that determines BER provided that the channel spacing is not large so that ACI does not diminish. Figure A.5 shows the same

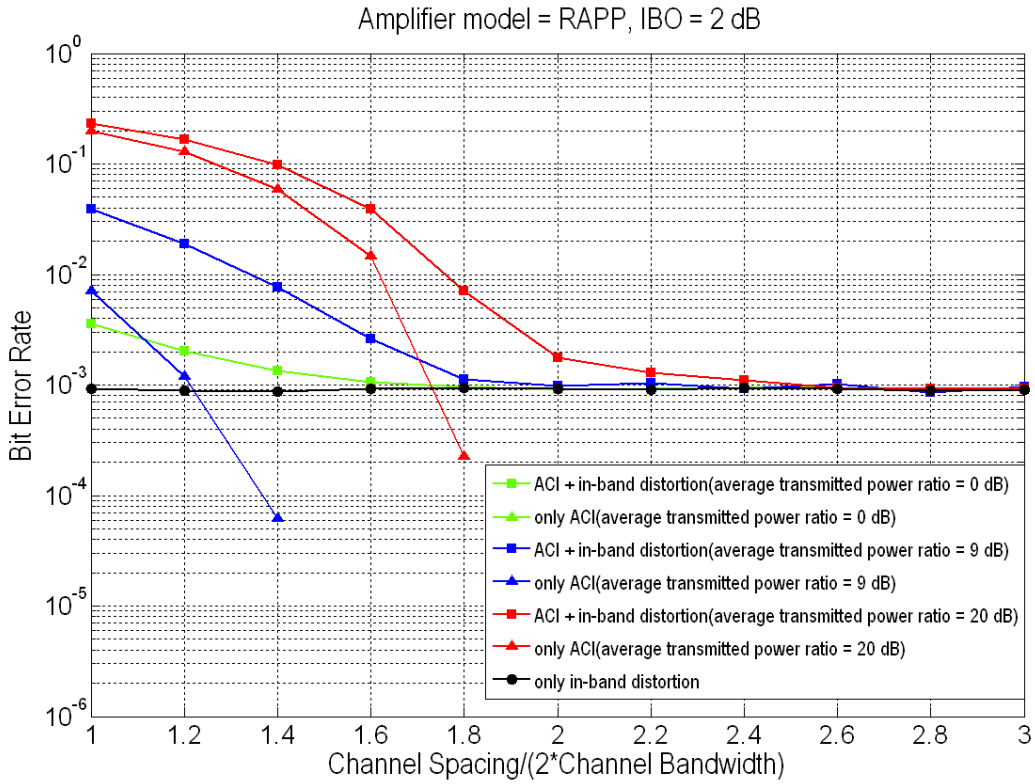


Figure A.5: BER of the middle transmitter as a function of channel spacing for different average transmitted power ratio values where amplifier model = Rapp model, IBO = 2 dB

plots as Figure A.4 for IBO = 2 dB. The behaviour of BER is similar to Figure A.4 so the same comments also apply to Figure A.5. The difference is that IBO is larger. This results in the reduction of both in-band distortion and adjacent channel interference. As a result, BER values become smaller for all cases but the behaviour of BER with respect to channel spacing and average transmitted power ratio stays the same. As seen in the figure, the BER level of in-band distortion becomes smaller since in-band distortion is reduced for higher IBO. Also the effect of ACI on BER diminishes for smaller values of channel spacing since ACI is reduced for higher IBO, too.

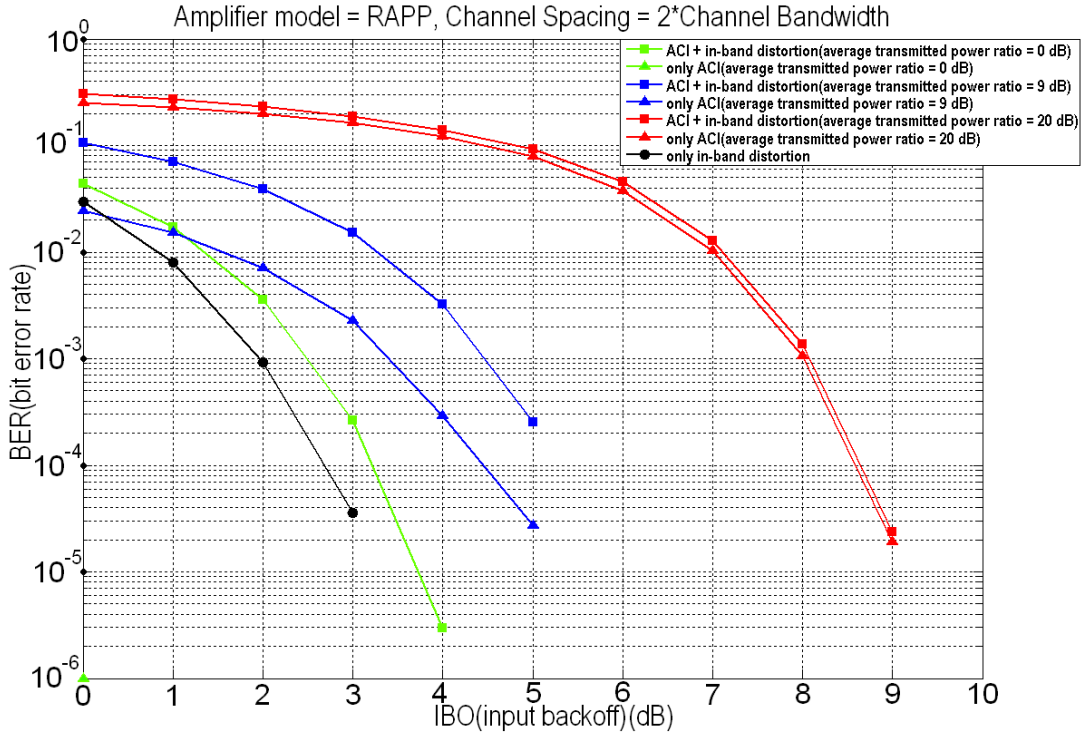


Figure A.6: BER of the middle transmitter as a function of IBO for different average transmitted power ratio values where amplifier model = Rapp model, Channel Spacing = 2*Channel Bandwidth

Figure A.6 shows BER of the middle transmitter as a function of IBO for different average transmitted power ratio values. Channel spacing is equal to 2*bandwidth of middle channel for all the plots in the figure. This is the worst case for BER in terms of channel spacing. For this value of channel spacing, the

3 channels are side-by-side with no separation between their ends. As seen in the figure, BER values decrease as IBO increases because in-band distortion and ACI are both reduced when IBO increases. Like the previous cases, the effect of ACI on BER increases when the average transmitted power ratio value increases because when it increases, ACI also increases. As a result, " in-band distortion + ACI " and " only ACI " cases approach each other as average transmitted power ratio value increases. When average transmitted power ratio value is small, the BER values of " only ACI " cases are smaller than the BER values of " only in-band distortion " case. As average transmitted power ratio value increases, the situation reverses and the BER values of " only ACI " cases become larger than the BER values of " only in-band distortion " case, which means that ACI becomes more dominant than in-band distortion. As seen in the figure, the BER value becomes zero in all of the plots after certain values of IBO. The reason for this is that as IBO increases, the amplifier behaves more linearly and after a certain value of IBO, the amplifier behaves almost linearly resulting in approximately no ACI and in-band distortion. Another observation is that the IBO value after which the effect of ACI on BER diminishes increases with increasing average transmitted power ratio. Figure A.7 shows the same plots as Figure A.6 for channel spacing = 3.2*bandwidth of middle channel. Similar behaviour is observed as Figure A.6. So the comments that apply to Figure A.6 also applies to this figure. The difference is that channel spacing is larger and this weakens the effect of ACI on BER. The BER values of " only in-band distortion " case stays the same but the BER values of cases that contain ACI are smaller. Also since ACI is weaker, the difference between the BER values of " in-band distortion + ACI " cases and the BER values of " only in-band distortion " case is smaller. Since ACI is weaker, its effect on BER diminishes for smaller values of IBO. Another observation is that for the value of channel spacing in the figure, ACI has no effect on BER when the channels have the same average power(average transmitted power ratio = 0 dB). When average transmitted power ratio increases

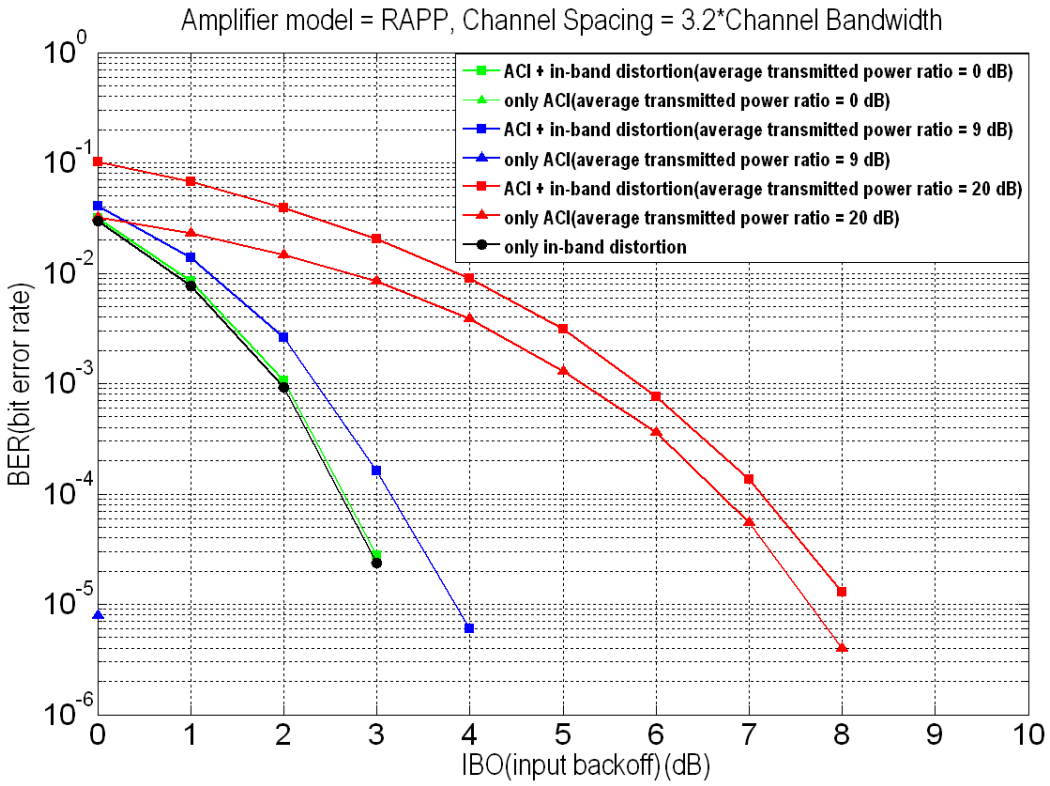


Figure A.7: BER of the middle transmitter as a function of IBO for different average transmitted power ratio values where amplifier model = Rapp model, Channel Spacing = 3.2*Channel Bandwidth

over 0 dB, ACI starts to affect BER and its effect on BER increases as average transmitted power ratio increases. According to the figure, average transmitted power ratio value must be at least 20 dB for ACI to be more dominant on BER than in-band distortion when the channel spacing has the value in the figure. Looking at figures A.6 and A.7, it seems that increasing IBO has a stronger effect on in-band distortion than ACI.

Figure A.8 shows BER of the middle transmitter as a function of average transmitted power ratio for different channel spacing values. IBO is equal to 0 dB for all of the plots in the figure and this is the worst case for BER in terms of IBO. As seen in the figure, the effect of ACI on BER increases as average transmitted power ratio value increases. It is also observed that as channel spacing increases, the effect of ACI on BER decreases. The minimum value that the average transmitted power ratio must take for ACI to affect BER increases

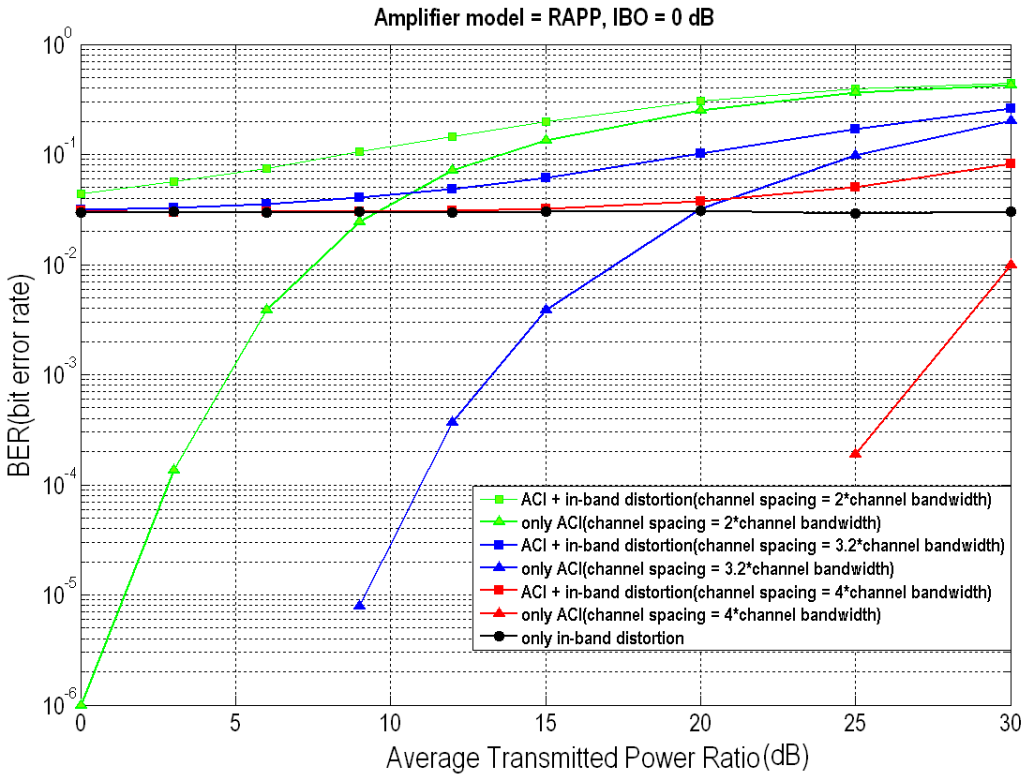


Figure A.8: BER of the middle transmitter as a function of average transmitted power ratio for different channel spacing values where amplifier model = Rapp model, IBO = 0 dB

as channel spacing increases. For ACI to affect BER, average transmitted power ratio must certainly take a value larger than 0 dB. Figure A.9 shows the same plots as Figure A.8 for IBO = 3 dB. Similar behaviours are observed as Figure A.8. The difference is that IBO is larger. As a result, in-band distortion and ACI is reduced and all cases have smaller BER values compared to Figure A.8. The value that average transmitted power ratio should take for ACI to affect BER becomes larger compared to Figure A.8. The BER value caused by in-band distortion is reduced. The value that average transmitted power ratio should take for ACI to be more dominant on BER than in-band distortion is also reduced compared to Figure A.8. This figure also supports the claim that increasing IBO affects in-band distortion more than ACI.

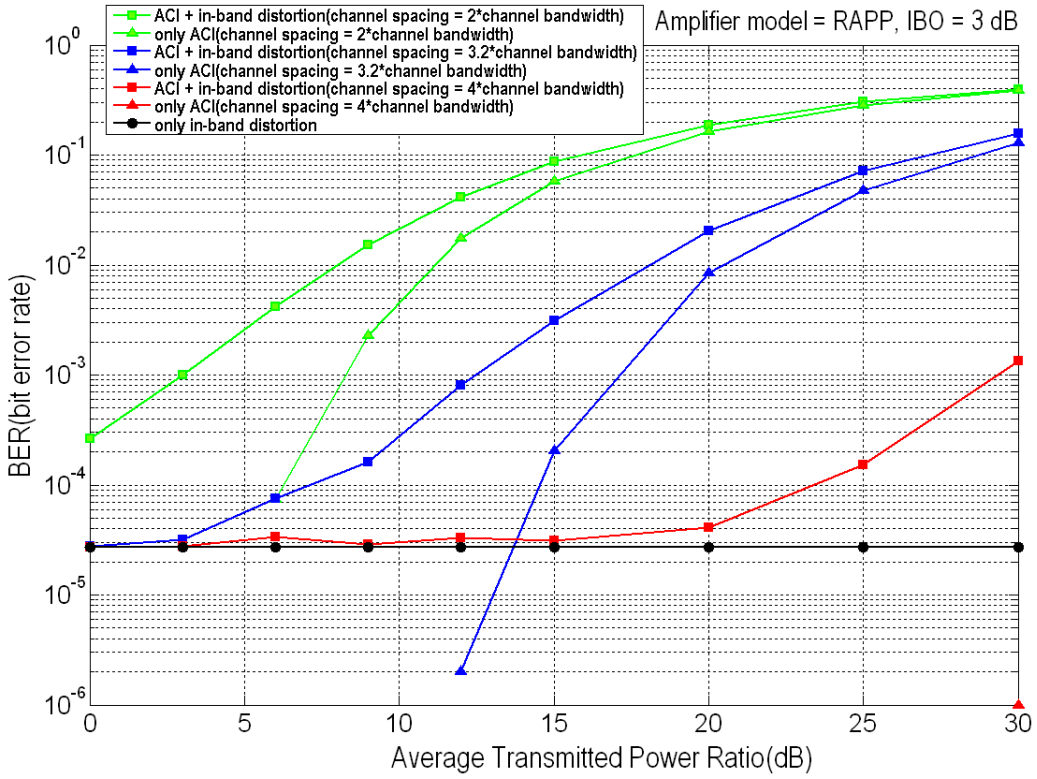


Figure A.9: BER of the middle transmitter as a function of average transmitted power ratio for different channel spacing values where amplifier model = Rapp model, IBO = 3 dB

A.4 Conclusion

In this chapter, the effect of in-band distortion and adjacent channel interference on the performance of a 16-QAM-OFDM system was investigated. For this purpose, the system model shown in Figure A.1 was simulated. The system model consists of three transmitters with identical nonlinear power amplifiers. The transmitters operate at equally spaced frequencies. The lower and upper transmitters create adjacent channel interference for the middle transmitter. The effect of this adjacent channel interference on the performance of the middle transmitter was investigated. The performance criterion was BER. The important parameters in the simulations were IBO of the amplifiers, frequency separation between adjacent channels and the ratio of average transmitted powers of the upper and lower transmitters to the average transmitted power of the middle

transmitter. The simulation results show that when the transmitters have equal average transmitted power, it is the in-band distortion that determines BER whatever the values of IBO and frequency separation between adjacent channels are. When the interfering transmitters have larger average transmitted powers than the middle transmitter, the values of IBO and frequency separation between adjacent channels determine whether in-band distortion or ACI is dominant. By increasing the average transmitted powers of interfering transmitters, ACI can be made more dominant than in-band distortion in determining BER for every IBO and frequency separation value.

Bibliography

[1] R. Maršálek, "Power amplifier linearization using digital baseband adaptive predistortion," Ph.D. dissertation, University of Marne-la-Vallée, Année, 2003.

[2] P. B. Kenington, *High Linearity RF Amplifier Design*. Norwood, MA: Artech House, 2000.

[3] K. Miehle, "A new linearization method for cancellation of third order distortion," Master's thesis, The University of North Carolina at Charlotte, Charlotte, 2003.

[4] C. B. Haskins, "Diode predistortion linearization for power amplifier radio frequency integrated circuits in digital radios," Master's thesis, Virginia Polytechnic Institute and State University, Blacksburg, VA, 2000.

[5] S. P. Stapleton, "Adaptive feedforward linearization for rf power amplifiers," Agilent Technologies, Tech. Rep., June 2001.

[6] F. H. Raab *et al.*, "Power amplifiers and transmitters for rf and microwave," *IEEE Trans. Microwave Theory Tech.*, vol. 50, no. 3, pp. 814–826, March 2002.

[7] W. M. David Su, "An ic for linearizing rf power amplifiers using envelope elimination and restoration," Hewlett Packard Communications and Optics Research Laboratory, Tech. Rep. HPL-98-186, November 1998.

[8] F. H. Raab *et al.*, "L-band transmitter using kahn eer technique," *IEEE Trans. Microwave Theory Tech.*, vol. 46, no. 12, pp. 2220–2225, December 1998.

[9] L. Sundström, "Digital rf power amplifier linearisers analysis and design," Ph.D. dissertation, Lund University, Lund, 1995.

[10] Y. Nagata, "Linear amplification technique for digital mobile communications," in *Proc. IEEE* 39^{th} *Vehicular Tech. Conf.*, vol. 1, San Francisco, CA, May 1989, pp. 159–164.

[11] J. Patel, "Adaptive digital predistortion linearizer for power amplifiers in military uhf satellite," Master's thesis, University of South Florida, Tampa, FL, 2004.

[12] J. K. Cavers, "A linearizing predistorter with fast adaptation," in *Proc. IEEE* 40^{th} *Vehicular Tech. Conf.*, Orlando, FL, May 1990, pp. 41–47.

[13] J. Cavers, "Amplifier linearization by adaptive predistortion," U.S. Patent 5 049 832, Sept. 17, 1991.

[14] W. G. Jeon, K. H. Chang, and Y. S. Cho, "An adaptive data predistorter for compensation of nonlinear distortion in ofdm systems," *IEEE Transactions on Communications*, vol. 45, no. 10, pp. 1167–1171, Oct. 1997.

[15] H. Besbes and T. Le-Ngoc, "A fast adaptive predistorter for nonlinearly amplified m-qam signals," in *IEEE Global Telecommunications Conference, 2000*, vol. 1, San Francisco, CA, USA, Nov. 2000, pp. 108–112.

[16] A. Saleh, "Frequency-independent and frequency-dependent nonlinear models of twt amplifiers," *IEEE Transactions on Communications*, vol. 29, no. 11, pp. 1715–1720, Nov. 1981.

[17] C. Rapp, "Effects of hpa-nonlinearity on a 4-dpsk/ofdm-signal for a digital sound broadcasting system," in *Proceedings of the Second European Conference on Satellite Communications*, Liége, Belgium, Oct. 1991.

[18] N. S. Sirdani, "Adaptive digital linearisation of high power amplifier for linear modulation," Master's thesis, Chalmers University of Technology, Gothenburg, Sweden, 2003.

[19] J. C. Pedro and N. B. Carvalho, *Intermodulation Distortion in Microwave and Wireless Circuits*. Norwood, MA: Artech House, 2003.

[20] K. Gard, "Autocorrelation analysis of spectral regrowth generated by nonlinear circuits in wireless communication systems," Ph.D. dissertation, University of California, San Diego, La Jolla, CA, 2003.

[21] V. T. Davide Dardari and A. Vaccari, "A theoretical characterization of nonlinear distortion effects in ofdm systems," *IEEE Transactions on Communications*, vol. 48, no. 10, pp. 1755–1764, Oct. 2000.

[22] E. Costa and S. Pupolin, "M-qam-ofdm system performance in the presence of a nonlinear amplifier and phase noise," *IEEE Transactions on Communications*, vol. 50, no. 3, pp. 462–472, Mar. 2002.

[23] C. Rapp, "Effects of hpa-nonlinearity on a 4-dpsk/ofdm-signal for a digital sound broadcasting system," in *Proceedings of the Second European Conference on Satellite Communications*, Liége, Belgium, Oct. 1991.